Maria Inês Gonçalves Monteiro
Licenciatura em Ciências da Engenharia Química e Bioquímica

Forward osmosis membranes tailored by hydrogel coatings

Dissertação para obtenção do Grau de Mestre
em Engenharia Química e Bioquímica

Orientador: Professor Andrew Livingston e Professora Isabel Coelhoso
Co-orientador: Ruslan Kochanov

Júri:

Presidente: Professora Doutora Maria Ascensão C. F. Miranda Reis
Arguente: Doutor Svetlozar Gueorguiev Velizarov

FACULDADE DE CIÊNCIAS E TECNOLOGIA
UNIVERSIDADE NOVA DE LISBOA

Outubro de 2012

Maria Inês Gonçalves Monteiro

Forward osmosis membranes tailored by hydrogel coatings

Dissertação para obtenção do Grau de Mestre
em Engenharia Química e Bioquímica

Outubro de 2012

Acknowledgements

I would like to express my deep gratitude to Professor Andrew Livingston (Imperial College, London) and Professor Isabel Coelhoso (Faculdade de Ciências e Tecnologia, Universidade Nova de Lisboa), for all their useful and constructive recommendations on this project. I also would like to thank, Ruslan Kochanov (Imperial College, London), for his guidance, patience and useful elucidations.

I would also like to thank Andrew's group for their support and friendship.

ABSTRACT

Forward osmosis (FO) is a promising process to substitute reverse osmosis (RO), as a lower cost and more environmentally friendly desalination process. However, FO still presents some drawbacks, in particular the several internal concentration polarization (CP) effects and insufficient salt selectivity. In order to overcome these disadvantages, this study focuses on the use of hydrogel surface-coated FO membranes to minimize internal CP effect in water purification, and also to improve membrane salt rejection. For this, a series of crosslinked poly(ethylene glycol) (PEG)-based hydrogels were synthesized, by the photopolymerization of poly(ethylene glycol) diacrylate (PEGDA) and the monomer (PEG) in the presence of a photoinitiator. The water uptake and salt permeability of the resulting films were controlled by manipulating the composition ratio of PEGDA and the monomer PEG, by varying the water content in the prepolymerization mixture and the UV-exposure time. High water uptake and low salt permeability values were observed for the films prepared with 50wt% of water content (50%PEGDA). The hydrogels were applied using different techniques (pressure, soaking and coating) to a cellulose acetate (CA) membrane prepared by phase inversion. However, only one technique was effective, surface coating. The CA membranes coated with these hydrogels materials showed an improvement in NaCl rejection (≅100%) and in some cases an enhancement of 100 and 120% of the original water flux (50% PEGDA coating on the active layer and on the porous support, respectively; in PRO mode). The 50%PEGDA coated membrane (with a coating on the porous support) has also shown reduction of the internal CP effects.

Keywords: forward osmosis (FO), surface coating, hydrogel, poly(ethylene glycol) diacrylate, internal concentration polarization.

RESUMO

A osmose direta (OD) é um processo promissor para substituição da osmose inversa no processo de dessalinização, já que é mais económico e menos prejudicial para o meio ambiente. No entanto, a OD ainda apresenta alguns inconvenientes, nomeadamente o efeito de polarização da concentração (PC) interna e baixa seletividade. De forma a contornar estes problemas, o presente estudo tem como objetivo a preparação de membranas de OD revestidas por um hidrogel, a fim de minimizar o efeito de PC interna e também melhorar a rejeição da membrana aos sais. Para tal, diferentes hidrogéis de polietileno glicol (PEG) foram preparados através da fotopolimerização de diacrilado de polietileno glicol (PEGDA) e do monómero PEG, na presença de um fotoiniciador. A absorção de água e a permeabilidade ao sal dos filmes preparados foram controlados pela variação das razões de PEGDA e do monómero PEG, pela variação do teor de água na mistura de prepolimerização e pela variação do tempo de exposição à luz UV. Os filmes preparados com 50% de teor em água (50%PEGDA) obtiveram elevados valores de absorção de água e baixos valores de permeabilidade ao sal. Os hidrogéis foram aplicados através de diferentes técnicas (pressão, imersão e revestimento) a uma membrana de acetato de celulose (AC), preparada pela técnica de inversão de fase. Porém, apenas uma das técnicas resultou, o revestimento de superfície. Assim, as membranas AC revestidas com hidrogel apresentaram uma rejeição ao NaCl superior (≅100%) e, em alguns casos, uma melhoria de 100 e 120% do fluxo de água original (para as membranas com revestimento de 50%PEGDA na camada activa e suporte poroso, respectivamente; no modo PRO). Igualmente, a membrana revestida com 50%PEGDA (revestimento sobre o suporte poroso) apresentou uma redução do efeito de PC interna.

Termos chave: osmose direta, revestimento de superfície, hidrogel, diacrilado de polietileno glicol, polarização da concentração interna.

INDEX

FIGURES CAPTION

TABLES CAPTION

ABREVIATIONS

AA - Acrylic acid

AMPS - 2-acrylamido-2-methylpropane-sulfonic acid

CA - Cellulose Acetate

CEOP - Cake-enhanced osmotic pressure

CP - Concentration polarization

CTA - Cellulose triacetate

DIW - Deionized water

FO - Forward Osmosis

HTI - Hydration Technologies Inc

ICP - Internal concentration polarization

iCVD - Initiated chemical vapour deposition

MA - Methacrylic acid

MD - Membrane distillation

M_w - Molecular weight

NF - Nanofiltration

OMBR - Osmotic membrane bioreactor

OMD - Osmotic membrane distillation

PEGDA - Poly(ethylene glycol) diacrylate

PEGDE - Poly(ethylene glycol) diglycidyl ether

PEGMA - Poly(ethylene glycol) methacrylate

PRO - Pressure retarded osmosis

RO - Reverse osmosis

SPM - 3- sulfopropylmethacrylate

TGA - Thermogravimetric analysis

TFC - Thin film composite

UF - Ultrafiltration

VSA - Vinylsulfonic acid

NOMENCLATURE

c_b^* - Solubility of benzoic acid in water (mol.m^{-3})

c_b - Concentration of benzoic acid in water (mol.m^{-3})

d_h - Hydraulic diameter (m)

k - Mass transfer cefficient (m.s^{-1})

l - Thickness (μm)

$\mathbf{m_{dry}}$ - Mass of the dry hydrogel film (g)

$\mathbf{m_{wet}}$ - Mass of the wet hydrogel film (g)

t - Time (h)

A - Membrane water permeability (L.m^{-2}.h^{-1}.bar^{-1})

A_m - Membrane surface area (m^2)

B - Membrane salt permeability (L.m^{-2}.h^{-1}.bar^{-1})

D_S - Salt diffusivity coefficient (m^2.s^{-1})

J_i - Flux of component i (L.m^{-2}.h^{-1})

J_w - Water flux (L.m^{-2}.h^{-1})

J_s - Salt flux (g.m^{-2}.h^{-1})

P_S - Salt permeability coefficient (m^2.s^{-1})

K_S - Salt partition coefficient

R - Ideal gas constant (J. K^{-1}.mol^{-1})

R - Solute rejection (%)

T - Temperature (K)

Re - Reynolds number

S - Structural parameter (mm)

Sc - Schmidt number

Sh - Sherwood number

GREEK SYMBOLS

$\boldsymbol{\omega_w}$ **-** Water uptake (%)

$\boldsymbol{\pi_D}$ **-** Osmotic pressure of the draw solution (bar)

$\boldsymbol{\pi_F}$ **-** Osmotic pressure of the feed solution (bar)

$\Delta\boldsymbol{\pi}$ **-** Osmotic pressure difference (bar)

$\Delta\boldsymbol{\pi_{eff}}$ **-** Effective osmotic pressure difference driving force (bar)

$\Delta\boldsymbol{\pi_m}$ - Osmotic pressure difference across the membrane (bar)

$\boldsymbol{\varphi}$ **-** Osmotic coefficient (bar.dm^3.g^{-1})

$\Delta\boldsymbol{P}$ **-** Pressure difference (bar)

$\Delta\boldsymbol{V_{H_2O}}$ **-** Water volume variation in the draw/feed solution (dm^3)

$\boldsymbol{\rho_w}$ **-** Mass density of water (g.dm^{-3})

$\boldsymbol{\rho_p}$ **-** Mass density of polymer (g.dm^{-3})

$\boldsymbol{\varepsilon}$ **-** Porosity (%)

$\boldsymbol{\tau}$ **-** Tortuosity

$\boldsymbol{\mu}$ **-** Chemical potential (energy/mole)

$\boldsymbol{\gamma}$ **-** Activity coefficient

1. INTRODUCTION

Water scarcity and the lack of drinking water are the most serious challenges of the twenty-first century. Currently, one third of the world's population lives in water-stressed countries and, by 2025, this figure is expected to rise to two-thirds (Elimelech, 2006). Increasing population growth and a warming global climate have created even greater disparities between the supplies of, and demands for, reliable fresh water sources. In several cases, conflicts over shared water have exacerbated already significant tensions between neighbouring states (McGinnis, et al., 2010). The need to alleviate water scarcity and ensure good water quality is a major challenge.

In highly industrialized countries, there are growing problems of providing adequate water supply and properly disposal of municipal and industrial used water. In developing countries, particularly those in arid parts of the world, there is a need to develop low-cost methods of acquiring new water supply while protecting existing water sources from pollution.

Under the threats of fresh water shortage, many engineers and researchers have been dealing with reclaiming polluted water, while others try to find other alternative sources. To overcome this problem, the desalination of seawater and other water sources, is becoming a more and more attractive method to produce high quality water for both industrial and domestic usage. Seawater and brackish water desalination technologies hold great promise to reduce water scarcity in arid and densely populated regions of the world. In pursuit of these goals, some techniques have already been developed, as multi-effect distillation, multistage flash, vapor compression, and the most popular reverse osmosis (RO) (Karagiannis, et al., 2008).

The reverse osmosis (RO) is a membrane separation process, which its main application is water treatment (seawater desalination, wastewater treatment, brackish water and water purification) (Cath, et al., 2006; Kim, et al., 2008; Peñate, et al., 2012). In this process, the water is forced to move across a selective permeable membrane against a concentration gradient, by applying pressure (greater than the osmotic pressure) (Cath, et al., 2006). Nevertheless, the RO process has some unavoidable disadvantages the energy costs of seawater and brackish water by RO desalination is too high for economic widespread use; it has also large brine discharge streams, requires the use of chemical cleaning agents and long term membrane replacement

cost (McGinnis, et al., 2010; Lee, et al., 2010). So, is important to find an alternative method for water purification and desalination, which lead to a process less expensive and easy to operate. In order to address some of the challenges still facing current seawater and brackish water desalination technologies, forward osmosis (FO) has gained attention as a possible solution.

2. FORWARD OSMOSIS PROCESS

Lately there has been an increase interest, of using the osmosis phenomenon or forward osmosis (FO) for water treatment instead of the RO process. The osmosis phenomenon was discovered by Nollet in 1748 (Nollet, et al., 1748), although few studies were conducted before the progress of membrane technology. Only in the past years the interests in osmotically driven processes has increased.

In osmotically driven membrane processes two solutions with different salt concentration are separated by a semipermeable membrane, which only allows small molecules (like water-molecules) pass. The difference of concentration between the two solutions creates a gradient that drives water across the membrane from the side of low salt concentration to the side of high salt concentration. An osmotic pressure (π) arises due to this concentration difference (see Figure 1), which is the pressure that applied to the more concentrated solution would prevent transport of water across the membrane.

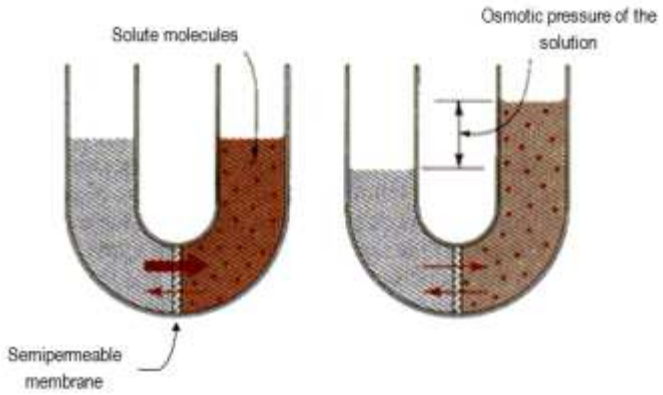

Figure 1 – Schematic illustration of osmosis and osmotic pressure (Rogers, et al., 2000)

The solute concentration (C_S) and the osmotic pressure (π) can be related by the van't Hoff equation, which is:

$$\pi = \frac{C_S RT}{M_w} \qquad (1)$$

Where R is the universal gas constant, T is the temperature and M_w is the molecular weight. It can be seen, in equation (1), that the osmotic pressure is proportional to the concentration and inversely proportional to the molecular weight (M_w). If the solute dissociates (as for instance salts) or associates, equation (1) must be modified. When dissociation occurs the number of moles increases and hence the osmotic pressure increases proportionally, whereas in the case of association the number of moles decreases as does the osmotic pressure. Substantial deviations from the van't Hoff law occur at high concentrations and with macromolecular solutions (Mulder, 1996).

For salt solutions the following van't Hoff equation is used:

$$\pi = n.\varphi.C_S.R.T \quad (2)$$

Where, n is the number of ions and φ is the osmotic coefficient.

Osmotically-driven membrane processes can be classified as forward osmosis (FO), pressure retarded osmosis (PRO, see section 2.8 d) and osmotic membrane distillation (OMD). This latter process, unlike FO and PRO, uses a porous hydrophobic membrane to separate two solutions (feed and osmotic solution) with different solute concentrations. The water passes through the membrane in the form of vapour, from the surface of the solution with higher vapor pressure (feed) to the surface of the solution with lower vapor pressure (osmotic agent), condensing. This migration of water in the form of vapor results in the concentration of the feed and dilution of the osmotic agent solution (Babu, et al., 2006).

Table 1 summarizes the main characteristics of the osmotically-driven membrane processes.

Table 1 - Summary of the main properties of the osmotically-driven separation processes (Khayet, et al., 2011; Achilli, et al., 2009; Qin, et al., 2012; Gostoli, 1999)

	FO	PRO	OMD
Typical separation	Low MW solutes (salt)	Low MW solutes (salt)	Low MW solutes (salt)
Application	Water purification	Power generation	Liquid concentration
Osmotic pressure	High (≈25 bar)	High (27 bar)	Low (≈3.5 bar)
Membrane	Asymmetric Hydrophilic	Asymmetric Hydrophilic	Asymmetric Hydrophobic

In the FO process is not necessary to apply pressure to the system, the water will flow to the permeate side due to an osmotic pressure differential (Δπ) across the membrane, caused by the concentrated solution in the permeate side (see Figure 2). Different names are used to name this solution; in this work the term draw solution will be used. So in this process the water will flow across the semi-permeable membrane from a saline stream into the highly concentrated draw solution, diluting it, thus it is possible to effectively separate the water from the saline feed water stream. The water is subsequently extracted from the dilute draw solution by removing the solute. In order to achieve an effective FO desalination, the draw solute must have a high osmotic efficiency (namely high solubility in water and low molecular weight), as to be easy and inexpensively separated to yield potable water, without being consumed in the process (Cath, et al., 2006; Chay; McCutvheon, et al., 2006).

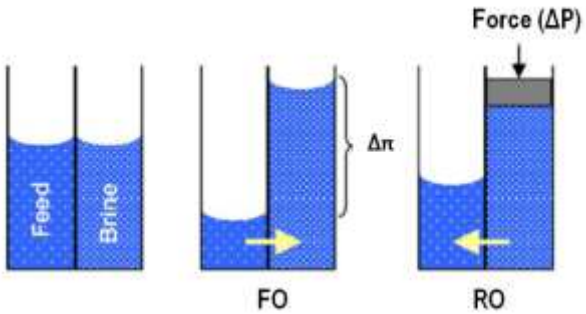

Figure 2- Solvent flows in FO and RO. For FO, ΔP is approximately zero and water diffuses to the more saline side of the membrane. For RO, water diffuses to the less saline side due to hydraulic pressure (ΔP>Δπ) (Cath, et al., 2006).

In the Table 2 is a summarized the advantages of FO process over the RO process.

Table 2- The Comparisons between RO and FO (Liu, et al., 2009)

Sort	Reverse Osmosis	Forward Osmosis
Driven pressure	High hydraulic pressure	Osmotic pressure difference
Water recovery	30%~50%	At least ~75%
Environment effect	Harmfully (concentrated brine)	Friendly
Membrane fouling	Seriously	Hardly
Modules	Compression resistance	Without particular desire
Application	Normal separation system	Temperature-sensitive system; Pressure sensitive system; Renew energy; Control release of drug
Energy Consumption	High energy expenditure (1.6 - 3.02 $kW.h.m^{-3}$) (Triwahyudi, 2007; Avlontis, et al., 2003)	Low energy demand (0.24 $kW.h.m^{-3}$, low temperature, 1.5M Feed) (Triwahyudi, 2007)
Equipments	High-pressure pumps; Energy recovery unit; Resistant high pressure pipelines; High investment in equipments	Low investment equipment

2.1. Overall advantages of Forward Osmosis

FO has a range of potential benefits, mainly due to the low hydraulic pressure required, holding a promise of low energy consumption, and so a decrease in operation costs. This is one of the most attractive points of FO, especially under the growing energy crises. However, this aim can only be achieve by choosing the appropriate draw solution and its regeneration method (Zhao, et al., 2012; Elimelech, et al., 2011; Qin, et al., 2012; Elimelech, 2006).

Recent studies have demonstrated that membrane fouling in FO is relatively low (Achilli, et al., 2009), more reversible (Mi, et al., 2010) and can be minimized by optimizing the hydrodynamics (Lee, et al., 2010). Therefore, avoiding the additional costs required to clean the membrane by chemical cleaning agents (unlike RO) (Lee, et al., 2010). Additionally, a variety of contaminants can be effectively rejected via the FO process (Cartinella, et al., 2006; Cath, et al., 2010).

FO also has the potential to help achieve high water flux and high water recovery due to the high osmotic pressure gradient across the membrane. High water recoveries could help reduce the volume of desalination brine, which is a major environmental concern for current desalination plants, particularly for inland desalination (Zhao, et al., 2012).

Furthermore, in the fields of liquid food and pharmaceutical processing, FO has the advantage of maintaining the physical properties (e.g. colour, taste and aroma) of the feed without deteriorating its quality since the feed is not pressurized or heated (Jiao, et al., 2004; Yang, et al., 2009). For medical applications, FO can assist in the release of drugs with low oral bioavailability (e.g. poor solubility) in a controlled manner by osmotic pumps (Shokri, et al., 2008). Due to having such a diverse range of potential benefits, FO has been proposed for use and investigated in a variety of applications.

2.2. System thermodynamics

The mathematical description of permeation in membranes is based in thermodynamics, that the driving forces of pressure, temperature, concentration, and electromotive force are interrelated and that the overall driving force producing movement of a permeant is the gradient in its chemical potential. So the flux, J_i, of component *i*, is described by

$$J_i = -L_i . \frac{d\mu_i}{dx} \qquad (3)$$

Where $^{d\mu_i}/_{dx}$ the gradient in chemical potential of component *i* and L_i is a coefficient of proportionality linking this chemical potential driving force with flux (Baker, 2000; Wijmans, et al., 1995). Restricting the chemical potential into driving forces generated only by concentration and pressure gradients, the chemical potential can be written as

$$d\mu_i = RTd\ ln(\gamma_i c_i) + \upsilon_i dp \qquad (4)$$

Where c_i is the molar concentration (mol.dml^{-3}) of component *i*, γ_i is the activity coefficient linking concentration with activity, *p* is the pressure, and v_i is the molar volume of component *i.* In incompressible phases, such as a liquid or a solid membrane, volume does not change with pressure. So equation (4) can be integrated with respect to concentration and pressure, giving

$$\mu_i = \mu_i^{\circ} + RT\, ln(\gamma_i c_i) + v_i(p - p_i^{\circ}) \qquad (5)$$

Where $\mu_i^{\circ}$is the chemical potential of pure i at reference pressure, p_i° (Wijmans, et al., 1995). In general the reference pressure, p_i° is defined as the saturation vapor pressure of i, $p_{i_{sat}}$.

To better describe the mechanism of permeation there are two models, the solution-diffusion model and the pore-flow model, which are illustrated in Figure 3. In the first model, the permeants dissolve in the membrane material and then diffuse through the membrane down a concentration gradient. The permeants are separated because of the differences in solubilities of the materials in the membrane and the differences in the rates at which the materials diffuse through the membrane. And in the second model, the permeants are transported by pressure-driven convective flow through tiny pores. Separation occurs because one of the permeants is excluded (filtered) from some of the pores in the membranes through which other permeants move (Baker, 2000; Wijmans, et al., 1995).

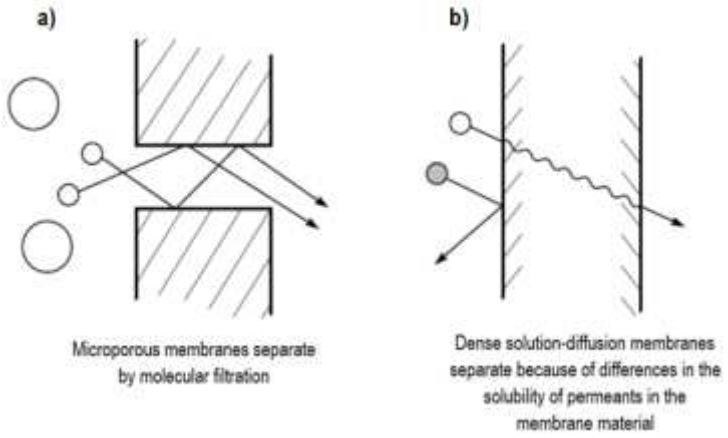

Figure 3- Molecular transport through membranes can be described by a flow through permanent pores (a) or by the solution-diffusion mechanism (b) (Baker, 2000)

These two models differ in the way the chemical potential gradient in the membrane phase is expressed. In the case of the solution-diffusion model, it is assumed that the pressure within a

membrane is uniform and that the chemical potential gradient across the membrane is expressed only as a concentration gradient. And in the case of the pore-flow model, the concentration of solvent and solute within the membrane are uniform and that the chemical potential gradient across the membrane is expressed only as pressure gradient (Wijmans, et al., 1995).

The solution-diffusion model was previously proven to have a good agreement between theory and experiment to describe the water transport in FO and RO (Wijmans, et al., 1995). To define this model, two assumptions have to be made. The first one is that the fluids on either side of the membrane are in equilibrium with the membrane material at the interface. The second assumption is that the pressure within the membrane is uniform (at a high pressure value, p_0) and the chemical potential gradient across the membrane is expressed only as a smooth gradient in solvent activity $\gamma_i c_i$ (as shown in Figure 4).

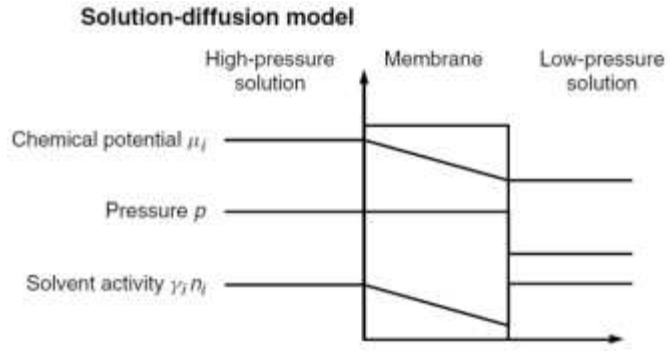

Figure 4- Pressure driven permeation of one-component solution through a membrane according to the solution-diffusion transport model, where $c_i = m_i \rho n_i$ (Baker, 2000)

Therefore, because no pressure gradient exists within the membrane, the water flux in the FO and RO processes can be described in terms of chemical potential by forces only generated by concentration, as it is shown in Figure 5.

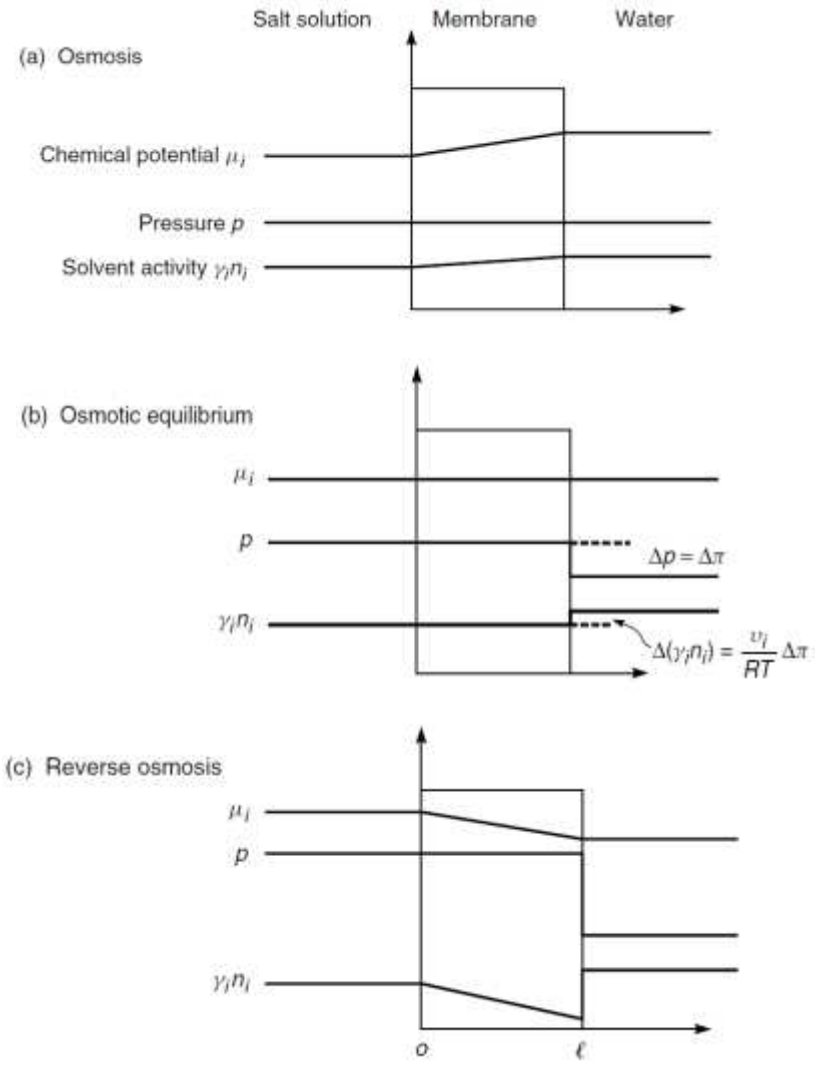

Figure 5 - Chemical potential, pressure, and solvent activity profiles through an osmotic membrane following the solution-diffusion model. The pressure in the membrane is uniform and equal to the high-pressure value, so the chemical potential gradient within the membrane is expressed as concentration gradient (where $c_i = m_i \rho n_i$) (Baker, 2000)

So the flux of component i (J_i) can be described by the following equation:

$$J_i = -\frac{RTL_i}{c_i} \cdot \frac{dc_i}{dx} \quad (6)$$

Where, R is the ideal gas constant, T is the temperature, and L_i is a coefficient of proportionality linking this chemical potential driving force. Equation (6) has the same form as Fick's Law, in which the term RTL_i/c_i can be replaced by the diffusion coefficient, D_i. So integrating over the thickness of the membrane gives

$$J_i = \frac{D_i(c_{i_{o(m)}} - c_{i_{l(m)}})}{l} \qquad (7)$$

In order, to achieve a general equation describing the water transport in the RO and FO processes, from the definition of chemical potential, it is assumed that the fluids on either side of the membrane are in equilibrium with the membrane material at the interface. Thus, equating the chemical potential in the solution and membrane phase at the feed-side interface of the membrane, gives

$$\mu_{i_0} = \mu_{i_{0(m)}} \quad (8)$$

Substituting the expression for the chemical potential, from equation (5), gives

$$\mu_i^{\circ} + RT\ln\left(\gamma_{i_0}^L c_{i_0}\right) + v_i\left(p_0 - p_{i_{sat}}\right) = \mu_i^{\circ} + RT\ln\left(\gamma_{i_{0(m)}} c_{i_{(m)}}\right) + v_{i_{0(m)}}\left(p_0 - p_{i_{sat}}\right) \quad (9)$$

Which leads to

$$\ln\left(\gamma_{i_0}^L c_{i_0}\right) = \ln\left(\gamma_{i_{0(m)}} c_{i_{(m)}}\right) \quad (10)$$

And thus

$$c_{i_{0(m)}} = \frac{\gamma_{i_{0(m)}}^L}{\gamma_{i_{0(m)}}} c_{i_0} \qquad (11)$$

Hence, defining a sorption coefficient K_i^L as

$$K_i^L = \frac{\gamma_{i_0}}{\gamma_{i_{0(m)}}} \quad (12)$$

Equation (11) becomes

$$c_{i_{0(m)}} = K_i^L . c_{i_0} \qquad (13)$$

In the RO process, a pressure difference exists at the permeate interface from p_0 within the membrane to p_l in the permeate solution. Thus, equating the chemical potentials across this interface obtains

$$\mu_{i_l} = \mu_{i_{l(m)}} \quad (14)$$

Substituting as before, for the chemical potential of an incompressible fluid, it leads to

$$\ln\left(\gamma_{i_l}^L c_{i_l}\right) = \ln\left(\gamma_{i_{l(m)}}^L c_{i_{l(m)}}\right) + \frac{v_i(p_0 - p_l)}{RT} \quad (15)$$

Rearranging and substituting for the sorption coefficient, K_i^L, gives the expression

$$c_{i_{l(m)}} = K_i^L . c_{i_l} . exp\left[\frac{-v_i(p_0 - p_l)}{RT}\right] \qquad (16)$$

The expressions for the concentrations within the membrane at the interface in equations (13) and (16) can now be substituted into the Fick's Law expression, equation (7), to yield

$$J_i = \frac{D_i K_i^L}{l}\left\{c_{i_0} - c_{i_l} exp\left[\frac{-v_i(p_0 - p_l)}{RT}\right]\right\} \qquad (17)$$

This equation can be simplified assuming that the membrane as high permeability, so $D_i . K_i^l / l \gg D_j . K_j^l / l$ (j refers to the salt component). Consider first, the water flux at the point which the applied hydrostatic pressure balances the water activity gradient (osmotic equilibrium, Figure 5 C) the flux of water across the membrane is zero. So equation (17) becomes

$$J_i = \frac{D_i K_i^L}{l}\left\{c_{i_0} - c_{i_l} exp\left[\frac{-v_i(p_0 - p_l)}{RT}\right]\right\} \qquad (18)$$

And thus:

$$c_{i_l} = c_{i_0} exp\left[\frac{v_i(\Delta\pi)}{RT}\right] \qquad (19)$$

At hydrostatic pressures higher than $\Delta\pi$, equations (17) and (19) can be combined to yield

$$J_i = \frac{D_i K_i^L c_{i_0}}{l}\left\{1 - exp\left[\frac{-v_i(\Delta p - \Delta\pi)}{RT}\right]\right\} \qquad (20)$$

A trial calculation shows that the term $-v_i(\Delta p - \Delta\pi)/RT$ is small under the normal RO conditions. So it can be used the simplification $1 - \exp(x) \to x$ as $x \to 0$ and the equation (20) becomes

$$J_i = \frac{D_i K_i^L c_{i_0} v_i(\Delta p - \Delta\pi)}{lRT} \quad (21)$$

This equation can be simplified, giving the general equation that describes the water transport in FO and RO:

$$J_w = A.(\Delta P - \Delta\pi) \quad (22)$$

Where J_w is the water flux, A the water permeability constant of the membrane and ΔP is the applied pressure. But, in the case of FO, ΔP is zero, and the driving force only depends on $\Delta\pi$. So for the FO process, the water flux is defined by

$$J_w = A.\Delta\pi \quad (23)$$

The water permeability constant (A) is dependent on the semipermeable membrane thickness, solubility of water into the membrane and diffusivity of water within the membrane (Kim, et al., 2008).

A simplified equation for the salt flux, J_s, through the membrane also, can be derived, starting with the equivalent equation (17), giving

$$J_S = B.(C_{s0} - C_{sl}) \qquad (24)$$

Where B is the salt permeability constant ($B = \frac{D_S K_S^L}{l}$).

From equations (23) and (24), the ratio between J_s/J_w can be derived to give the following relationship (where $\Delta\pi = n.\varphi.R.T$) (Xiao, et al., 2011):

$$\frac{J_S}{J_w} = \frac{B}{A}.\frac{1}{n.\varphi.R.T} \qquad (25)$$

This relationship demonstrates that the J_s/J_w ratio is directly dependent on the membrane separation characteristics (B/A) for a given operating condition ($n.\varphi.R.T \sim$ constant).

From this application of the solution-diffusion model, it can be obtained a measure of the ability of the membrane to separate the salt form the feed solution, the rejection coefficient, R, which is defined as

$$R = \left(1 - \frac{c_{S_l}}{c_{S_0}}\right).100\% \qquad (26)$$

2.3. Concentration polarization and fouling in osmotic processes

The main problem in membrane processes is the decline of flux as a function of filtration time due, most importantly, to concentration polarization (remaining constant once established) and membrane fouling (worsening as a function of time). They cause extra resistances on top of the membrane resistance and thus slow down the transport. These phenomena's are illustrated on Figure 6. Fouling refers to the accumulation of retained molecules or particles in the pores of the membrane or at the membrane surface. Concentration polarization (CP) refers to the effect of the build up of solute on the membrane surface (on the feed side) causing a diffusive solute flux from the membrane surface towards the feed, forming a kind of "dynamic" membrane, creating an extra resistance (Crespo, et al., 2005).

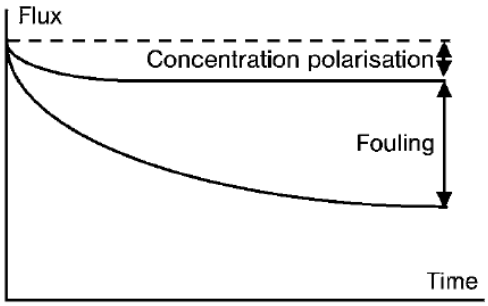

Figure 6- Flux decrease as function of time due to the combined effect of fouling and concentration polarization (Crespo, et al., 2005)

In the FO process, problems can occur on both sides of the membrane due to CP, so it is required special membranes for these processes. Consequently membranes with a conventional asymmetric structure (active layer on a porous support layer), can suffer from two types of CP phenomena, external CP and internal CP. Both of them can be manifested as a dilutive or concentrative CP (Cath, et al., 2006; Chou, 2010). Generally, external CP occurs at the surface of the active layer of the membrane and internal CP occurs within the porous support layer of the membrane (Zhao, et al., 2012).

a. External concentration polarization

As in pressure-driven membrane processes, external CP in FO occurs at the surface of the membrane active layer. The difference is that only concentrative external CP can take place in a pressure-driven membrane process (e.g. RO), while both concentrative and dilutive external CP may occur in an osmotically driven membrane process depending on the membrane orientation. The solute build up on the membrane active layer surface, due to the feed solution, is called concentrative external CP. Simultaneously, the draw solution in contact with the permeate side of the membrane is being diluted at the permeate-membrane interface by the permeating water. This is called dilutive external CP. Both of the phenomena reduce the effective osmotic driving force and the water flux. The undesirable effect of external CP can be minimized by increasing flow velocity and turbulence at the membrane surface (Cath, et al., 2006; Liu, et al., 2009; McCutvheon, et al., 2006).

Knowing the overall effective osmotic driving force is important to determine the flux performance in FO. Therefore is important to determine the concentration of the feed/draw on the membrane surface. In the case of concentrative external CP is necessary to quantify the feed at the active layer surface. This is not an easily measurable quantity, though it can be calculated from experimental data using boundary layer film theory (McCutcheon, et al., 2006). Determining the membrane surface concentration begins with the calculation of the Sherwood number for the appropriate flow regime. In general, the Sherwood (Sh) number is related to the Schmidt (Sc) and Reynolds (Re) numbers as follows (McCutcheon, et al., 2006; McCutvheon, et al., 2006; Baker, 2000; Mulder, 1996; Cath, et al., 2012):

$$Sh = a.Re^{b}Sc^{c}.\left(\frac{d_h}{L}\right)^{d} \quad (27)$$

Where, d_h is the hydraulic diameter (depends on the geometry of the system) and L is the length of the channel. The values a, b, c, d depend on the system geometry, type of fluid (Newtonian and non-Newtonian) and flow regime. The mass transfer coefficient, k, is related to Sh by

$$k = \frac{Sh.D_S}{d_h} \quad (28)$$

Where D_s is the solute diffusion coefficient. The mass transfer coefficient is then used to calculate what is called the concentrative external CP modulus:

$$\frac{\pi_{F,m}}{\pi_{F,b}} = exp\left(\frac{J_w}{k_F}\right) \quad (29)$$

Where J_w is the experimental permeate water flux, k_F is the mass transfer coefficient on the feed side, and $\pi_{F,m}$ and $\pi_{F,b}$ are the osmotic pressures of the feed solution at the membrane surface and in the bulk, respectively.

In the case of dilutive external CP, the modulus can be defined as above, except that in this case, the membrane surface concentration of the draw solute is less than that of the bulk:

$$\frac{\pi_{D,m}}{\pi_{D,b}} = exp\left(-\frac{J_w}{k_D}\right) \qquad (30)$$

Here, $\pi_{D,m}$ and $\pi_{D,b}$ are the osmotic pressures of the draw solution at the membrane surface and in the bulk, respectively.

To model the flux performance of the FO process in the presence of external CP, some corrections has to be made to $J_w = A.(\Delta P - \Delta\pi)$(22equation (23). This equation predicts flux as a function of driving force, without taking into account the concentrative or dilutive external CP, which may be valid only if the permeate flux is very low. When flux rates are higher, this equation must be modified to include both the concentrative and dilutive external CP (McCutcheon, et al., 2006):

$$J_w = A\left[\pi_{D,b}.\exp\left(-\frac{J_w}{k_D}\right) - \pi_{F,b}.exp\left(\frac{J_w}{k_F}\right)\right] \qquad (31)$$

However, no dense symmetric membranes are in use today for osmotic processes, due to the low hydraulic pressure used in FO. So, membrane fouling caused by external CP, has milder effects on water flux, comparing with the effects on pressure-driven membrane processes (Cath, et al., 2006; Gray, et al., 2006; McCutvheon, et al., 2006). Therefore the usefulness of this particular flux model is limited.

b. Internal concentration polarization

When a composite or asymmetric membrane consisting of a dense separating layer and a porous support is used in FO, two phenomena can occur depending on the membrane orientation. If the porous support layer of the asymmetric membrane faces the feed solution, a polarized layer is established along the inside of the dense active layer as water and solute propagate the porous support layer. This phenomenon, referred to as concentrative internal concentration polarization (illustrated in Figure 7 (b)), is similar to concentrative external CP, except that takes place within the porous layer. If the membrane is run in the opposite orientation (active layer of the membrane facing the feed solution and the porous support layer

facing the draw solution), when the water permeates the active layer, the draw solution within the porous substructure becomes diluted. This phenomenon is called dilutive internal CP (illustrated in Figure 7 (c)). These phenomena cannot be controlled by cross-flow since they occur within the membrane structure (McCutvheon, et al., 2006).

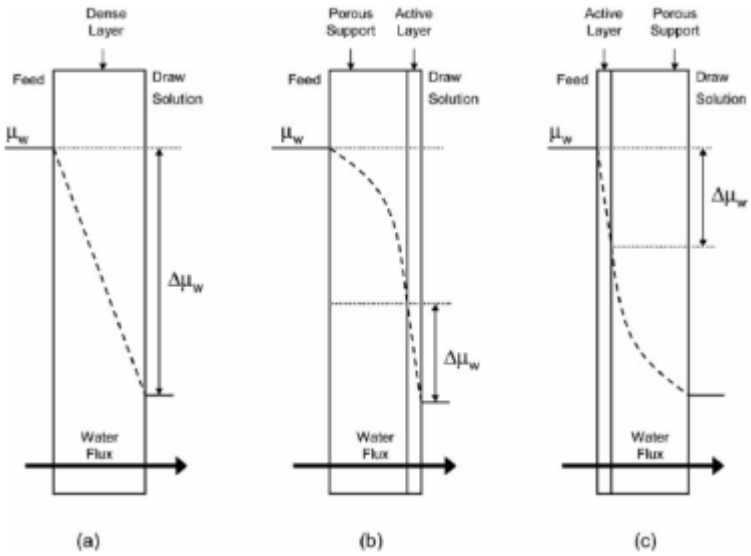

Figure 7 – Illustrations of driving forces profiles, expressed as water chemical potential, μ_w, for osmosis several membrane types and orientations. (a) A symmetric dense membrane. (b) An asymmetric membrane with the porous support layer against the feed solution; the profile illustrates concentrative internal CP. (c) An asymmetric membrane with the dense layer against the feed solution; the profile illustrates dilutive internal CP. The actual (effective) driving force is represented by $\Delta\mu_w$. External CP effects on the driving force are assumed to be negligible in this figure (McCutvheon, et al., 2006)**.**

From Figure 8, it can be seen that the osmotic pressure difference between the bulk feed and bulk draw solution ($\Delta\pi_{bulk}$) is higher than the osmotic pressure difference across the membrane ($\Delta\pi_m$) due to external CP and that the effective osmotic pressure driving force ($\Delta\pi_{eff}$) is even lower due to internal CP (Loeb, et al., 1973).

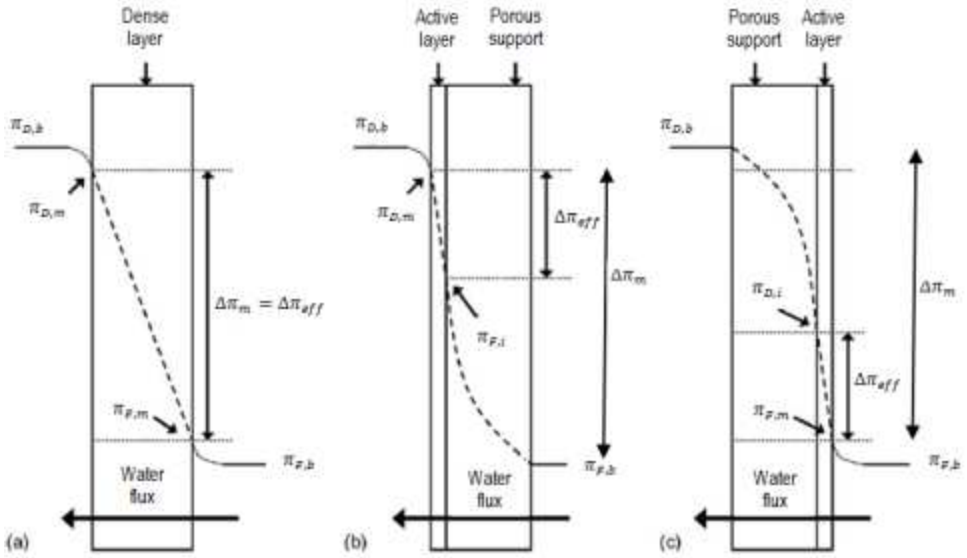

Figure 8- Illustration of osmotic driving force profiles for osmosis through several membrane types and orientations, incorporating both internal CP and external CP. (a) Symmetric dense membrane; the profile illustrates concentrative and dilutive external CP. (b) An asymmetric membrane with the dense active layer against the draw solution (PRO mode); (c) An asymmetric membrane with the porous support layer against the draw solution (FO mode); the profile illustrates dilutive internal CP and concentrative internal CP. Key: $\pi_{D,b}$ is the bulk draw osmotic pressure, $\pi_{D,m}$ is the membrane surface osmotic pressure on the draw side, $\pi_{F,b}$ is the bulk feed osmotic pressure, $\pi_{F,m}$ is the membrane surface osmotic pressure on the feed side, $\pi_{F,i}$ is the effective osmotic pressure of the feed in PRO mode, $\pi_{D,i}$ is the effective osmotic pressure of the draw solution in FO mode, $\Delta\pi_m$ is the osmotic pressure difference across the membrane, and $\Delta\pi_{eff}$ is the effective osmotic driving force (McCutcheon, et al., 2006)

The water and solute flux in a FO process can be modelled by coupling the solution-diffusion model with the diffusion-convection transport in the membrane support layer (Tang, et al., 2010; McCutcheon, et al., 2006). So, considering the PRO configuration, and applying the solution-diffusion model to the active layer, gives equation (23)$J_w = A.(\Delta P - \Delta\pi)$ (22) for the water flux (J_w), and equation (24) for the salt flux. Both equations considered the difference in concentration/osmotic pressure between the draw solution and the interface of FO support layer and active layer. For the solute transport in the support layer, the transport of solute into the support by convection ($J_w C$) and that due to the solute back-transport through the rejection layer (J_s) have to be balanced by the solute diffusion away from the support:

$$J_w C + J_s = D_{eff}\frac{dC}{dx} \qquad (32)$$

Where C is the solute concentration in the porous support layer at a distance x away from the interface between the rejection layer and the support layer, and D_{eff} is the effective diffusion

coefficient of solute. In a porous support layer with a porosity of ε, D_{eff} is related to the solute diffusion coefficient D by $D_{eff} = D\varepsilon$. The boundary conditions for equation (32) are:

- $x = 0$, $C = C_{support}$
- $x = l_{eff} = l\tau$

Where l is the actual thickness of the FO support layer, l_{eff} is the effective thickness of the support layer, and τ is the tortuosity of the support layer. Solving equation (32), substituting J_w and J_s with the equations obtained from the solution-diffusion model, gives:

$$\ln\left(\frac{C_{support}+B(C_{draw}-C_{support})/A(\pi_{draw}-\pi_{support})}{C_{feed}+B(C_{draw}-C_{support})/A(\pi_{draw}-\pi_{support})}\right) = \frac{J_w}{k_m} \qquad (33)$$

Where k_m is the effective mass transfer coefficient, which takes into account the impact that the porous support layer has on mass transfer, and it is given by

$$k_m = \frac{D_{eff}}{l_{eff}} = \frac{D}{\tau^{l}/_{\varepsilon}} = \frac{D}{S} \qquad (34)$$

Where S is the structural parameter, analogous to the boundary layer thickness for external CP in a typical reverse osmosis process, which is given by

$$S = \frac{\tau l}{\varepsilon} \quad (35)$$

Assuming that the osmotic pressure of a solution is proportional to its concentration, equation (33) can be simplified to:

$$\ln\left[\frac{\pi_{support}+{}^{B}/_{A}}{\pi_{feed}+{}^{B}/_{A}}\right] = \frac{J_w}{k_m} \qquad (36)$$

Where the $\pi_{support}$ can be determine by equation (23). Therefore,

$$J_w = k_m \ln\left(\frac{A\pi_{draw} - J_w + B}{A\pi_{feed} + B}\right) \qquad (37)$$

For the FO configuration, the flux equation can be similarly derived, giving:

$$J_w = k_m \ln\left(\frac{A\pi_{draw} + B}{A\pi_{feed} + J_w + B}\right) \qquad (38)$$

c. Membrane fouling

Like CP, membrane fouling is also an important and inevitable phenomenon in all membrane processes. Lower membrane fouling implies more product water, less cleaning and longer membrane life, thereby reducing operational and capital costs. However, membrane fouling in osmotically driven membrane processes is different from that in pressure-driven membrane processes due to low hydraulic pressure being employed in the former processes.

Membrane fouling in FO was primarily studied by Cath et al. (Cath, et al., 2005; Cath, et al., 2005), which reported that FO might have the potential of low membrane fouling since no sign of flux reduction due to fouling was observed in their studies. Lately FO has been used in OMBR for wastewater treatment mainly due to its low fouling and low energy consumption (Achilli, et al., 2009), which are the two major problems of membrane bioreactors. Achilli et al. (Achilli, et al., 2009) tested a submerged OMBR to treat domestic wastewater, with long-term (up to 28 days) experiments, the results showed that the water flux decline was mainly caused by membrane fouling. However, the flux could be recovered to approximately 90% of the initial value though osmotic backwashing. This indicates that membrane fouling does exist in FO, becoming obvious in long-term operation.

Furthermore, membrane fouling in FO and RO has been compared and is thought to be quite different from one another in terms of reversibility and water cleaning efficiency (Zhao, et al., 2012). Lee et al. (Lee, et al., 2010) observed that membrane fouling in FO is almost completely reversible while it is irreversible in RO. However, they attributed FO fouling to the accelerated cake-enhanced osmotic pressure (CEOP) due to reverse salt diffusion from the

draw solution (illustrated in Figure 9). When the draw solution is facing the membrane support layer, the draw solute accumulates at the surface of the active layer through reverse diffusion, enhancing the CP layer and reducing the net osmotic driving force. A draw solute with a smaller hydrated radius (e.g. NaCl) is more readily to cause CEOP compared with one with larger hydrated radius (e.g. dextrose) (Zhao, et al., 2012). Also, it was reported that FO fouling can be significantly minimized by increasing the cross flow velocity (Lee, et al., 2010).

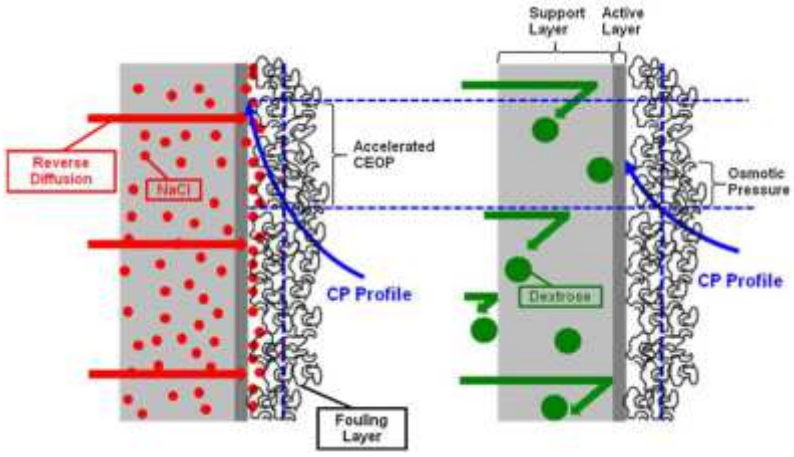

Figure 9 – A conceptual illustration of the effect of draw solute reverse diffusion on cake-enhanced osmotic pressure (CEOP) in FO for different draw solutions: a) NaCl and B) dextrose (Lee, et al., 2010)

Both, CP and membrane fouling are critical inevitable phenomena in FO processes because they increase the extra resistance of the membrane and thus reduce the overall membrane permeability. So to improve FO performance, it is necessary to understand these mechanisms.

2.4. Reverse solute diffusion

The reverse diffusion of solute from the draw solution through the membrane to the feed solution is also inevitable in osmotically driven membrane processes, due to the concentration differences. Hancok and Cath (Hancock, et al., 2009) suggested that the reverse diffusion of the draw solute have significant implications on the performance and sustainability of the FO process. Recent studies have correlated the reverse diffusion of the draw solute to membrane fouling. Lee et al. (Lee, et al., 2010) have demonstrated that reverse solute diffusion accelerate

CEOP and increase the fouling layer resistance. Therefore, multivalent ion solutions with lower diffusions coefficients may be preferable in some specific applications in which high rejection is desired (Zhao, et al., 2012). However, some multivalent ions (e.g. Ca^{2+} and Mg^{2+}) may interfere with the foulants in the feed solution after reverse diffusion, which is likely to aggravate membrane fouling (Zou, et al., 2011). Also, multivalent ion solutions may also introduce more severe internal CP because of their large ion sizes and lower solution diffusion coefficients (Zhap, et al., 2011). This solute transport is determined by the selectivity of the membrane active layer, but is independent of the draw solution concentration and the structure of the membrane support layer (Philip, et al., 2010). This finding has significant implications as it poses another criterion for the development of a new membrane: high selectivity of the membrane active layer. Furthermore, employing a multivalent ion solution as the draw solution may minimize the reverse solute diffusion and thus reduce membrane fouling, but the resultant higher internal CP and the potentially increased risk of fouling must be considered carefully. Overall, reverse solute diffusion has been one of the challenges in osmotically driven membrane processes and it should be fully considered and minimized in the developments/design of both FO membranes and draw solute (Zhao, et al., 2012).

2.5. Draw solutions

The osmotic pressure difference is the driving force in the FO process. So, the selection of optimal osmotic agents is one of the key factors for a higher water flux. The main criterions to select a suitable draw solution are as follows: the solute must have a high osmotic efficiency, namely high solubility in water and relatively low molecular weight, which can lead to high osmotic pressures; osmotic agents should ideally be inert, stable, neutral or near neutral pH, and non-toxic; solute must also be easily and inexpensively separated to yield potable water, without being consumed in the process (i.e., minimal reverse draw solute diffusion) which may lower the replenishing cost. Moreover, the draw solutions should not degrade the membrane chemically or physically (Liu, et al., 2009; Ge, et al., 2011). In particular, the last requirements

are crucial for the viability of the process at the municipal scale, and have direct consequence on the operating costs of a FO plant (Qin, et al., 2012).

Figure 10 shows the daily amount of draw solute that needs to be replenished for a FO process due to loss through the membrane for three different J_s/J_w scenarios. Current FO membranes could achieve J_s/J_w down to around 0.1 g.L^{-1} for NaCl (Scenario B), which means that a municipal scale FO plant with the capacity of 100000 m^3.d^{-1} will lose 10000 kg of NaCl on a per day basis, which need replenishment. From a logistics point of view, Scenario C needs no further consideration for a municipal scale FO plant, whereas Scenario A is technically not yet achievable with current FO membranes and for NaCl as the draw solute (Qin, et al., 2012).

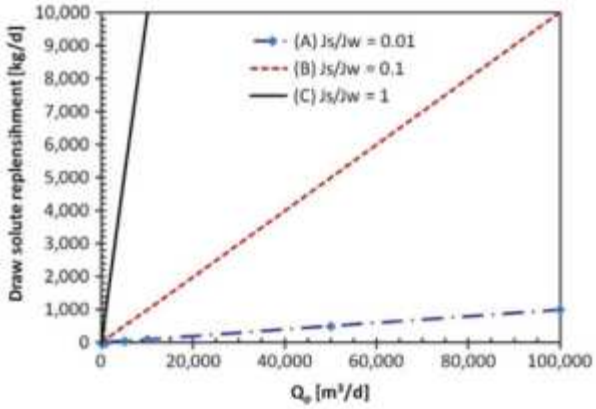

Figure 10- Daily requirement of draw solute replenishment (kg/d) as function of water production (m^3/d) derived based on equation (25) for the three scenarios: (A) J_s/J_w=0.01 g.L^{-1}; (B) J_s/J_w=0.1 g.L^{-1}; and (C) J_s/J_w=1 g.L^{-1} (Qin, et al., 2012)

Another way of evaluation is to consider the additional operating costs to a FO desalination plant due to the replenishment for the lost draw solutes for scenarios of various draw solute cost and J_s/J_w Table 3 show different scenarios, with a range of draw solutes prices and a range of J_s/J_w ratios. Typically, costs for various types of draw solutes range between \$10.kg^{-1} and \$100.kg^{-1} (Lee, et al., 2010), such that commonly available chemicals such as NaCl may be represented by the \$10 per kg cost range, whereas other more specialized chemicals may be represented by the \$100 per kg costs range. It is also assumed that specific low cost draw solute at the \$1 per kg cost range will be developed in the future.

Table 3 – Additional operating costs to a FO desalination plant for replenishment of lost draw solutes (Qin, et al., 2012)

Draw solute cost		J_s/J_w		
		(A) J_s/J_w=0.01 g.L^{-1}	**(B) J_s/J_w=0.1 g.L^{-1}**	**(C) J_s/J_w=1 g.L^{-1}**
1.	1\$.kg^{-1}	**0.01 \$.m^{-3}**	**0.1 \$.m^{-3}**	1 \$.m^{-3}
2.	10 \$.kg^{-1}	**0.1 \$.m^{-3}**	1 \$.m^{-3}	10 \$.m^{-3}
3.	100\$.kg^{-1}	1 \$.m^{-3}	10 \$.m^{-3}	100 \$.m^{-3}

The range of desalination cost for a municipal scale plant (size > 60000 m^3.d^{-1}) is typically 0.5-1\$ per m^3 of water produced (Karagiannis, et al., 2008). On the basis that the additional operating cost due to replenishment for lost draw solutes should not exceed 10-20% of the desalination cost for a municipal scale FO plant, a practical cost limit for draw solute replenishment may be set as 0.1\$.m^{-3} (i.e. scenario I-(A), I-(B) and II-(A)) (Qin, et al., 2012). Can be concluded that the economical viability of a municipal scale FO desalination plant it is not achieved by using expensive draw solute with very low J_s/J_w (i.e. scenario III-(A)); neither with a low-cost draw solute with high J_s/J_w (i.e. I-(C)). The discussion here makes clear that both J_s/J_w and draw solute cost are crucial factors for selecting an appropriate draw solution for FO application.

The draw solutions can be composed of different types of solutions and mixtures, like salt solutions with different concentrations (some examples are showed in Figure 11; also seawater, Dead seawater and Salt Lake water), mixtures of water and another gas (e.g. sulphur dioxide) or liquid (e.g. aliphatic alcohols), mixture of gases (e. g. ammonia and carbon dioxide gases) (McGinnis, et al., 2006), 2-methylimidazole, sodium salts of polyacrylic acid (PAA-Na) (Ge, et al., 2011), albumin, dendrimers with sodium ions attached to the surface (Adham, et al., 2007), urea, ethylene glycol (Young, et al., 2011), dextrose (Gray, et al., 2006; Lee, et al., 2010), ethanol, fructose solution (Kim, et al., 2011), glucose solution, and, glucose and fructose solution (Cath, et al., 2006; Chay). More specifically for fruit juice concentration application, also can be used as draw solution, glycerol, cane molasses and corn syrup (Jiao, et al., 2004). In a new nanotechnological approach, naturally non-toxic magnetoferritin is tested as a naturally non-toxic solute for draw solutions, which can be rapidly separated from aqueous streams using a magnetic field (Cath, et al., 2006; Liu, et al., 2009).

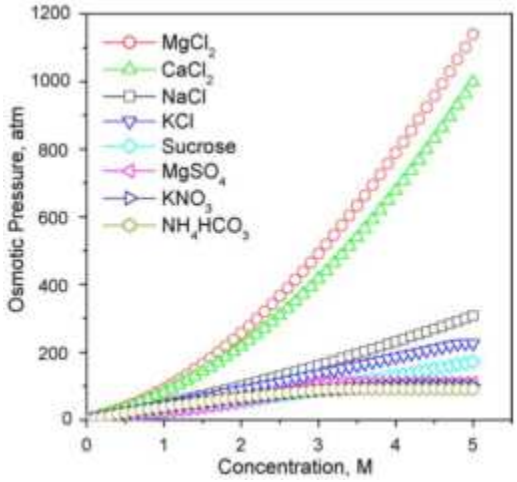

Figure 11 - Osmotic pressures as a function of solution concentration at 25º C for various potential draw solutions. Data were calculated using OLI Stream Analyzer 2.0 (Cath, et al., 2006)

a. Permeate recovery

Different types of draw solute have been studied in the past four decades and so, the processes to separate the draw solution from the permeate differs widely. This process should achieve high recovery of the draw solution (to minimize losses), be affordable, and be able to produce high-quality product water (Achilli, et al., 2010). In this section some of the processes already tested will be described.

Batchelder in 1965 (Batchelder, 1965), suggested the permeate recovery from the draw solution (sulphur dioxide) by heated gas stripping operation in which the heated draw solution would pass in counter-current with warm air in a stripping column. Such operation could be operated at 66 ºC to 88 ºC.

In the same year, Glew (Glew, 1965), used the process of distillation to recover the permeate from the draw solution (sulphur dioxide).

Frank in 1972 (Frank, 1972), recovered the permeate from the aluminium sulphate draw solution by using a chemical precipitating agent, calcium hydroxide.

In 1992, Yaeli (Yaeli, 1992) used a low pressure reverse osmosis process to remove the permeate from a glucose draw solution.

McGinnis in 2002 (McGinnis, 2002), suggested a two-stage FO process that relies on the use of draw solutes having high temperature dependence solubilities such as potassium nitrate (KNO_3) and sulphur dioxide (SO_2). In the first stage the pre-heated feed solution contact with

KNO_3 along a semi-permeable membrane. The permeate is recovered by cooling down the diluted draw solution in a heat exchanger by incoming seawater, which promotes the KNO_3 precipitation.

In 2005, McCutcheon et al. (McCutcheon, et al., 2005), recovered the permeate from ammonium bicarbonate draw solution by a moderate heating, in order to promote the decomposition of the dissolved salts into ammonia and carbon dioxide gases.

In the same year, Cath et al. (Cath, et al., 2005) suggested the use of osmotic distillation to separate the water from the NaCl draw solution.

Adham et al. in 2007 (Adham, et al., 2007), suggested to use magnetic nanoparticles as draw solution, the permeate was recovered by using a canister separator. Oriard et al. (Oriard, et al., 2007), also using the same draw solution, recovered the permeate by applying a magnetic field to the dilute draw solution.

The Adham Group (Adham, et al., 2007) also suggested the use of dendrimers as draw solution, which can be reconcentrated by using a wide range of pH values. This group tested as well albumin as draw solution to recover the permeate, the diluted draw solution was heated making the albumin solution denatured and solid.

2.6. Membrane types

Although the osmosis phenomenon was discovered in 1748 (Mulder, 1996), no progress on membrane development was made. Early studies focused on the mechanism of osmosis through natural materials. Special attention has been given to FO only with the development of synthetic membrane materials since the first Loeb-Sourirajan asymmetric cellulose acetate RO membrane with high flux and high salt rejection was developed in 1960's (see Appendix 1) (Qin, et al., 2012).

In general, any dense, non-porous, and selectively permeable material can be used as membrane for FO. Such flat sheet and hollow fiber membranes have been tried for various applications of FO in the past forty years (Cath, et al., 2006; Qin, et al., 2012).

Batchelder (Batchelder, 1965) in 1965 was the pioneer, using natural cellulose as membrane material. In the same year, Glew (Glew, 1965) used a cooper ferrocyanide membrane. Frank in 1972 (Frank, 1972) tested a homemade CA RO membrane and a CA flat sheet (RO-97) membrane from Eastman Chemical Products, Inc. to desalinate sea water. Votta et al. in 1974 (Votta, et al., 1974) and Anderson in 1977 (Anderson, 1977) tested several commercially available and an in-house CA RO membranes to treat dilute wastewater by FO using a simulated seawater draw solution. Kravath and Davis in 1975 (Kravath, et al., 1975) used a CA flat sheet RO membrane (KP 98) from Eastman and a CA hollow fiber from Dow to desalinate seawater by using glucose as draw solution. Goosens and Van-Haute in 1978 (Goosens, et al., 1978) investigated CA RO membranes reinforced with mineral fillers to evaluate whether the membrane under FO conditions can predict the properties under the RO conditions. However, performance of the membranes tested mentioned above were not explored. Mehta and Loeb in 1979 (Mehta, et al., 1979) investigated the performance of flat sheet DuPont B-9 membrane and hollow fiber B-10 Permasep RO membrane.

In the 1970's, there were no FO membranes available, only RO. So all studies involving osmosis (mostly PRO studies) used RO membranes, either flat sheet or tubular, and in all cases, researchers observed lower fluxes than expected. The flux reduction was due to the fact that RO membranes had a thick porous support which caused a very large internal CP (Loeb, et al., 1997).

In the 1990s, a special FO membrane with significant improvement in water flux was developed by Osmotek Inc. (now Hydratation Technologies Inc., HTI) (Salter, 2005). SEM images of this type of FO membrane are shown in Figure 12. The membrane is made of cellulose triacetate (CTA), the thickness is less than 50 μm and its structure is quite different from a standard RO membrane. A unique feature is its lack of thick support layer. Instead, the embedded polyester mesh provides mechanical support for the membrane.

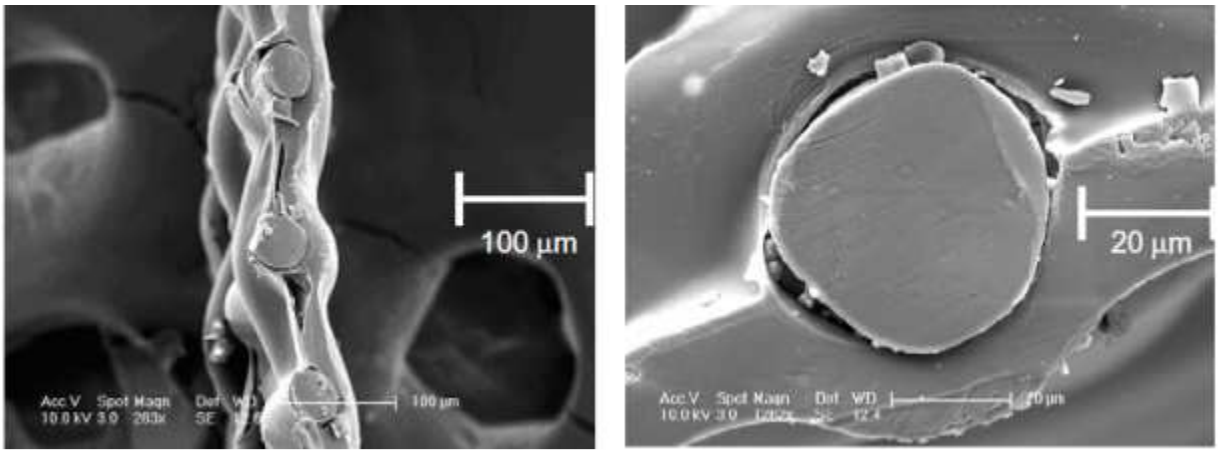

Figure 12 – SEM photographs of cross sections of forward osmosis (CTA) membrane of HTI's FO membrane. A polyester mesh is embedded between the polymer material for mechanical support. The membrane thickness is less than 50 µm, much thinner than the RO membranes used (McCutcheon, et al., 2005)**.**

The CTA-FO membrane from HTI has been successfully used in commercial applications has water purification for military emergency relief and recreational purposes (e.g. Hiker's backpack) (Salter, 2005). Results from various investigations are presented in Table 4.

Table 4 – FO performance of CTA-FO membrane from HTI

Year	Feed Solution	Draw solution	Orientation (towards)	J_W (LMH)	J_s (g.MH)	J_s/J_W ($g.L^{-1}$)	Ref.
2005	0.5 M NaCl	6 M NH_4HCO_3	Feed	23	-	-	(McCutcheon, et al., 2005)
2008	DIW	0.5 M NaCl	Feed	6.2	8.6	1.39	(Cornelissen, et al., 2008)
	DIW	0.5 M NaCl	Draw	8.5	7.4	0.87	(Cornelissen, et al., 2008)
2009	DDW (double deionised water)	0.5 M NaCl	Draw	10.0 (A) 6.5 (B) 4.0 (C)	11 (A) 4.0 (B) 0.1 (C)	1.1 (A) 0.61 (B) 0.025(C)	(Achilli, et al., 2009)
2010	DIW	0.6 M NaCl	Feed	9.6	7.2	0.74	(Lee, et al., 2010)
2011	DIW	1.0 M NaCl	Feed	15.8	12.18	0.45	(Zou, et al., 2011)
	DIW	1.0 M NaCl	Draw	26.8	19.07	0.711	(Zou, et al., 2011)

Currently, the FO membranes developed can be classified into three categories: phase inversion-formed membranes, thin film composite (TFC) membranes and chemically modified membranes (see Appendix 1) (Zhao, et al., 2012). The main configuration used is flat sheet, but since two cross-flow channels are required at both sides of the FO membrane, hollow fiber configuration is more suitable for FO desalination process, as one may simultaneously

induce/force flow on both sides of a hollow fiber membrane in a simpler manner (Qin, et al., 2012). In addition, hollow fiber membranes have the advantages of self-support and high packing density compared to flat sheet configuration (Qin, et al., 2012).

An overview of a few selected recent examples of membrane development for FO is given in Table 5.

So far, commercially available RO membranes and membranes based on celluloce triacetate (CTA), cellulose acetate (CA), polybenzimidazole (PBI) and aromatic polyamide have been developed for FO processes (Chung, et al., 2012).

Table 5- Recent FO membranes developed

Year	Membrane	Configuration	Draw solution	Feed solution	Orientation (Towards)	J_w (LMH)	J_s (g.MH)	J_s/J_w ($g.L^{-1}$)	Ref.
2008	TS80 NF Thin film composite	Flat sheet	1.5 M $MgSO_4$	DIW	Draw	1.1	-	-	(Cornelissen, et al., 2008)
2008	Asymmetric Cellulose Acetate	Flat sheet	0.5 M NaCl	Fresh water	Draw	1.3	-	-	(Gerstandt, et al., 2008)
2009	PBI-based dual layer NF	Hollow fiber	5.0 M $MgCl_2$	DIW	Feed	33.8	0.55	0.02	(Yanq, et al., 2009)
2009	Dual-layer (PBI-PES/PVP)	Hollow fiber	5.0 M $MgCl_2$	DIW	Draw	24.8	1.0	0.04	(Yanq, et al., 2009)
2010	Cellulose Acetate	Hollow fiber	2.0 M $MgCl_2$	DIW	Draw	7.3	0.53	0.07	(Su, et al., 2010)
2010	CA-double dense layer	Flat sheet	0.5 M $MgCl_2$	DIW	Top-DS Bottom-DS	40-80 30	-	-	(Wang, et al., 2010)
2010	Thin film composite polyamide	Hollow fiber	0.5 M NaCl	DIW	Feed Draw	A - 12.9 B - 32.2 A - 5.0 B - 14	A - 5.03 B – 3.54 A – 10.6 B – 24.5	A - 0.39 B - 0.11 A - 2.12 B - 1.75	(Wang, et al., 2010)
2010	Thin film composite polyamide	Flat sheet	1.5 M NaCl	DIW	Draw	18	-	-	(Yip, et al., 2011)
2011	Cellulose acetate/cellulose triacetate cast on a nylon fabric	Flat sheet	1.2 M $MgSO_4$	0.6 M NaCl	Draw	6.1-6.5	-	-	(Sairam, et al., 2011)
2011	Thin film composite polyamide	Flat sheet	5.0 M NaCl	DIW	Feed	69.8	-	-	(Wang, et al., 2012)
2011	PAI substrate treated by PEI	Positively charged hollow fiber	0.5 M $MgCl_2$	DIW	Feed	1%PEI – 8.36 2%PEI – 9.74	<0.4	-	(Setiawan, et al., 2011)
2011	PAN substrate, multiple PAH/PSS	Flat sheet	1.0 M $MgCl_2$	DIW	Feed	28	-	-	(Saren, et al., 2011)

	polyelectrolyte layers								
2011	PES/sulfonated polymer substrate, Polyamide active layer	Flat sheet	2.0 M NaCl	DIW	Feed	33.0	-	-	(Widjojo, et al., 2011)
2011	PSf support, polyamide active layer	Flat sheet	0.5 M NaCl	10 mM NaCl	Feed Draw	9.5 18.1	2.4 6.3	0.25 0.35	(Wei, et al., 2011)
2011	PES cast on PET fabric	Flat sheet	3.0 M NaCl	DIW	Draw	32	8.76	0.3	(Yu, et al., 2011)
2011	Cellulose ester	Flat sheet	2.0 M NaCl	DIW	Draw	CA – 7.7 CTA – 9.4 CAP – 7.6 CAB – 7.4	CA – 3.8 CTA – 12.5 CAP – 921.1 CAB – 1520	CA – 0.5 CTA – 1.3 CAP – 121.2 CAB – 205.4	(Zhang, et al., 2011)
2011	PES nanofiber support, polyamide active layer	Flat sheet	1.5 M NaCl	DIW	Feed	33.6	-	-	(Anon., 2011)
2012	PAI substrate treated by PEI	Positively charged flat sheet	0.5 M $MgCl_2$	DIW	Feed Draw	29.6 19.2	<0.8 <0.5	0.03	(Qiu, et al., 2012)

In summary, the desired characteristics of FO membranes are very thin and high dense skin layer for high water flux (high water permeability, A) and high solute rejection (low salt permeability, B); a thin substrate with maximum porosity for minimal internal CP (small mass transfer coefficient, k_m); hydrophilicity of the skin layer for reduction of membrane fouling; and tolerance to chemicals for cleaning and draw solution. Currently, only Hydration Technologies Inc. provides the commercially available CTA-FO membranes. However, these membranes do not meet the requirements for an ideal FO membrane; only have a narrow range of pH tolerance for cleaning, whereas other types of FO membranes are still at the stage of laboratory development. Further breakthrough in the development of improved FO membranes is critical for advancing the technology for seawater desalination (Qin, et al., 2012).

2.7. Membranes modules and devices

Different module configurations can be used to hold or pack membranes for FO. Laboratory-scale modules have been designed for use with either flat sheet or tubular/capillary (e.g. hollow fibers) membranes. Large-scale applications have been designed and built with flat sheet membranes in plate-and-frame configuration (Cath, et al., 2006). Other modules also referred, are spiral-wound and bag configuration (Cath, et al., 2006; Trent, et al., 2010; Loeb, 2002). Each configurations has advantages and limitations that must be taken into account when planning the research or developing the application. Primarily has to take into account the differences between continuous flow and batch operation.

In continuous flow FO applications, the draw solution is repeatedly reconcentrated/refreshed and reused. In this mode, the feed solution is recirculated on the feed side of the membrane and the reconcentrated/refresh draw solution is recirculated on the permeate side (see Figure 13). For this reason, modules that use flat sheet membranes are more complicated to build and operate for the FO process compared to pressure-driven processes. For example, in the case of the spiral-wound module, (one of the most common packing configurations in the membrane industry) cannot be used in its current design for FO because a liquid stream cannot be forced to flow on the support side (inside the envelope) (Cath, et al., 2006).

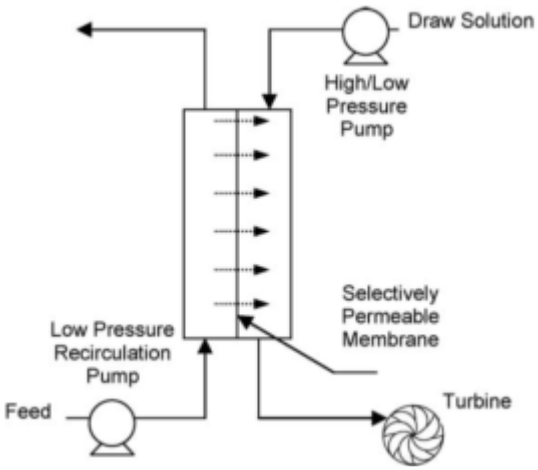

Figure 13 – Flows in FO and PRO processes. Feed water flows on the active side of the membrane and draw solution flows counter-currently on the support side of the membrane. In PRO, the draw solution is pressurized and is released in a turbine to produce electricity (Cath, et al., 2006)

In batch FO applications, the draw solution is diluted once and is not reconcentrated for further use. In this mode of operation, the device used for FO is most often disposable and is not reused. Applications using this mode of operation include hydration bags for water purification and osmotic pumps for drug delivery (Cath, et al., 2006; Kim, et al., 2008).

The generally available semi-permeable polymeric membranes are flat sheet membranes, even with their limitations. For continuous flow operation of an FO process, flat sheet membranes can be use either a plate-and frame configuration or in a unique spiral-wound configuration (Cath, et al., 2006).

a. Plate-and-frame

The simplest device for packing flat sheet membranes is a plate-and-frame module. In this configuration, the feed and the draw flow on opposite sides of a flat sheet membrane (see Figure 14) with a minimal total pressure applied on the membrane (Cath, et al., 2005). These modules can be constructed in different sizes and shapes ranging from lab-scale devices to full-scale systems. The main limitations of plate-and-frame elements for membrane applications are lack of adequate membrane support and low packing density. The lack of adequate membrane support limits the operation to a low hydraulic pressure and/or operation at similar pressures on both sides of the membrane (demanding for high process control). Low packing density leads to a larger system footprint, higher capital costs, and higher operating costs (labour for membrane replacement) (Cath, et al., 2006). Other limitations of this configuration include problems with internal and external sealing, difficult in monitoring membrane integrity, and limited range of operation conditions (for example: flow velocities and pressures) (Cath, et al., 2005).

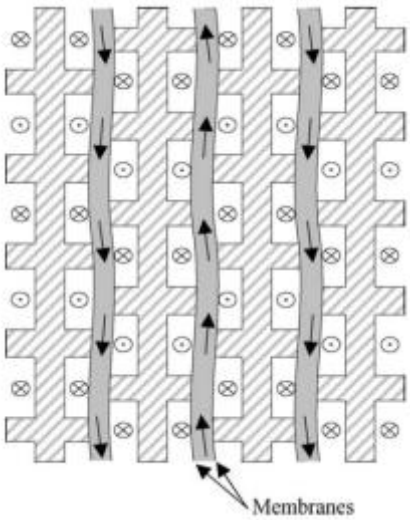

Figure 14 – Cross-section of plate-and-frame module, (⊙) Flow of the draw in one direction; (⊗) Flow of draw in the other direction; gray area – flow of the feed; Cross-hatched area – polycarbonate areas (Cath, et al., 2005)

b. Spiral wound

The commercially available spiral-wound membrane elements are only for RO applications. This configuration operates with only one stream (the feed stream) flowing under direct control of its flow velocity tangential to the membrane (see Figure 15). The permeate stream flows very slowly in the channel formed by the two glued membranes and its composition and flow velocity are controlled by the properties of the membrane and the operating conditions. So, for this design, it cannot operate in FO mode (active layer facing the draw solution) because the draw solution cannot be forced to flow inside the envelope formed by the membranes (Cath, et al., 2006).

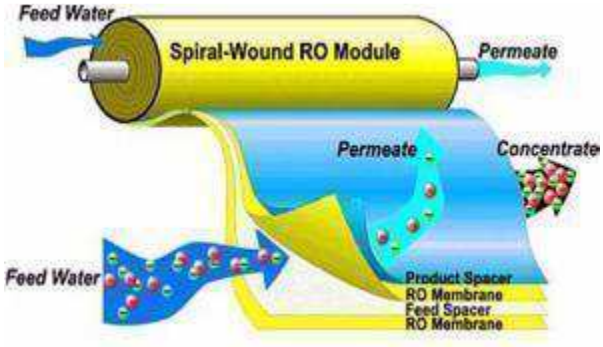

Figure 15- Schematic representation of a RO spiral-wound module[1]

[1] http://www.water-technology.net/projects/perth/perth4.html

Mehta (Mehta, 1982) produced an exclusive spiral-wound module for FO, where both outside-in and inside-out operation can be used. This element is only efficient for PRO applications. The module has four ports and is different from the regular module used in RO, which have only three ports (see Figure 16). The four port configuration allows for independent flow control on the two sides of the membrane, but due to design limitations the hydraulic pressure difference across the membrane cannot be higher than 25 atm. The draw solution flows through the spacers and between the rolled membranes, in the same way that a feed stream flows in a spiral-wound element for RO. However, unlike RO modules, the central collecting tube is blocked halfway though so that the feed solution cannot flow to the other side. Instead, an additional glue line at the centre of the membrane envelope provides a path for the feed to flow inside the envelope. In this configuration, the feed flows into the first half of the perforated central pipe, is then forced to flow into the envelope, and then flows out through the second half of the perforated central pipe. The draw solution outside of the envelope can be pressurized similar to the way it is done in spiral-wound membrane elements for RO.

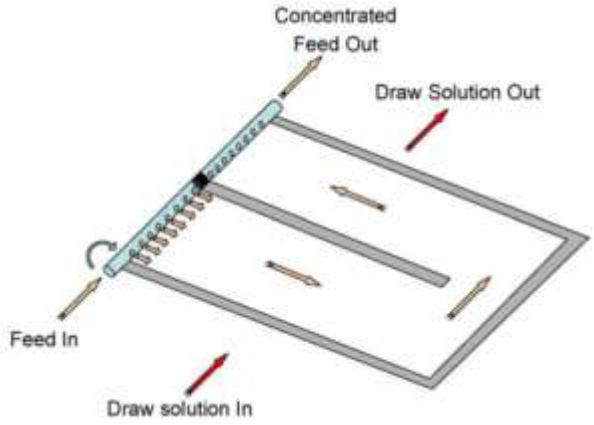

Figure 16- Flow patterns in a spiral-wound module modified for FO. The feed solution flows through the central tube into the inner side of the membrane envelope and the draw solution flows in the space between the rolled envelopes (Cath, et al., 2006; Mehta, 1982)**.**

c. Tubular

Tubular membranes (tubes or hollow fibers) are practical to use in continuously operated FO processes, because are self-supported (i. e. they can support high hydraulic pressure without deformation and they can be easily packed in bundles directly inside a holding vessel), are of

simple fabrication, have high packing density and allow liquids to flow freely on both sides of the membrane (a flow pattern necessary for FO) (Cath, et al., 2006; Mallevialle, et al., 1996; Qin, et al., 2012). Furthermore, the hollow fiber membranes are more suitable for FO because do not need a thick support layer, which will result in reduced internal CP and enhanced performance.

The major difference between hollow fiber and tubular membranes is the flow regime that can be achieve. In hollow fibers (small internal diameter, <1mm) the linear cross-flow velocity is low (from 0 to 2.5 $m.s^{-1}$), which can induce external CP and fouling. In tubular membranes (large internal diameters, 1-2.5 cm) can operate at high cross-flow fiber velocities (up to 5 $m.s^{-1}$), which reduce the CP and fouling (Mallevialle, et al., 1996).

d. Hydration bags

The hydration bag is another configuration of flat sheet FO membrane. Consists in a double lined bag; the internal bag is made of an FO membrane and the external bag is a sealed plastic bag containing the FO bag and the feed water to be treated. The FO membrane bag is filled with draw solution (e.g. sugary syrup) (Cath, et al., 2006)[2].The application of this technology will be further described in section 2.8 b.

2.8. Applications of forward osmosis

Forward osmosis has been investigated in a wide range of applications, they are still limited, but are emerging in the field of wastewater treatment and water purification, seawater desalination, food processing, pharmaceutical applications, and power generation. The following section summarizes the past, present and future applications of FO.

[2] http://www.nasa.gov/mission_pages/shuttle/behindscenes/sts-135_FOB.html.

a. Waste water treatment

In this field of application several modern applications of FO have been published in the literature. These include concentration of dilute industrial wastewater, investigation on treatment of landfill leachate, a study on direct potable reuse of wastewater in advanced life support systems for space applications, and an investigation on concentration of liquids from anaerobic sludge digestion at a domestic wastewater treatment facility. Nevertheless, in most wastewater treatment applications FO is not the final process, but a rather a high-level pretreatment step before an ultimate desalination process.

Concentration of diluted waste water

The first studies for FO was the industrial application for wastewater treatment, published in 1974 (Votta, et al., 1974) and 1977 (Anderson, 1977). The purpose of the investigation was to use low energy process to treat industrial wastewater, containing very low concentrations of heavy metals, for possible reuse. The system used for the tests was a bench-scale; the membranes were the newly commercialized cellulose RO membranes. There feasibility was studied for concentrate dilute real or synthetic wastewater streams containing copper and chromium. The authors observed much lower fluxes than the calculated (fluxes obtained~ 0 - 4.51 $L.m^{-2}.h^{-1}$; fluxes calculated: 10 – 17 $L.m^{-2}.h^{-1}$, from the mass transfer equation and manufacturer data for the membranes tested in RO mode under equivalent conditions), because of the effects of internal CP in RO membranes. Attempts to investigate the effects of external CP on flux by varying the feed and draw solution flow rates yielded inconclusive results.

The draw solution used was simulated seawater, since it is a potentially inexpensive source available in coastal areas. The passage of sodium chloride from the draw (1 g NaCl for every 11.5 – 688 g water) and the diffusion of feed contaminants towards the draw solution occurred at a higher rate than expected. To avoid these effects, different approaches to enhance salt rejection were investigated including chemical treatment of the membrane and thermal

treatment. The treatment of the membrane chemically showed no effect on flux or rejection, while the thermal treatment resulted in elevated salt rejection but decreased water flux.

Due to the poor performance of the RO membranes, further pilot-scale testing of the process was called off. The authors concluded that membranes must be improved and specifically "tailored" for the FO process to be feasible for water treatment.

Concentration of landfill leachate

The water collected by the liners at landfills is a complex mixture. Landfill leachate consists in four general types of pollutants: organic compounds, dissolved heavy metals, organic and inorganic nitrogen, and total dissolved solids (TDS). To treat this mixture there are two commercially available treatments, mechanical evaporation (e. g. vapor compression, vertical tube falling film, horizontal tube spray film, forced circulation) and membrane processes (RO and FO) (Cath, et al., 2006). An evaluation showed that the membrane process can be very effective in the treatment of landfill leachate (Full Scale Experience of Direct Osmosis Concentration Applied to Leachate Management, 1999) this process used the combination of FO and RO techniques.

The company Osmotek Inc., in 1998, constructed the first pilot-scale FO system to test the concentration of landfill leachate at the Coffin Butte Landfill in Corvallis Oregon[3]. For the tests it was used a CTA membrane and a NaCl as draw solution. The results achieved were, a water recover of 94-96% with high contaminant rejection, the flux decline was not apparent at the processing of raw leachate, but was observed a flux decline of 30-50% during the processing of concentrated leachate and an almost complete flux restoration was achieved after cleaning.

The success of the pilot-scale system led to the design and construction of a full-scale system (Full Scale Experience of Direct Osmosis Concentration Applied to Leachate Management, 1999). The first step in the leachate treatment is acidification. This step brings metal precipitates and other solids into solution. The acidified leachate is then passed through a six step forward osmosis stage. In each stage the water in the leachate is osmotically drawn from the leachate into a 6% solution of NaCl. This process concentrates the leachate from the

[3] http://www.rimnetics.com/osmotek.htm

raw state to the final concentrated state. The high concentration leachate is then mixed into Portland cement and returned to the land fill. The water that has been extracted from the leachate into the 6% NaCl solutions is then sent to the reverse osmosis stage. The second final stage of purification is accomplished by three passes through reverse osmosis purifiers to extract the purified water from the concentrated saline solution. The concentrated saline solution is then recycled and used again for the FO step. The pure water, or permeate, is pumped to a holding pond where it is oxygenated and then used to irrigate a tree farm (Aslow, 1998).

The advantage of this method is not saving in energy, but rather in the fact that the FO process is more resistant to fouling from leachate feed than a RO process alone would be (Full Scale Experience of Direct Osmosis Concentration Applied to Leachate Management, 1999).

Other companies, also used this method, like CATALYX Inc[4] and Delta Triqua[5].

Direct potable reuse for advanced life support systems

Long-term human missions in space require a continuous and self-sufficient supply of fresh water for consumption, hygiene and maintenance. The three main sources of wastewater that can be reclaimed and reused in long-term space missions are hygiene wastewater, urine, and humidity condensates (Wieland, 1994; Cath, et al., 2005). The system to treat these wastewaters must be reliable, durable, redundant, capable of recovering a high percentage of the waste water, economical, and lightweight. Additionally, this system should operate automatically with low maintenance and minimal consumables. Different specialized systems have been evaluated by the U. S. National Aeronautics and Space Administration (NASA) over the years. These included the International Space Station (ISS) Baseline, which utilizes filtration beds and oxidation post-treatment; the ICB Bioreactor (BIO) system, which utilizes biodegradation followed by RO, oxidation, and ion exchange post-treatment; the vapor phase catalytic ammonia reduction (VPCAR) system, which uses distillation and oxidation; and the direct osmosis (DO) and osmotic distillation (OD) as pretreatment for RO[6] (Cath, et al., 2005). A

[4] http://www.catalyxinc.com/forward-osmosis.html
[5] http://www.triqua.eu/triqua/fs3_site.nsf/htmlViewDocuments/AEDC3A38607F1868C12577890038866C
[6] http://www.sti.nasa.gov/tto/spinoff2000/er3.htm

preliminary evaluation showed that the DOC system is the best option, has it showed the lowest mass equivalence and relatively low power requirements (Cath, et al., 2005).

The DOC system is a proprietary wastewater treatment system that was developed by Osmotek Inc. (Corvallis, Oregon). The NASA DOC test unit consists of a core RO cascade and two DO pretreatment stages, the first of which (DOC#1) utilizes a DO process only and the second (DOC#2) utilizes a combination of DO and OD to assist in rejecting small compounds, like urea, that easily diffuse through the semipermeable membrane. In DO, a hypertonic solution (referred to as an osmotic agent (OA)) is recirculated on the permeate side of the membrane, while wastewater is recirculated on the feed side (Cath, et al., 2005; Cath, et al., 2005).

Recently NASA have come with a new idea, to use waste-treatment bags has radiation shielding in the space habitat walls and has source of freshwater. As the water supply is used up, the bags will switch to treating wastewater and become a permanent addition to the space walls (see Figure 17)[7].

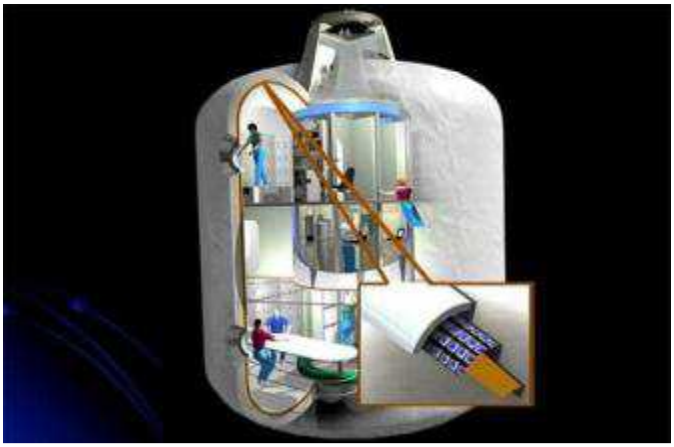

Figure 17- Illustration of NASAS's shield space station[7]

Concentration of digested sludge liquids

Every day, wastewater treatment plants produce large quantities of sludge, which is often treated on an anaerobic or aerobic digester, for further degradation of the recalcitrant organic solids and for the stabilization of the sludge. After the digestion, the sludge is normally dewatered using a centrifuge, producing a biosolids fraction and a liquid fraction (i. e., a

[7] http://www.innovationnewsdaily.com/47-space-habitats-membrane-walls-110120html.html

centrate). The centrate is nutrient-rich (e.g., ammonia, ortho-phosphate, organic nitrogen), with suspended and dissolved solids. The common practice for centrate treatment is to combine the centrate with the influent raw wastewater, resulting in an effluent rich in ammonia and phosphorous. The treatment and removal of this liquid stream from the treatment plant could greatly reduce operating costs and improve the water quality of the final effluent from the treatment facility. Furthermore, if successfully concentrated, the centrate could be economically transported and beneficially used as a fertilizer. To mitigate the liquid stream problems, a process is needed that can either remove both nitrogen and phosphorous or reduce volume of centrate (Holloway, et al., 2007).

In the study (Holloway, et al., 2007), it was investigated the advantages, limitations and economics, of using FO as pretreatment for RO concentration of centrate. The experiments were conducted on a bench-scale FO batch to determine if FO is a viable process for centrate treatment, using different centrate feed solutions and draw solutions (DS) concentrations. The feed solutions used in the investigation were raw centrate (directly collected from the dewatering centrifuges), filtered centrate (106 μm sieve, mesh #104) and deionized water (DI). For each feed solution evaluated, two sets of experiments were conducted: one at constant feed solution concentration and the other at increasing feed solution concentration. The draw solution used was NaCl, ACS grade dissolved in DI water, with the concentration of 70g.L^{-1}, for all experiments. The membrane used in all the experiments is a cellulose triacetate (CTA) (Hydratation Technologies, Inc., Albany, OR). At the end, it was demonstrated that FO is capable of concentrating both raw and pretreated centrate and providing high rejection of nutrients of interest, the performance and the flux increased when the centrate was treated prior to the FO (see Figure 18).

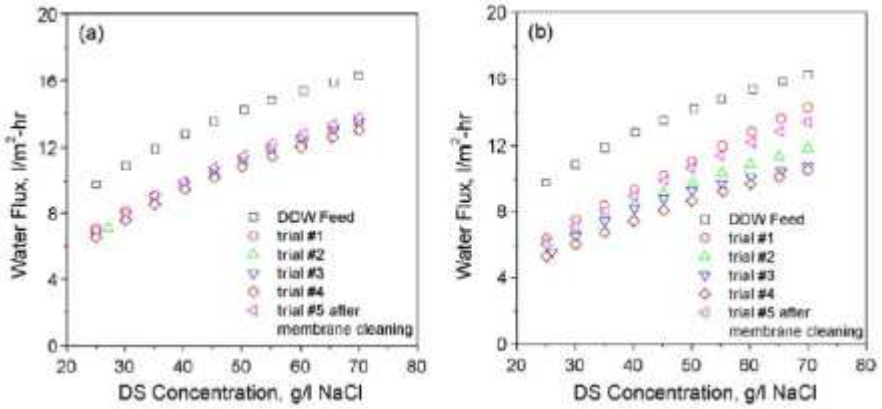

Figure 18 - water flux as a function of draw solution (DS) concentration during FO concentration of (a) pretreated centrate and (b) non-treated centrate. Flux decline between trials is due to organic and suspended solids fouling (Holloway, et al., 2007)

Due to more stringent regulations, extensive treatment of wastewater is becoming increasingly important. One of the latest trends in wastewater treatment is the development of membrane bioreactors (MBR). MBRs have several advantages over conventional treatment technologies, such as reduced footprint and an extensive decomposition of wastewater resulting in high effluent quality. Because of this, reuse of biologically treated wastewater becomes both technically and economically interesting and viable, as an alternative source for irrigation water, process water and even drinking water. For the latter, it is need to associate a FO process after the MBR. However MBRs have some disadvantages, as the high energy demand (compared with the conventional wastewater treatment) and membrane fouling (caused by the presence of natural organic matter (NOM) and biofouling). To avoid these problems, an innovative compact osmotic membrane bioreactor (OMBR) is currently under development. This technique combines activated sludge treatment and FO membrane separation with a RO post-treatment. OMBR as the same advantages as MBRs but don't suffer from irreversible fouling and don't require high energy demand. The OMBR is believed to be a more compact system than conventional MBR systems. Furthermore the OMBR will result in better water quality because of the double barrier against NOM and emerging contaminants (Zhu, et al., 2011; Cornelissen, et al., 2008).

In the study (Zhu, et al., 2011), the feasibility of applying FO to the simultaneous thickening, digestion and dewatering of waste activated sludge was investigated. The experiments were conducted at bench-scale FO setup, the membrane used in the study was supply by Hydration Technology (HTI, Albany, Oregon US) and different types of DS were used, using as draw

agents NaCl, $CaCl_2.2H_2O$, $MgCl_2$, $NaHCO_3$ and Na_2SO_4, at different concentrations. After 19 days of operation, the total reduction efficiencies of the simultaneous sludge thickening and digestion systems in terms of mixed liquor suspended solids (MLSS) and mixed liquor volatile solids (MLVSS) were approximately 63.7% and 80% respectively. The MLSS concentration reached 39 $g.L^{-1}$ from an initial value of 7 $g.L^{-1}$, indicating a good thickening efficiency. The flux was primarily reduced due to the decrease of apparent osmotic pressure difference (see Figure 19). FO dewatering performance was greatly affected by the sludge depth.

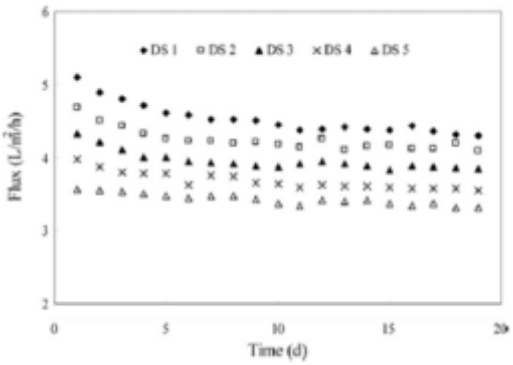

Figure 19 - Variation in water flux with the operation time under different DS concentrations

b. Hydration bags

Hydration bags are one of the few commercial applications of FO (see Figure 20). This concept was developed for military, recreational, and emergency relief situations when reliable drinking water is scarce or not available. This device is slower than the other purifications systems but, requires no power and only fouls minimally[8]. The high selectivity of the FO membrane ensures that the permeating water is free of microorganisms, most macromolecules and most ions.

In the hydration bags, an edible draw solution (e.g. sugar or beverage powder) is packed in a sealed bag made of a semi-permeable FO membrane (Cath, et al., 2006). Immersing the bag in an aqueous solution, the water will diffuse into the bag diluting the initially solid draw solution, producing a consumable sweet drink containing nutrients and minerals. In this regard, hydration bags represent an ultimate treatment process; not a pretreatment process.

[8] http://www.htiwater.com/divisions/military_regulatory/case_studies.html

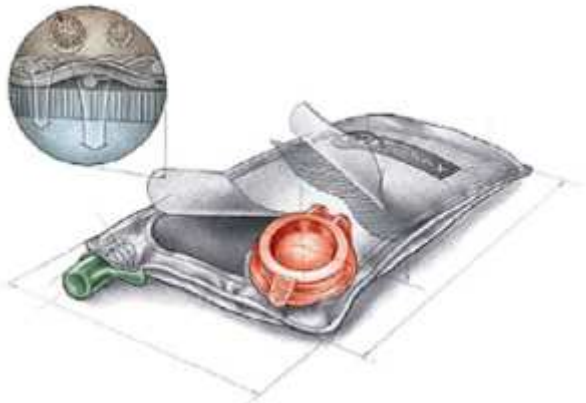

Figure 20 – Illustration of water purification hydration bag (Cath, et al., 2006)

c. Seawater desalination

Since the 1970s that FO has been proposed for the removing of salts from saline water. Several patents have been awarded for different methods and systems for water desalination by FO (Batchelder, 1965; Glew, 1965; Frank, 1972; Stache, 1989; McGinnis, 2002; Hough, 1970; Yaeli, 1992; Lampi, et al., 2005); however, most of them have not be matured or proven feasible.

The FO desalination processes, generally, involve two steps: osmotic dilution of the draw solution and fresh water generation from the diluted draw solution. All FO processes can be classified into two types according to the differences of final water generation method. One method is the use of thermolytic draw solutions which can be decomposed into volatile gases (e.g. CO_2 or SO_2) by heating after osmotic dilution. Therefore, drinking water can be recovered and the gases can be recycled during the thermal decomposition. McGinnis (McGinnis, 2002) described a new FO method for seawater desalination using a combination of draw solutes (KNO_3 and SO_2). This method takes advantage of the temperature dependent solubilities of the solutes (e.g. saturated KNO_3 precipitated with cooling and SO_2 can be removed by heating). McCutcheon et al. (McCutvheon, et al., 2006) proposed a mixture of highly soluble gases, ammonia (NH_3) and carbon dioxide (CO_2) as draw solution for water desalination. The resultant highly soluble and thermolytic ammonium bicarbonate (NH_4HCO_3) draw solution can yield high water fluxes and result in high feed water recoveries.

The second method for FO desalination uses water-soluble salts or particles as the draw solutes, and fresh water is generated from the diluted draw solution by other methods. Khaydarov and Khaydarov (Khaydarov, et al., 2007) proposed the utilization of solar power to produce fresh water from diluted draw solution after osmotic dilution. Tan and Ng (Tan, et al., 2010) proposed a hybrid forward osmosis-nanofiltration (FO-NF) system for seawater desalination, using seven different draw solutes (i.e., NaCl, KCl, $CaCl_2$, $MgCl_2$, $MgSO_4$, and $C_6H_{12}O_6$). Ling and Chung (Ling, et al., 2011) used an integrated FO-UF (forward osmosis-ultrafiltration) system for water desalination, using hydrophilic nanoparticles as draw solutes. Cath et al. (Cath, et al., 2010) employed FO as an osmotic dilution process using seawater as the draw solution for impaired water purification in a hybrid FO-RO process. Also, similar hybrid FO-RO systems were proposed to generate potable (Yangali-Quintanilla, et al., 2011) and the osmotic power of RO brine (Bamaga, et al., 2011). In these combined processes (FO-NF or FO-RO), FO offers several major benefits as, high quality drinking water due to the multi-barrier protection, reduced RO fouling because of the pre-treatment by FO, recovery of osmotic energy of RO brine, low energy input and no need for chemical pre-treatment. In fact, the FO process acts as a pre-treatment process (i.e. osmotic dilution) in the second type of FO desalination. To get fresh water, further water recovery methods must be used to desalinate the diluted draw solution (Zhao, et al., 2012).

Now, the main obstacles for employing FO process as the desalination method is the lack of high-performance membranes and a draw solution which can both have higher osmosis pressure and easily be removed from the product water (Liu, et al., 2009). Moreover, when considering seawater desalination, especially when high water recovery is desired, FO can only be utilized only if the draw solution can induce a high osmotic pressure (Peñate, et al., 2012).

d. Power generation

The dependence on limited fossil fuels and the threat of global warming have raised great interest in alternative energy sources. One potential source, is harvesting electric power by mixing fresh and salt water. This concept of harvesting energy, from the osmotic pressure difference of two solutions is not a new idea and was developed in the mid-1950s (Pattle, 1954).

Unlike conventional energy from fossil fuel sources, salinity-gradient energy or so-called “blue” energy is renewable and sustainable (Post, et al., 2008). Theoretically the energy that can be generated per m^3 river water is 2.5 MJ when mixed with a large surplus of seawater or 1.7 when mixed with 1 m^3 sea water (Veerman, et al., 2009). It is estimated that the gross power potential of this energy source is up to 2.4-2.6 TW, which is sufficient to supply the global electricity demand (2TW) or 16% of the total present energy consumption (Veerman, et al., 2009; Zhao, et al., 2012). Pressure retarded osmosis (PRO) is one method that can be used to realize this energy.

The principle of power generation by PRO is illustrated in Figure 21. When concentrated seawater and diluted fresh water (i.e. river water) are separated by a semipermeable membrane, water will diffuse from the feed side into the draw solution side (i.e. seawater) that is pressurized. The pressurized and diluted seawater is then split into two streams: one going through a hydroturbine to generate power by depressurizing the diluted seawater, and the other one passing through a pressure exchanger to assist in pressuring the seawater and thus maintaining the circulation (Zhao, et al., 2012; Achilli, et al., 2009).

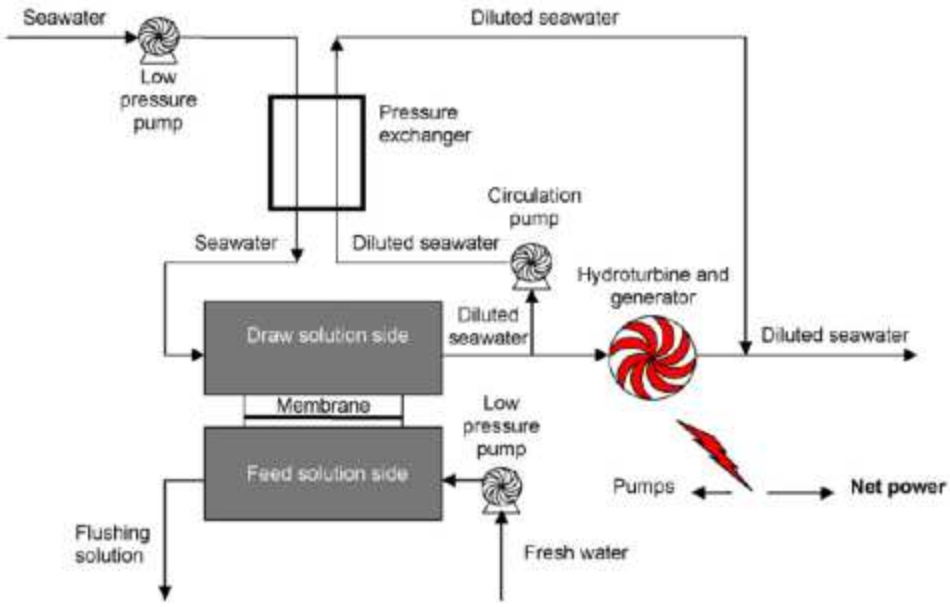

Figure 21- Schematic of a pressure-retarded osmosis (PRO) power plant (Achilli, et al., 2009)

In PRO, the power that can be generated per unit membrane area (i.e., the power density) is equal to the product of the water flux (J_w, defined in equation (22)) and the hydraulic pressure differential across the membrane (ΔP) (Achilli, et al., 2009):

$$W = J_w.\Delta P = A.(\Delta\pi - \Delta P).\Delta P \qquad (39)$$

The power density varies with the osmotic pressure difference, the applied hydraulic pressure difference and mainly determined by the membrane characteristics. For example, the earlier investigations using polyamide or cellulose acetate RO membranes with low water permeability achieved lower power densities (Loeb, et al., 1976; Mehta, 1982; Loeb, et al., 1978). Achilli et al.'s (Achilli, et al., 2009) recent study using the commercial FO membrane with higher water permeability obtained a higher power density. A more recent study using their lab-prepared PRO membranes specifically designed for power generation reported the higher power density (up to 10 W/m^2) (Yip, et al., 2011). A desirable PRO membrane for power generation should have favourable characteristics, such as high water permeability, high salt rejection and minimized internal CP via the optimization of the membrane support layer (Lee, et al., 1981). Since both processes depend on the same semi-permeable membranes, the development and future success of PRO for power generation will, in turn, have great influence on the success of FO.

e. Food processing

In the food industry, it is often necessary to remove water from liquid food to increase the stability, improve shelf life and reduce storage and transportation costs. Vacuum evaporation is the predominant method used to produce liquid food concentrates, but has several drawbacks, has deteriorates the sensory (colour, taste, aroma) and nutritional value (vitamins, etc) of the finish product (concentrate). Compared with the conventional methods, FO can provide advantages in maintaining the physical properties of the food without deteriorating its quality, because operates at low temperatures and low pressures, also as the potentially of low membrane fouling compared to pressure-driven membrane processes (Petrotos, et al., 2001;

Cath, et al., 2006). For that reason, FO has been widely used to concentrate various water-containing foods, including tomato juice (Petrotos, et al., 1998; Petrotos, et al., 1999), mushrooms (Torringa, et al., 2001), fruit juice (Garcia-Castello, et al., 2009; Garcia-Castello, et al., 2011; Nayak, et al., 2011; Babu, et al., 2006; Jiao, et al., 2004), pears (Park, et al., 2002), carrots (Uddin, et al., 2004), papayas (El-Aouar, et al., 2006; García, et al., 2010), potatoes (Eren, et al., 2007), apricots (Khoyi, et al., 2007), strawberries (Changrue, et al., 2008), pineapples (Lombard, et al., 2008) and peppers (Ozdemir, et al., 2008).

In spite of the FO process advantages, the lack of optimized membranes and an effective recovery process for the draw solution are the main limitations to transforming FO into a full-scale process in the food industry (Cath, et al., 2006).

f. Pharmaceutical applications

In the pharmaceutical industry, FO has two types of applications: osmotic drug delivery and the enrichment of pharmaceutical products (Santus, et al., 1995; Yang, et al., 2009; Herbig, et al., 1995; Lin, et al., 2003; Thombre, et al., 1999).

Osmotic drug delivery systems are based on the principle of osmosis. There are different types of osmotic drug delivery systems, as tablets/capsules coated with semi-permeable membranes containing micro-pores (see Figure 22 A), polymer drug matrix systems, and self-formulating in line systems for parenteral drug delivery called osmotic pumps (Figure 22 B; e.g. Rose-Nelson pump, Higuchi-Leeper pump, Higuchi-Theeuwes pump and elementary osmotic pump) (Santus, et al., 1995; Herbig, et al., 1995; Lin, et al., 2003; Thombre, et al., 1999). These osmotic drug delivery systems are used for oral administration, and have been widely used in medical fields.

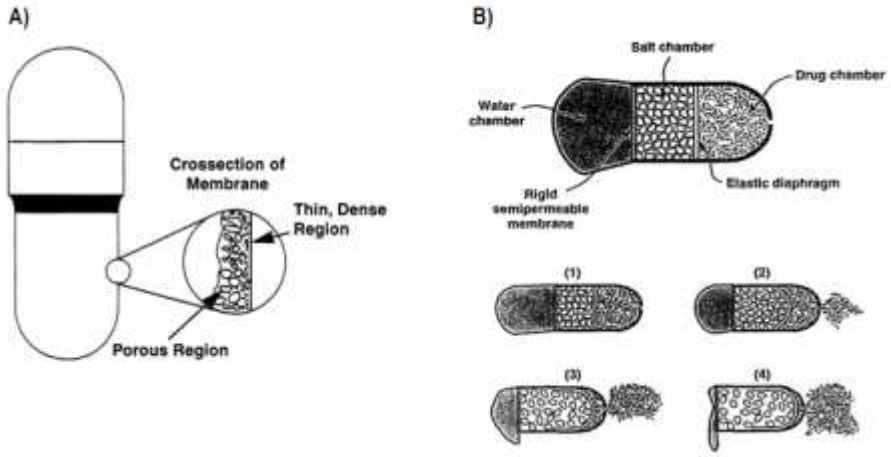

Figure 22- Schematic representation of FO applications for osmotic drug delivery systems. A) Schematic view of the asymmetric membrane capsule (Thombre, et al., 1999); B) Principle of the three-chamber Rose-Nelson osmotic pump first described (Santus, et al., 1995)

Another application of FO is the enrichment of pharmaceutical products (e.g. protein, lysozyme and flavonoids). Generally, these pharmaceutical products are heat sensitive and have large molecule sizes; therefore, FO can have some advantages over conventional chemical or thermal concentration methods. Yang et al. (Yang, et al., 2009) were able to enrich a lysozyme solution with high purity by forward osmosis, without denaturing and changing its configuration. Nayak and Rastogi (Nayak, et al., 2010) used FO to enrich to concentrate anthocyanin extract, and found that the FO process has several advantages over the thermal concentration, in terms of higher stability and lower browning index. Wang et al. (Wang, et al., 2011) studied the concentration of protein solutions (specifically a bovine serum albumin solution) using a forward osmosis-membrane distillation (FO-MD) system.

In the fields of pharmaceutical and food concentration, the concentrates of FO are the target products, which is quite different from desalination and wastewater treatment. Because there is no need to further separate water from the diluted draw solution, FO has great potential in food and pharmaceutical product concentration (Zhao, et al., 2012).

g. Other applications

FO has also been proposed for many other applications. Talaat (Talaat, 2010; Talaat, 2009) proposed that FO had the potential to be used for dialysis fluid regeneration. Phuntsho et al. (Phuntsho, et al., 2011) investigated the use of fertilizers as draw solute for direct fertigation.

The most pronounced benefit revealed by their study was that the dilute draw solution could be used for irrigation directly, without any separation.

FO can also play an important role in the production of biomass energy and the protection of the environment. FO has been proposed to optimize the growth and harvesting of microalgae, which will be used to produce biofuels, while simultaneously treating water (OMEGA system; see Figure 23) (Hoover, et al., 2011).

Figure 23- Schematic of the Offshore Membrane Enclosure for Growing Algae (OMEGA) system. Inset shows the permeation through and rejection by FO membrane in contact with the seawater. The top of the enclosure, which is in contact with atmosphere, contains specialized membranes that allow the passage of sunlight and the exchange of CO_2/O_2 to facilitate the algae photosynthesis (Hoover, et al., 2011)

A recent study has integrated FO in a novel way into microbial fuel cells for wastewater treatment, water extraction and bioelectricity generation (Zhang, et al., 2011). The FO process was also proposed to osmotic dilute the desalination brine, from the desalination plant, before it is discharged into the sea, which will benefit the marine ecological system (Hoover, et al., 2011). Employing FO as a means of membrane cleaning to reduce chemical use has been investigated in recent studies (Hoover, et al., 2011; Qin, et al., 2010; Ramon, et al., 2010).

3. MOTIVATION AND OBJECTIVES

As mentioned before, FO has the potential to replace the current seawater and brackish water desalination processes (e.g. RO) due to its low fouling propensity, high feed water recovery and low energy requirement. However, FO technology presents some drawbacks as the lack of suitable membrane and draw solution.

In order to overcome the FO membrane limitations, i.e. the occurrence of internal CP and improve the membrane salt selectivity; an application of a surface coating or fill the membrane pores with a hydrophilic compound can be one solution (see Appendix 2). This compound, in ideal circumstances, will act as a high flux, water selective barrier, eliminating or minimizing salt contact with the membrane pores. To achieve this goal, a hydrogel material was selected.

Hydrogel materials are crosslinked polymer networks with high affinity to water; they swell significantly in water, but do not dissolve in it. These materials do not have sufficient mechanical properties, by themselves, to serve as membranes (Sagle, et al., 2009).

Coatings of hydrogel have already been applied with success in some membrane processes such, as: reverse osmosis, osmotic distillation and ultra-filtration. Some of the polymers reported are: poly(vinil alcohol) (Wang, et al., 2006; Bolto, et al., 2009), alginic acid-silica (Xu, et al., 2005), polyethersulfone (Peeva, et al., 2012), methyl methacrylate-hydroxy poly(oxyethylene) methacrylate (Choi, et al., 2012), polyether–polyamide (Li, et al., 2007), poly(ethylene glycol) methacrylate (La, et al., 2012) and poly(ethylene glycol) diacrylate (Wu, et al., 2010; Sagle, et al., 2009; Ju, et al., 2010; Sagle, et al., 2009), mixture of poly(ethylene glycol) diacrilate and poly(ethylene glycol) (La, et al., 2011), poly(ethylene glycol) methacrylate (Peeva, et al., 2010), poly(2-dimethylaminoethyl methacrylate, poly(1,1'-dihydroperfluorooctyl methacrylate), poly(1,1,2,2-tetrahydroperfluorooctyl acrylate) (Nagai, et al., 2001).

Poly(ethylene glycol) (PEG)-based hydrogels (see Figure 24) are versatile materials that are highly hydrophilic, readily chemically modified, and biocompatible. These polymers derive their high hydrophilicity from the ethylene oxide linkages in the polymer backbone. Unmodified PEG chains are soluble in water, but crosslinking renders them insoluble. Chemical modification of PEG chain ends facilitates crosslinking. For example, the chain ends can be terminated with acrylate groups, which can then crosslink via polymerization (Sagle, et al., 2009). This polymer

has already been applied with success as coatings for reverse osmosis membranes (Wu, et al., 2010; Ju, et al., 2009; La, et al., 2011; Sagle, et al., 2009).

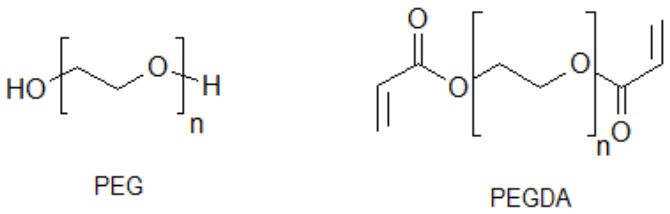

Figure 24- Chemical structure of hydrogel components; PEG- poly(ethylene glycol) monomer, PEGDA-poly(ethylene glycol) diacrylate

In this study, PEG-based materials were considered as potential FO membrane coatings/filling for use in applications such as seawater desalination. The hydrogel was synthesized by UV-photopolymerization of PEGDA aqueous solutions, using 1-hydroxycyclohexyl phenyl ketone (HCK) as the photoinitiator (see Figure 25). The monomer PEG does not react with the PEGDA net, so it will be only dispersed in it.

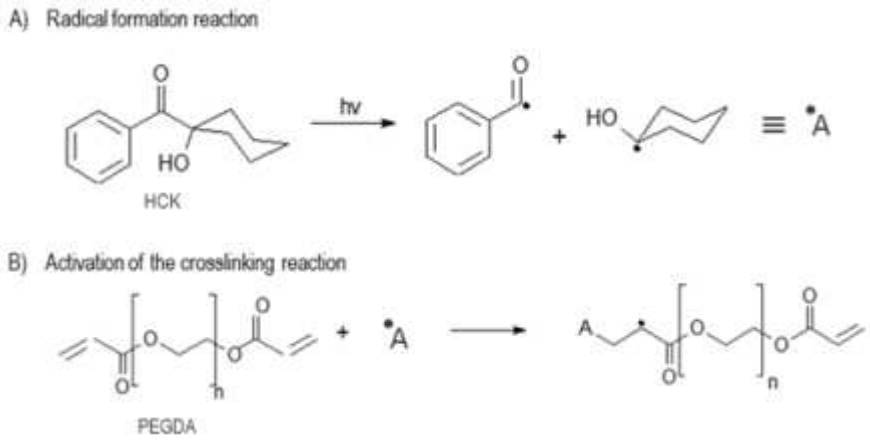

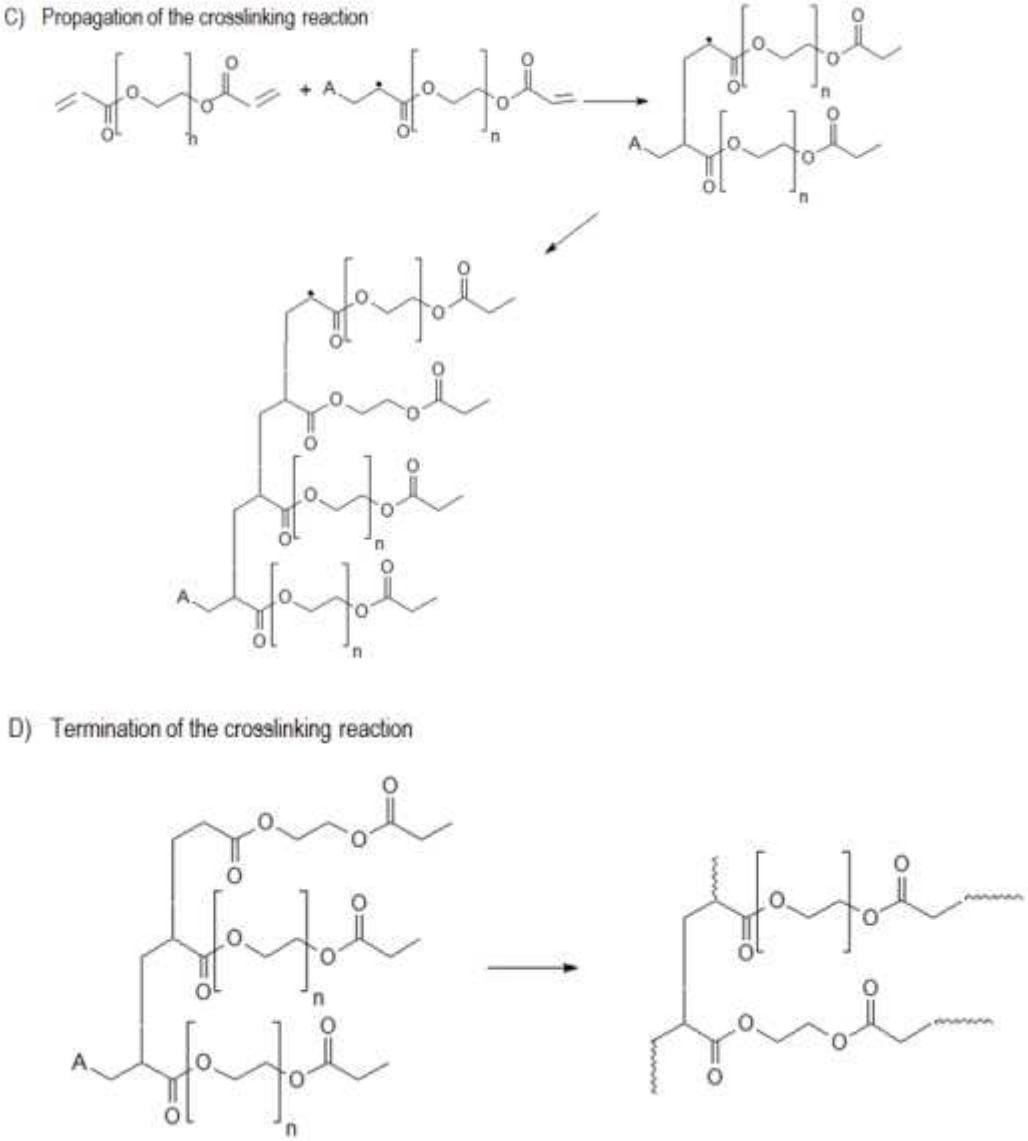

Figure 25- Free radical polymerization of PEGDA

The PEG-based hydrogels were impregnated in the membrane structure by different techniques, as soaking, coating and impregnation by pressure. In order to obtain, the support/active layer, coated or pores filled with hydrogel (see Figure 26).

Figure 26- Illustration of the expected hydrogel treatment effect on the membranes

The scope of this research includes:

- The effect of solvent/co-solvent ratio on membrane performance;
- The effect of the porous support on the membrane performance;
- PEG-based hydrogel free-standing films characterization;
- Determination of external mass transfer coefficients in the FO cell;
- The influence of the PEG-based hydrogel coatings in the membrane performance.

4. MATERIALS AND METHODS

4.1. Materials

For the membrane preparation, the polymer cellulose acetate (CA), the solvents 1,4- dioxane and acetone, and also, polyvinyl pyrrolidone (PVP, used to paste the nylon support fabric to the glass plate), were all purchased from Sigma-Aldrich and used as received. The porous support used was a non-woven backing of nylon fabric (SEFAR NITEX 03-25/19) with a thickness of 65 μm, porosity of 19% and 25 μm mesh opening obtained from SEFAR Ltd, UK, and a polyester support with a thickness of 110 μm.

The crosslinking agent used in the coatings, poly(ethylene glycol) diacrylate (PEGDA, Mw= 575 (n=10) and 700 $g.mol^{-1}$(n=13)), the monomer poly(ethylene glycol) (PEG, Mw= 3000 and 35000 $g.mol^{-1}$) and the photoinitiator was 1-hydroxycyclohexyl phenyl ketone (HPK), were all obtained by Sigma-Aldrich and used as received.

The salts used for the FO tests, magnesium chloride ($MgCl_2$), magnesium sulphate ($MgSO_4$) and sodium chloride (NaCl), were both purchased from Sigma-Aldrich.

.

4.2. Membrane preparation

Nylon fabric was pasted to the glass using a 10 wt% polyvinyl pyrrolidone (PVP-K60) solution in water. The polymer solutions were prepared by dissolving CA (15 wt %) in 1,4-dioxane at room temperature. Solutions were then cast on the nylon support, using an adjustable casting knife (Elcometer 3700) on an automatic film applicator (Braive Instruments), followed by immediate immersion in a water bath at room temperature. The casting height of the casting knife was set at 150 μm.

To study the influence of changing the active layer internal structure, the previous dope solution was compared to three more dope solutions which were prepared, with CA (15 wt %) in a mixed solvent acetone/1,4-dioxane, with the following weight ratios: 1:3; 1:1 and 3:1. Table 6 contains the membrane nomenclature used in the section 5.2. The method for the preparation of the membrane was the same as described before.

Table 6- Nomenclature of membranes used to test the effect of solvent/co-solvent ratio on membrane performance

Title	Dope composition (wt%)
A	15% CA 85% dioxane
B	15% CA 63.8% dioxane 21.3% acetone
C	15% CA 42.5% dioxane 42.5% acetone
D	15% CA 21.3% dioxane 63.8% acetone

The effect of the porous support layer in the membrane performance was studied with the dope solution first described but cast on a polyester support. The thickness of the casting knife was also set at 150 µm.

The resulting membranes were stored in water.

4.3. Hydrogel synthesis and characterization

Prepolymerization mixtures containing, 25 wt%, 50 wt% and 75 wt% of PEGDA (Mw= 575 and 700 $g.mol^{-1}$) were prepared by combining the crosslinker with 0.1 wt% of photoinitiator. The 50 wt% composition was chosen to study the effect of adding the monomer PEG to the prepolymerization mixture (PEG3000/PEGDA and PEG35000/PEGDA), to increase the coating solution viscosity. The mixtures containing the monomer PEG (Mw=3000 and 35000 $g.mol^{-1}$) were prepared by combining 40 wt% PEGDA (Mw=700 $g.mol^{-1}$) with 0.1 wt% of photoinitiator and 20 wt% of the monomer. Table 7 show the composition of each hydrogel prepared.

Table 7 – Composition of the hydrogels prepared

Entry nº	Hydrogel	Prepolymerization mixture composition
1	25% PEGDA	- PEGDA (Mw=575/700) =25 wt% - PEG = 0 - HCK = 0.1 wt%
2	50% PEGDA	- PEGDA (Mw=575/700) =50 wt% - PEG = 0 - HCK =0.1
3	75% PEGDA	- PEGDA (Mw=575/700) =75 wt% - PEG =0 - HCK = 0.1 wt%
4	PEG35000/PEGDA	- PEGDA (Mw=700) = 40 wt% - PEG (Mw=35000) = 20 wt% - HCK = 0.08 wt %
5	PEG3000/PEGDA	- PEGDA (Mw=700) = 40 wt% - PEG (Mw=3000) =20 wt% - HCK = 0.08 wt %

To study the hydrogel salt and water transport properties, free-standing films were prepared by first placing a control volume (3.6 mL and 5 mL) of prepolymerization mixture in a petri dish. Then, the mixture was exposed to a UV crosslinking apparatus (UVP's B-100, 365 nm in $mW.cm^{-2}$). Different exposure times were tested for 25 wt% PEGDA prepolymerization mixture (90 s, 150 s and 300 s), the other mixtures were exposed for 150 s. The polymer films were soaked in deionized water for several days following the polymerization. The films were thoroughly washed with water for 24 hours, on the first day to remove any residual component not bound to the network.

The CA membranes were impregnated with the hydrogel using different techniques, see Figure 27. One of the techniques was coating, making one or three coatings on the membrane support or active layer. For this, a few drops of prepolymerization mixture were put on the top (on the active layer) or bottom (on the porous support) of the membrane, and then the surface was smoothed with a metal rod. Afterwards the membrane was irradiated with UV light for 150 s. This operation was repeated depending on the number of coatings desired. The other technique used was soaking; a membrane was soaked in the prepolymerization mixture for two hours and then was smoothed with a metal rod, following by a UV crosslinking for 150 s. Also, pressure was used to force the impregnation of the hydrogel in the membrane structure, using a dead-end cell; unfortunately this technique turns out to damage the membranes.

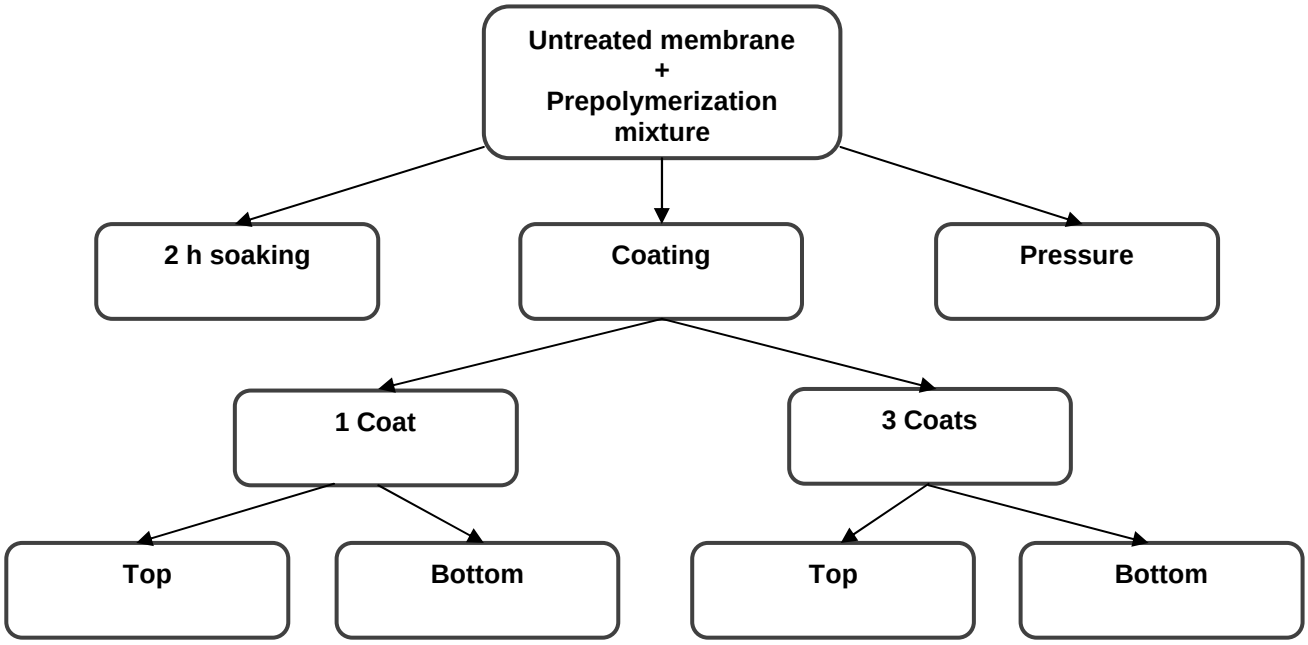

Figure 27 - Schematic illustration of membrane treatments used

4.4. Hydrogel films characterization

Crosslinked PEGDA free-standing films were characterized in terms of water and salt transport properties.

a. Water transport properties

Water uptake of free-standing hydrogel films was measured gravimetrically. Films were equilibrated in DIW for a minimum of 1 h, patted dry, and quickly weighed using an analytical balance (Sartorius CP3245). Afterwards, the samples were dried overnight on an oven (Gallenkamp Vacuun Oven) at 50 ºC and weighed again, to determine the mass of the dry film. This process was repeated two times to ensure that weight was constant. The water uptake, ω_w, was calculated as follows:

$$\omega_w = \left(\frac{m_{wet} - m_{dry}}{m_{dry}}\right).100 \quad (40)$$

Where m_{wet} is the mass of the wet film and m_{dry} is the mass of the dry film.

The volume fraction of water in the swollen network, υ_w, was calculated assumind ideal mixing behaviour (Sagle, et al., 2009) :

$$\upsilon_w = \frac{\frac{m_{wet}-m_{dry}}{\rho_w}}{\frac{m_{wet}-m_{dry}}{\rho_w}+\frac{m_{dry}}{\rho_H}} \qquad (41)$$

Where, ρ_w is the water density (1000 g.L^{-1}) and ρ_H is the hydrogel polymer density (Ju, et al., 2010).

b. Salt transport properties

Salt transport properties were characterized by using the method of kinetic desorption. In this method, the hydrated films with a thickness between 100-130 µm were cut, each one, to a 50 mL centrifuge tube filled with a solution of 0.6 M NaCl, for 24 h at ambient temperature, to ensure its equilibrium with the NaCl solution. The films were then removed from the NaCl solution, and any excess salt solution was removed with a tissue. The film was then quickly transferred to another 50 mL centrifuge tube filled with deionized water (the extraction solution). The solution in the centrifuge tube was stirred vigorously using a stir bar to achieve a uniform distribution of NaCl in the extraction solution during the desorption process and the solution was kept at room temperature. The NaCl concentration in the extraction solution as a function of time was determined by collecting samples of 0.5 mL at different times during the experiment. The samples were then analysed by inductively coupled plasma atomic emission spectroscopy (ICP-AES) (Perkin Elmer instruments, Optima 2000DV) to obtain the corresponding concentration change through time.

The desorption results were fit to the following Fickian diffusion model to calculate the NaCl diffusivity, D_S, in the polymer (Ritger, et al., 1987; Ganji, et al., 2010):

$$D_s = \frac{\pi l^2}{16}\left[\frac{d(M_t/M_\infty)}{d(t^{1/2})}\right]^2 \qquad (42)$$

Where M_t is the total amount of NaCl extracted from the polymer at time t, M_∞ is the total amount of NaCl extracted from the polymer as time approaches infinity, and $d(M_t/M_\infty)/d(t^{1/2})$

is the slope of the linear potion of M_t/M_∞ as function of $t^{1/2}$, which is observed when M_t/M_∞ is smaller than 0.6 (Ritger, et al., 1987; Ganji, et al., 2010).

The NaCl partition coefficient in the polymer, K_s, by definition, is the ratio of the amount of NaCl in the film (M_∞) per unit hydrated film volume divided by the NaCl concentration in the solution where the film was originally equilibrated (i.e. 0.6 M) (Yasuda, et al., 1968).

The salt permeability coefficient, P_s, can be estimated from the measured diffusion and partition coefficients (Wijmans, et al., 1995):

$$P_s = D_s . K_s \qquad (43)$$

4.5. Membrane characterization

The membranes were characterized in terms of morphology and structure measuring their thickness, porosity and water uptake. Digital microscope (DM) and scanning electron microscopy (SEM) pictures were obtained. The membrane capability to retain the hydrogel compound was measured by thermogrametry analysis. The performance of the membranes was evaluated by the flux, permeability and salt rejection, and their hydrophobicity – hydrophilicity characteristics by contact angle.

a. Membrane porosity, ε

For the measurement of porosity, small pieces of the membranes were taken from water followed by careful and quick removal of the excess water on the surface by tissue paper. The membranes were then weighed (m_1, g), after that were allowed to dry in air for 24h at room temperature, and then weighed (m_2, g). The latter value was confirmed after 2 days. The water content is thus calculated as $m_1 - m_2$, and the dry weight of the membrane is m_2. Since the density of both, water (ρ_W, 1000 g.L^{-1}) and CA (1310 g.L^{-1}) are known, their volumes can be calculated separately, and the overall porosity (%) is obtained by

$$\varepsilon = \frac{(m_1 - m_2)/\rho_W}{m_2/\rho_p + (m_1 - m_2)/\rho_W} . 100 \qquad (44)$$

b. Thickness, l

The membranes thickness was directly measured by a micrometer (Mitutoyo IP65, Coolant Proof), with the membrane wet, to simulate the membrane in the test environment.

c. Water uptake

The membranes water uptake was measured gravimetrically, using the same method used in section 4.4 a.

d. Scanning electron microscopy (SEM)

Surface and cross-sectional images of FO membranes were recorded using JEOL 5610 field emission scanning electron microscope FESEM. Samples were mounted onto SEM stubs, and coated with chromium using a chromium sputter coater (EMITECH K575).

e. Digital microscope

The images of the surface morphology of the untreated and hybrid membranes with contrast were captured by a digital microscope (DinoCapture, AM2011-Dino-Lite Basic). To obtain a higher contrast in the images, the membranes were colored using a green dye (green food colouring, Langdale).

f. Thermogravimetric analysis (TGA)

The weight loss studies versus temperature were performed by using a Thermogravimetric Analyzer TGA Q50 (TA Instruments). The dry samples were held at 40ºC for 2 min and the temperature was then raised to 600ºC at rate of 10ºC/min under air condition.

The membranes used in the experiment were prepared by a prepolymerization mixture of 50 wt% of PEGDA (Mw=700 $g.mol^{-1}$).

g. Water contact angle

The hydrogel-coated and the untreated membrane active layer were characterized by contact angle in order to compare their hydrophilicity. The water contact angle measurements were performed using a contact angle goniometer (DSA 10, Krüss GmbH), at room temperature. Five measurements were made and results were averaged for each membrane.

4.6. Membrane performance in FO

Figure 28 describes the apparatus used on the laboratory-scale FO experiments. The crossflow cell is composed of two chambers; the dimensions of each one are 7.5 cm of diameter and 8 mm deep. Two permanent magnet pumps (RS components 244-2917) were used to pump both the feed and draw solutions, at constant rate (v_F ~22.5 L.h^{-1} and v_D~ 30 L.h^{-1}). The set-up was kept at room temperature. The draw solution and the feed solution rested on a balance (Denver Instruments S-8001) each, and weight changes were measured over time to determine the permeate water flux. Both sides of the membranes were tested, FO (active layer facing the draw) and PRO mode (active layer facing the feed). The tests using DIW as feed solution had a duration of approximately 30 min. When the feed solution was 0.6 M NaCl, the tests have duration of approximately 1 h.

In all the experiments, the draw solution pump was always kept with a slightly higher rate than the feed solution pump, in order to detect possible defects in the membrane.

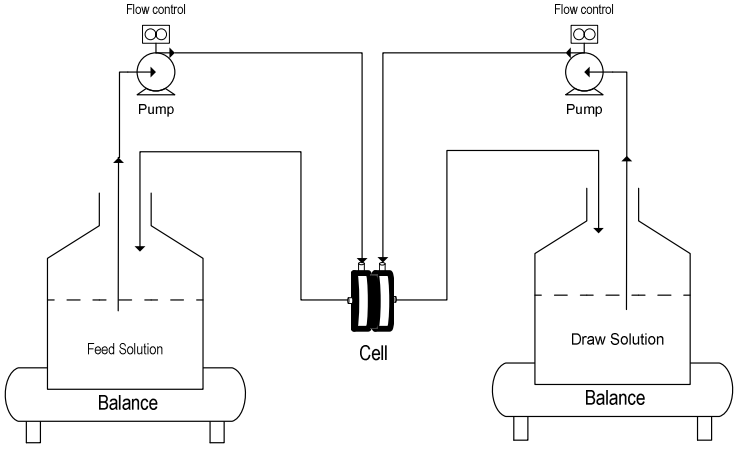

Figure 28- Schematic diagram of the lab-scale FO experimental set-up

The draw solution was prepared with 0.5 M of $MgCl_2$ or 1.25 M $MgSO_4$ in deionized water (DIW). The feed, depending on the test required, was DIW or a solution of 0.6 M of NaCl in DIW.

The theoretical osmotic pressure was calculated using the concentration at the start of the experiment, using the following equation (preciously mentioned in section 2):

$$\pi = n.\varphi.C_S.R.T \quad (2)$$

The φ values were taken from (Achilli, et al., 2010)). During the experiment the actual osmotic driving force will vary as result of the dilution of the draw solution/concentration of feed solution.

The water flux was determined by measuring the weight change of the draw and feed solution over a selected time period. As water transports across the membrane from the feed solution into the draw solution, the draw solution weight increases, and therefore the feed solution weight decreases. So the partial water flux (J, $L.m^{-2}.h^{-1}$, abbreviated as LMH) is given by:

$$J_{\Delta t} = \frac{\Delta V_{H_2O}}{A_m.\Delta t} \quad (45)$$

Where $J_{\Delta t}$ is the flux in a certain time interval (Δt), the ΔV_{H_2O} is the gained/lost water volume in a certain Δt, and A_m is the membrane surface area. For every test the average water flux was calculated, for both sides (draw and feed solutions), and corrected with regard to the concentration/dilution of the draw/feed solution. The average water flux (J_w) between the feed and draw side was considered, to minimize the possible errors.

The partial water permeability of the membrane was calculated as below:

$$A_{\Delta t} = \frac{J_{\Delta t}}{\pi_D - \pi_F} \quad (46)$$

Where $A_{\Delta t}$ is the partial permeability in a certain time interval (Δt) and, π_D and π_F are respectively the osmotic pressure in the draw and feed solution. The average permeability (A_w)

between, the permeability calculated from the feed side and draw side was considered, to minimize the possible errors.

To determine the membrane rejection for NaCl, a sample was taken from the feed and draw solution on the beginning and the end of every test (when the feed was 0.5 M NaCl). The samples were then analyzed by inductively coupled plasma atomic emission spectroscopy (ICP-AES) (Perkin Elmer instruments, Optima 2000DV) to determine the concentration change of salt in the solutions. Based on the amount of water passed into the draw solution during the course of the experiment and the amount of NaCl in the draw solution, the permeate NaCl concentration is determined. The percent salt rejection R is then calculated from:

$$R = \left(1 - \frac{C_p^{Draw_{end}}}{C_F^{Feed_{beginning}}}\right) \times 100 \quad (47)$$

Where $C_p^{Draw_{end}}$ is the permeate NaCl concentration in the end of the experiment and $C_F^{Feed_{beginning}}$ is the feed NaCl concentration at the beginning of the experiment.

4.7. The influence of hydrogel thickness in water flux

In order to study the influence of hydrogel thickness in water permeability, the plot flux vs hydrogel thickness was made, using the water permeability value from Ju et al. (Ju, et al., 2009) (5.3 L.μm.(m^2.h.bar)$^{-1}$).

4.8. Determination of external mass transfer coefficients in the FO cell

The external mass-transfer coefficients in the cross-flow cell were estimated from independent measurements of dissolution of a plate of benzoic acid into water at two different cross-flow rates: 18 and 60 L.h^{-1}, at 30°C. To prepare this test, a layer of molten benzoic acid was poured into the cross-flow cell and allowed to solidify so as to present a surface of benzoic acid at about the same depth in the cell as a membrane surface would reside. Water, with kinematic viscosity near to that of the docosane solutions, was circulated though the cell at flow

rates 50 and 120 $L.h^{-1}$, dissolving the benzoic acid. The benzoic acid concentration in the water was monitored, using the UV analysis (Perkin-Elmer FT-IR Spectrometer; absorbance at 2928 cm^{-1}), as a function of time (t), allowing calculation of the mass-transfer coefficient (k_b) from the equation (Peeva, et al., 2004):

$$\ln \frac{c_b^*}{c_b^* - c_b} = \frac{k_b A}{V} t \quad (48)$$

Where c_b is the concentration of benzoic acid in water at time t, c_b^* is the solubility of benzoic acid in water, V is the volume of the water solution at time t, and A is the surface area of the benzoic acid layer.

Mass-transfer coefficients for NaCl, $MgSO_4$ and $MgCl_2$ were estimated based on the benzoic acid mass-tranfer coefficients values and mass-transfer coefficient correlations available in the literature. In general, the Sherwood (Sh) number is related to the Schmidt (Sc) and Reynolds (Re) numbers as follows (Mulder, 1996):

$$Sh = \frac{k d_h}{D} = a.Re^b Sc^c \left(\frac{d_h}{L}\right)^d \quad (49)$$

Where $d_h$is the hydraulic diameter, which depends on the geometry of the system. The values, a, b, c and d, depend on the system geometry, type of fluid (Newtonian or non-Newtonian) and flow regime. By assuming that the system's hydrodynamics and geometric conditions are constant, the correlation can be reduced to:

$$k \propto \eta^{(c-b)} D^{(1-c)} \quad (50)$$

Therefore, the ratio of the solute mass-transfer coefficient to the benzoic acid mass-transfer coefficient can be expressed as:

$$\frac{k_{solute}}{k_b} \propto \left(\frac{\eta_{solute}}{\eta_b}\right)^{(c-b)} \left(\frac{D_{solute}}{D_b}\right)^{(1-c)} \quad (51)$$

Several correlations are available in the literature for the cross-flow cells (Gekas, et al., 1987). The correlations have Reynolds number exponents (b in the above equations) ranging from 0.65 to 0.875. The Schmidt number exponents (c in the above equations) range from 0.25 to 0.6. One widely used correlation is the Chilton-Colburn correlation (Peeva, et al., 2004):

$$Sh = 0.023Re^{0.8}Sc^{0.33} \quad (52)$$

A correlation specific to the cell used in this study, where the flow is tangential, is not available, however the benzoic acid data from this study suggested and exponent for Re of around 0.8. For that reason, the Chilton-Colburn correlation was used as a basis for calculating the mass-transfer coefficients for NaCl, $MgSO_4$ and $MgCl_2$. Note that it was necessary to assume that the contents of the cross-flow cell are well mixed and that turbulent flow conditions are valid in order to perform these calculations.

The diffusion coefficient for benzoic acid (0.8 x 10^{-9} $m^2.s^{-1}$) was obtained from the literature (Irandoust, et al., 1986), for $MgSO_4$ (1.11 x 10^{-9} $m^2.s^{-1}$) was taken from (Applin, et al., 1984), and for NaCl and $MgCl_2$ (1.5 x 10^{-9} $m^2.s^{-1}$ and 1.02 x 10^{-9} $m^2.s^{-1}$, respectively) was taken from (Lobo, 1993).

5. RESULTS AND DISCUSSION

In this chapter was used the standard nomenclature was used (Cath, et al., 2012), so PRO mode stands for support layer facing the feed solution and FO mode stands for support layer facing the draw solution. The first FO experiments (section 5.2) were run using $MgSO_4$ as draw solute, but due to economical reasons the following experiments were run using a solution of $MgCl_2$ (Achilli, et al., 2010); the osmotic driving force was kept the same.

5.1. Determination of external mass transfer coefficients in the FO cell

In order to correct the osmotic pressure values on the membrane surface due to the external concentration polarization effects, the mass transfer coefficient of the boundary layers was calculated using the benzoic acid dissolution tests (Peeva, et al., 2004). Table 8 presents the values obtained for the mass-transfer coefficient for the solutes used in the FO tests.

Table 8- Mass-transfer coefficients of the FO test solutes obtain form the benzoic acid dissolution experiments

Compound	Mass transfer coefficient at 18 $L.h^{-1}$ flow rate (10^{-5} $m.s^{-1}$)	Mass transfer coefficient at 60 $L.h^{-1}$ flow rate (10^{-5} $m.s^{-1}$)
NaCl	3.9	6.8
$MgSO_4$	3.0	5.6
$MgCl_2$	3.2	5.3

From the results obtain in Table 8, the osmotic pressure at the membrane surface was corrected using the following equations:

$$\pi_{D,m} = \pi_{D,b}.exp\left(-\frac{J_w}{k_D}\right) \quad (53)$$

and

$$\pi_{F,m} = \pi_{F,b}.exp\left(\frac{J_w}{k_F}\right) \quad (54)$$

from section 2.3 a. The mass-transfer coefficients used were the ones calculated with 18 $L.h^{-1}$ flow rate, since this value is the closest to the experimentally used.

5.2. The effect of solvent/co-solvent ratio on membrane performance

a. Membranes morphology

Different CA membranes were prepared by varying the dope solution solvent ratios of acetone and dioxane, Figure 29, shows the morphology observed under SEM pictures of the different CA membranes.

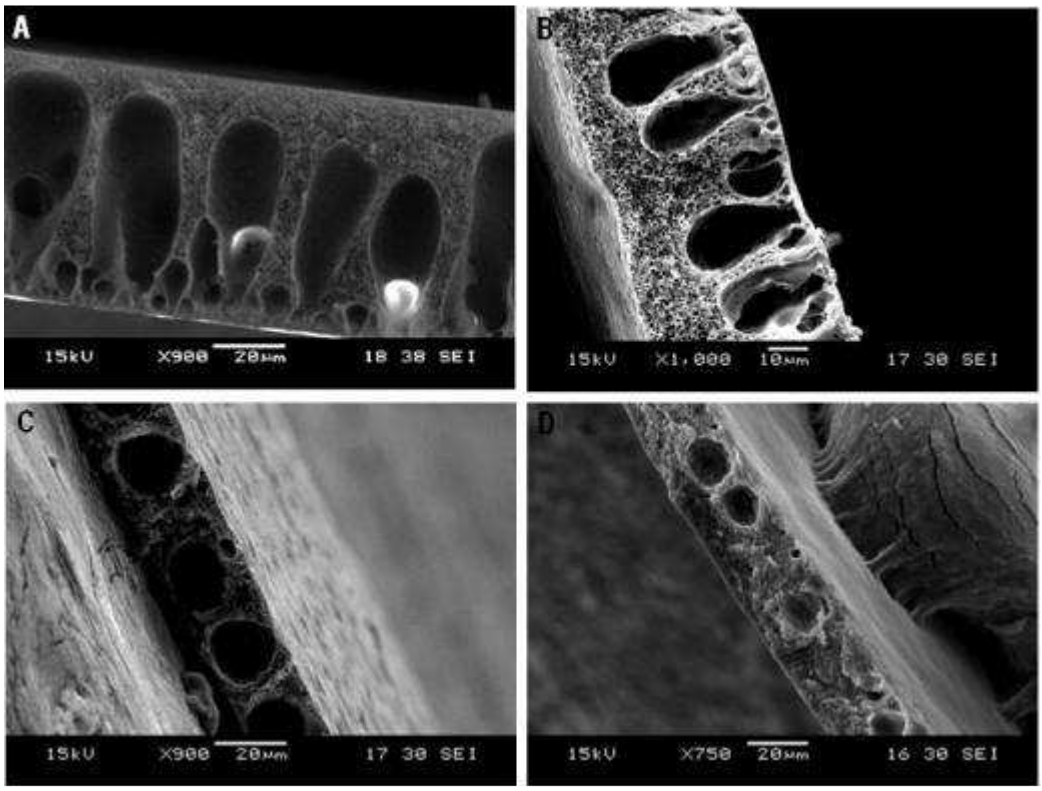

Figure 29- SEM image of membrane cross-section: A) Membrane A; B) Membrane B; C) Membrane C and D) Membrane D

The images obtained by SEM, show that increasing the amount of dioxane in the dope solution induces the formation of a macrovoid structure (see Figure 29 A and B), while, increasing the acetone concentration induces the formation of a more dense structure (see Figure 29 C). The finger-like structure (macrovoid) formation is due to the affinity between dioxane and water, which causes an instantaneous demixing, meaning that the membrane is

formed immediately after immersion in the non-solvent bath. The relatively dense structure formed with the acetone addition is due to a delayed demixing during the precipitation process, which causes faster water diffusion than solvents outflow. Figure 29 B shows the case where the dope solution has a weight ratio of 1:1 for the two solvents, and therefore the membrane shows an intermediate structure between the two latter cases.

b. Membrane performance

The water flux, permeability and rejection were evaluated for the different CA membranes, to verify the effect of altering the membrane structure in their performance. Both sides of the membrane were tested in crossflow mode. For all the experiments, the draw solution was 1.25 M $MgSO_4$ and the feed was DIW or 0.6 M NaCl. The experimental results are shown in Table 9. To minimize the errors due to the mass balance differences, the flux and permabilities showed correspond to the average flux between, the flux calculated from the weight change in the feed side and the draw side. Also, the first 20 min of every experience weren't considered because, in most cases, the first values didn't match with the behaviour of the other values.

Table 9 - Performance of the CA membranes in the FO system

Entry nº	Membrane	Feed solution	Draw solution	J_w (LMH)	A_w (LMH.bar^{-1})	R (%)
1	A	0.6 M NaCl	1.25 M $MgSO_4$	1.54	0.08	89.6
2	B	0.6 M NaCl	1.25 M $MgSO_4$	1.42	0.07	81.2
3	C	0.6 M NaCl	1.25 M $MgSO_4$	0.97	0.05	86.3
4	D	0.6 M NaCl	1.25 M $MgSO_4$	0.81	0.04	84.0
Entry nº	Membrane	Feed solution	Draw solution	J_w (LMH)	A_w (LMH.bar^{-1})	R (%)
1	A	0.6 M NaCl	1.25 M $MgSO_4$	0.89	0.05	96.4
2	B	0.6 M NaCl	1.25 M $MgSO_4$	0.77	0.04	96.0
3	C	0.6 M NaCl	1.25 M $MgSO_4$	0.78	0.04	97.0
4	D	0.6 M NaCl	1.25 M $MgSO_4$	0.91	0.05	95.9

From the results obtained in Table 9 for the membrane in PRO mode, it can be seen that adding acetone to the dope solution decreases the membrane performance, i.e. the water flux, water permeability and the membrane selectivity decreases. Although in FO mode this behavior is not so linear, the membranes present almost the same performance results. This latter result may be just irregular, since the other values show that the performance decreases with the increasing amount of acetone. The drop on the membrane flux and permeability (with increasing acetone) is due to the densification of the membrane internal structure. However, this densification is just apparent, because the membrane rejection also drops, which means that the membrane structure is still very porous. In the case where the membrane is in FO mode, the rejection is almost constant for all the four cases, which may be due to the low and similar flux results obtained.

Another remark that can be taken from Table 9 is the different membrane performances by changing the membrane orientation (PRO mode as superior flux results than FO mode). This result can be explained by the different internal CP effects that the membrane support layer is subjected. In PRO mode the membrane is subjected to concentrative internal CP and in FO mode to dilutive internal CP. The dilutive internal CP has more severe effect on the membrane flux, since in this configuration the membrane experienced even more severe internal CP. For the FO mode configuration, the water flux through the membrane drastically dilutes the concentration of draw solution inside of the membrane support structure, which results in a huge loss of the effective osmotic driving force (Gray, et al., 2006; Tang, et al., 2010).

c. Membrane parameters

The CA membranes parameters were obtained with the membrane in PRO mode. The thickness of the membrane was obtained by direct measurement. The parameters, porosity (ε), mass transfer coefficient (k_m), structural parameter (S) and tortuosity (τ), were calculated by the following equations (mentioned in section 2.3 b and 4.5 a):

$$\varepsilon = \frac{(m_1 - m_2)/\rho_W}{m_2/\rho_p + (m_1 - m_2)/\rho_W} . 100 \qquad (44),$$

$$k_m = \frac{J_w}{\ln\left(\frac{A\pi_{draw} - J_w + B}{A\pi_{feed} + B}\right)} \quad (55),$$

$$S = \frac{D}{k_m} \quad (56)$$

and

$$\tau = \frac{S.\varepsilon}{l} \quad (57)$$

The parameters results are presented in Table 10.

Table 10- Parameters of the CA membranes

Membrane	l (μm)	ε (%)	k_m (10^{-6}m.s^{-1})	S (mm)	τ
A	111.5	55.1	7.4	0,20	1.14
B	85	48.3	7.2	0.21	1.19
C	76	33.6	5.2	0.29	1.29
D	70	30.6	4.1	0.37	1.61

The membranes parameters results presented in Table 10 show that increasing the amount of acetone in the dope solution makes the membrane structure worst, as it can be seen by the increasing value of the membrane structural parameter (S). The membrane S value is an intrinsic membrane parameter used to determine the degree of internal CP of the FO membrane, and is crucial in evaluation of the membrane performance (Park, et al., 2011). So, the lower the S value, the less severe is the internal CP. Therefore, much less internal CP would be expected with membrane A during FO processes, and the effective driving force would be preserved to the highest extent.

From the results obtained, of the membrane performance, selectivity and parameters, membrane A was chosen as the base membrane for all the subsequently experiments.

5.3. Cellulose acetate membrane performance

The base membrane performance was tested in the FO system, using $MgSO_4$ and $MgCl_2$ as draw solutions (2.1 and 2.9 M for $MgSO_4$; 2.5, 3.7 and 5.0 M for $MgCl_2$), and NaCl as feed solution (0.6 M). Figure 30 shows the effect of increasing the driving force in the water flux, by increasing the concentration of the bulk draw solution.

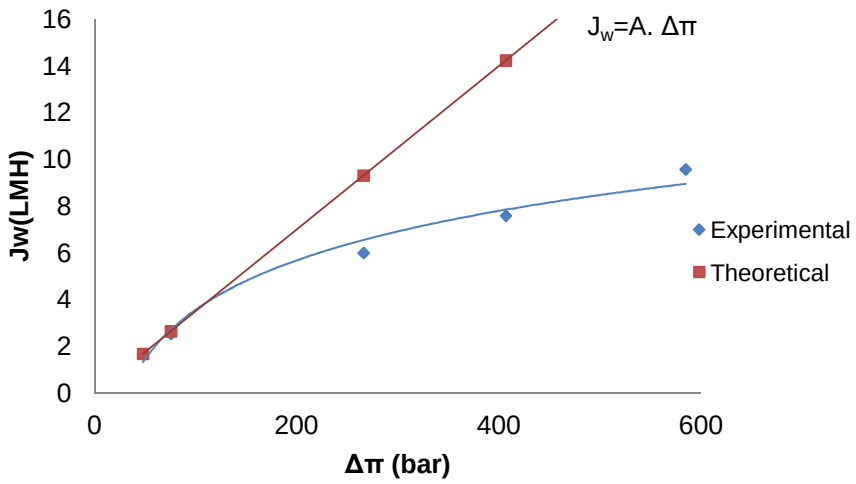

Figure 30- Base membrane water flux over a range of osmotic pressure differences; PRO mode. The theoretical line was illustrated by considering Aw constant

The increasing of driving force as expected shows an increase in the water flux, however based on equation (23) this flux increase should be linear to the osmotic pressure difference, and from Figure 30 the flux shows a non-linear behaviour, especially at higher driving forces. This phenomenon is attributed to the internal CP; most likely due to the solutes in the feed water entering the porous support as a result of the water flux from feed to draw solution (convection) (Tang, et al., 2010). In addition, some solutes also transmit through the CA rejection layer from the high concentration draw solution into the support. This causes a major concentration build-up in the membrane support layer (concentrative internal CP), which reduces the effective driving force (osmotic pressure difference across the dense rejection layer) and causes severe flux reduction (McCutcheon, et al., 2005; Tang, et al., 2010). This behaviour is explained by the internal CP model (section 2.3 b) which predicts that the degree of internal CP depend exponentially on membrane flux due to the salt convection and diffusion, which explained why the experimental flux deviated more severely from the ideal flux at higher draw solution concentrations (i.e. higher driving forces).

5.4. The effect of the porous support on the membrane performance

In order to test the effect of the porous support on the membrane performance, a polyester fabric was tested. This support is used in reverse osmosis membranes, to provide mechanical support.

Table 11 characterizes the two membranes prepared with different supports in terms o thickness and porosity.

Table 11- Characteristics of the base CA membrane, with different porous support

Support	l (μm)	ε (%)
Nylon	111.5	55.1
Polyester	142.8	24.5

From the results obtained it can be seen that the polyester support has lower porosity and higher thickness, which will affect negatively the membrane performance. Since the desired characteristics of the FO membranes is a thin support layer with maximum porosity for minimal internal CP.

a. Membrane performance

The FO system performance of the membranes differing on the support layer is present Figure 31.

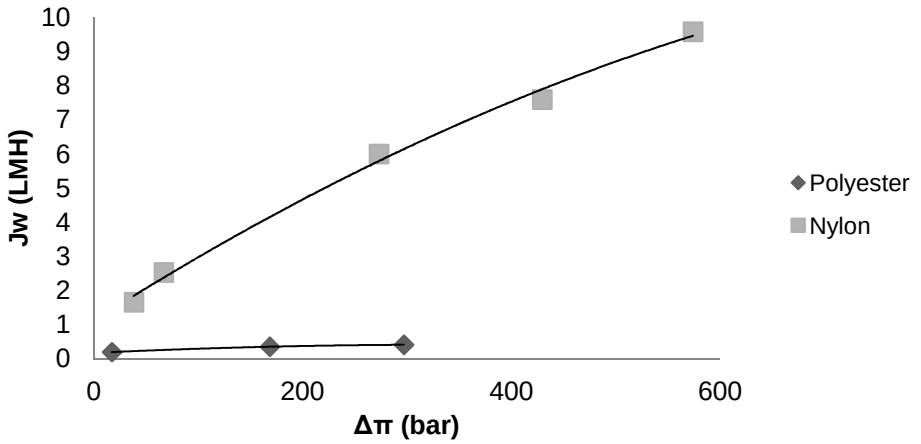

Figure 31 – Performance of the CA membranes prepared with different porous supports, test in PRO mode

The FO tests results show that changing the membrane support to polyester worsens the membrane performance, as was expected from the characteristics of the two membranes (see

Table 11). The internal CP becomes less severe for membranes with thinner and porous support layers due to their reduced mass transfer resistance (Tang, et al., 2010).

b. Membrane parameters

In Table 12 are presented the values of the base membrane parameters, with different porous supports.

Table 12- Parameters of the base CA membrane, with different porous supports.

Support	k_m (10^{-6}m.s^{-1})	S (mm)	τ
Nylon	4.9	0.28	1.56
Polyester	2.3	0.64	1.10

The results for the membrane parameters show that changing the membrane support layer as big influence in the structural parameter. It can be seen that the polyester support as a bigger value of S than the nylon support, which explains the several internal CP effect that the polyester support suffers, drastically reducing the water flux (see Figure 31).

Notice that changing the operation conditions (in this case the draw solute) as a expected slight influence in the membrane S value (Gray, et al., 2006; Park, et al., 2011), which in this case result in small increase (comparing with Table 10).

So, from the results obtained in this chapter was concluded that the best support for the FO experiments is the nylon support, so its utilization remained.

5.5. PEG-based hydrogel free-standing films characterization

Table 13 summarizes the water transport properties of free-standing films of the hydrogels used in this study. It can be seen that, for each series of samples, the water uptake (ω_w) and the volume fraction of water (v_w) increases as prepolymerization water content increases, also at the same water content, the equilibrium ω_w and $v_w$increases as the concentration of ethylene oxide units in the network increases (increasing Mw). In addition, the introduction of

the monomer PEG to the prepolymerization mixture (from the base 50%PEGDA) also increases the ω_w and the $v_w$of the films. This is due to the fact that these factors affect the crosslinking density of the polymer, removing/giving to the polymer network more mobility and freedom to swell. Regarding the variation of the UV-exposure time, for the 25wt% prepolymerization mixture, almost doesn't affect the water uptake of the polymers. In summary, increasing the water content in the prepolymerization mixture, using longer PEGDA or adding PEG to the prepolymerization mixture increases the equilibrium water uptake of the polymer as well as the volume fraction of water in the swollen network.

Table 13 – Water transport properties of free-standing hydrogel films

Entry nº	Polymer	Hydrogel	UV exposure (s)	ω_w (wt%)	v_w
1	PEGDA (Mw=575 g.mol^{-1})	25% PEGDA	90	275.9	0.75
2		25% PEGDA	150	267.4	0.76
3		25% PEGDA	300	267.8	0.75
4		50% PEGDA	150	103.2	0.54
5		70% PEGDA	150	60.4	0.40
6	PEGDA (Mw=700g.mol^{-1})	25% PEGDA	90	248.8	0.75
7		25% PEGDA	150	246.6	0.75
8		25% PEGDA	300	228.4	0.73
9		50% PEGDA	150	115.7	0.58
10		70% PEGDA	150	87.7	0.51
11		PEG35000/PEGDA	150	203.7	0.71
12		PEG3000/PEGDA	150	210.9	0.72

The NaCl transport properties of the free-standing films was characterized by kinetic desorption experiments, the results are show in Table 14.The results obtained are consistent with the water uptake results; the NaCl transport properties increase when the water content in the prepolymerization mixture increase, and with the addition of PEG in the prepolymerization mixture. However, for the content of 50wt% (in PEGDA Mn=700g.mol^{-1}), this linearity doesn't happened, the salt transport properties have the lowest values. Concerning the tests of UV-exposure time, it can be seen that varying the period of exposure affects the salt transport in the hydrogel. The PEGDA with low molecular weight shows an increase of salt diffusivity and permeability when the UV exposure time is increase from 90s to 150s, but when the exposure time is increased from 150s to 250 s both salt diffusivity and permeability decreases. The high

molecular weight polymer behaves differently, having the lowest value of salt diffusivity at an exposure time of 150 s, and the salt permeability increases with the exposure time. All of the salt diffusion coefficients in the hydrogel films are lower than the NaCl diffusivity in pure water (1.6 x 10^{-5} $cm^2.s^{-1}$, 25º C) which is reasonable. The partition coefficient has opposite behaviours for the two polymers, when the UV exposure time is varied. So when the exposure time increases, the K_s for the low molecular weight polymer decreases and for the high molecular weight increases. Summing up, adding water or PEG to the prepolymerization mixture decreases the crosslinking density thereby increasing NaCl diffusivity and permeability

Table 14 - Salt transport properties of free-standing hydrogel films

Entry nº	Polymer	Hydrogel	UV exposure (s)	D_s ($10^{-6}cm^2.s^{-1}$)	K_s ($\frac{g_{NaCl}/cm^3 film}{g_{NaCl}/cm^3 solution}$)	P_s ($10^{-7}cm^2.s^{-1}$)
1	PEGDA (Mw=575g.mol^{-1})	25% PEGDA	90	1.49	0.34	5.09
2		25% PEGDA	150	2.39	0.31	7.36
3		25% PEGDA	300	2.25	0.25	5.63
4		50% PEGDA	150	0.51	0.13	0.67
5		70% PEGDA	150	1.20	0.04	0.54
6	PEGDA (Mw=700g.mol^{-1})	25% PEGDA	90	0.64	0.10	0.65
7		25% PEGDA	150	0.28	0.25	0.72
8		25% PEGDA	300	0.38	0.39	1.52
9		50% PEGDA	150	0.006	0.20	0.01
10		70% PEGDA	150	1.05	0.05	0.54
11		PEG35000/PEGDA	150	0.20	0.60	1.22
12		PEG3000/PEGDA	150	0.02	0.27	0.06

The partition coefficient data were compared to the model proposed by Yasuda et al (Yasuda, et al., 1968), where the free volume of polymer/diluent system can be expressed by:

$$K_s = K_p \nu_p + K_w \nu_w \qquad (58)$$

Where K_s is the measured NaCl solubility coefficient, K_p and K_w are the partition coefficients of the polymer and water respectively, and ν_p and ν_w are the volume fractions of polymer and water, respectively, in the swollen polymer. If the NaCl will not permeate through the polymer

matrix by itself, K_p would be zero. Also, K_w is by definition one. Therefore equation (60) is simplified to (Yasuda, et al., 1968):

$$K_s = \nu_w \qquad (59)$$

Where in this case, ν_w is the water volume fraction measured.

In Figure 32 the NaCl partition coefficient is related to the water volume fraction. As is shown the measured partition coefficients are near bellow the line given by equation (59), so the concentration of salt dissolved in most of the hydrogel is slightly less than predicted by the latter model outlined. Thus, these hydrogels acts to exclude some salt from their network. These results indicate that the materials exhibit some solubility selectivity to water over NaCl, which is important for desalination membrane coatings.

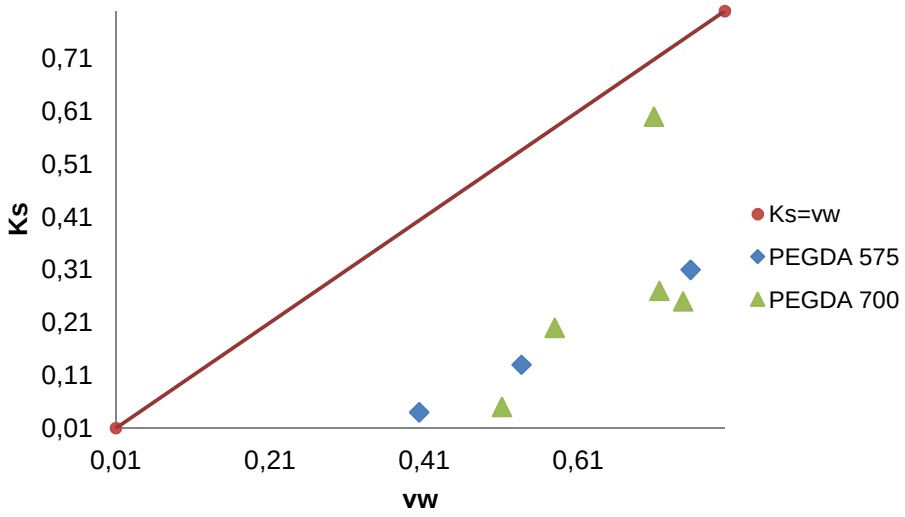

Figure 32 – Correlation between NaCl partition coefficients and polymer water volume fractions

From the results obtained the high molecular weight polymer was chosen, because presented the lowest values for salt transport properties and still, a high water uptake. The UV exposure time selected was 150 s because the water uptake maintains high and the salt transport properties have the values between 90s and 300 s.

5.6. The influence of PEG-based hydrogel coatings on membrane performance

a. Membrane morphology observations

The membranes surface morphology was analysed by digital microscope (DM) and scanning electron microscopy (SEM).

Digital microscope images

The membranes surface morphologies were observed by digital microscope analysis, the results are shown in Figure 33 and Figure 34.

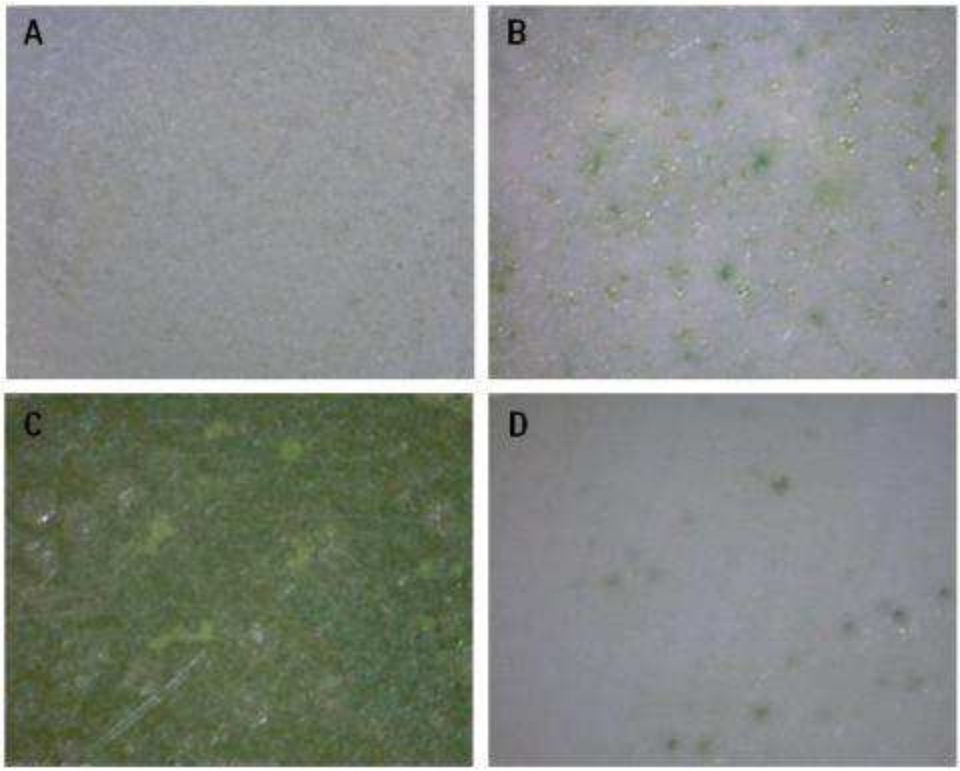

Figure 33 – Digital microscope images of top surface morphology, at 200x, of the A) untreated membrane; B) membrane with one PEDGA (prepolymerization mixture of 50wt% PEGDA) top coating; C) membrane soaked for 2 hours on a PEGDA solution; D) membrane with one top coat (prepolymerization mixture of PEG35000/PEGDA)

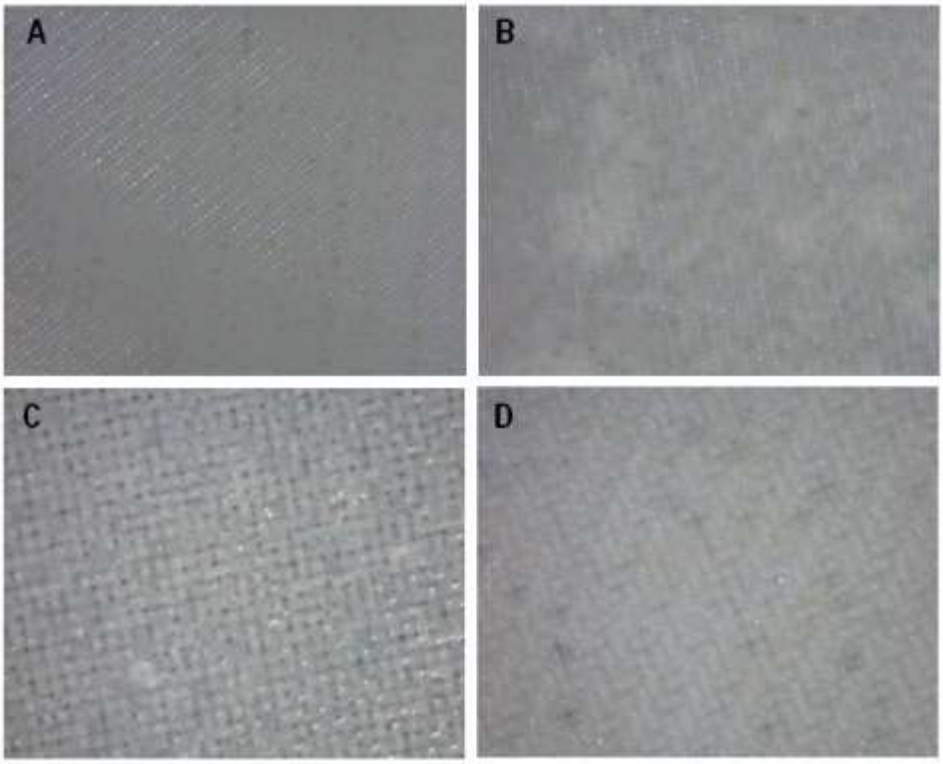

Figure 34 - Digital microscope images of bottom surface morphology, at 200x, of the A) untreated membrane; B) membrane with one PEDGA (prepolymerization mixture of 50wt% PEGDA) bottom coating; C) membrane soaked for 2 hours on a PEGDA solution; D) membrane with one bottom coat (prepolymerization mixture of PEG35000/PEGDA)

From the images obtained, is clear the presence of hydrogel on the treated membranes. However it can be seen, that some of the treatments used, do not generate a uniform hydrogel film. In the case where the membranes have one coat bottom/top (Figure 33 B and Figure 34 B) it is clear that some zones have a higher amount of hydrogel than others. When the membrane is soaked in the hydrogel solution, it can be seen that the amount of hydrogel on the membrane increases and the film is more uniform. In order to create a more uniform coating, the prepolymerization viscosity was increased by adding the monomer PEG. The membranes prepared with one coat bottom/top of the PEG35000/PEGDA solution, show a more thick and uniform film, which corresponds to a big improvement of the coating morphology; however, because the prepolymerization mixture is very viscous it is difficult to remove/avoid air bubbles in the solution (Figure 33 D) which creates small defects on the hydrogel film.

Scanning electron microscopy images

Images of the membranes surface and cross-section were observed by SEM.

Figure 35 shows the top surface of the untreated membrane and the membranes with top coatings. As can be seen, the modified membranes have a smoother and nearly defect-free surface, unlike the unmodified membrane. Both pore narrowing and pore blocking because of surface modification were observed. Adding PEG to the prepolymerization mixture (i.e. increase the solution viscosity) have great effect on the uniformity of the coating, increasing it. Unfortunately, the coating is not totally defect-free (see Figure 33 D) due to air bubbles trapped in the polymer solution and some “cracks” formed with the hydrogel formation.

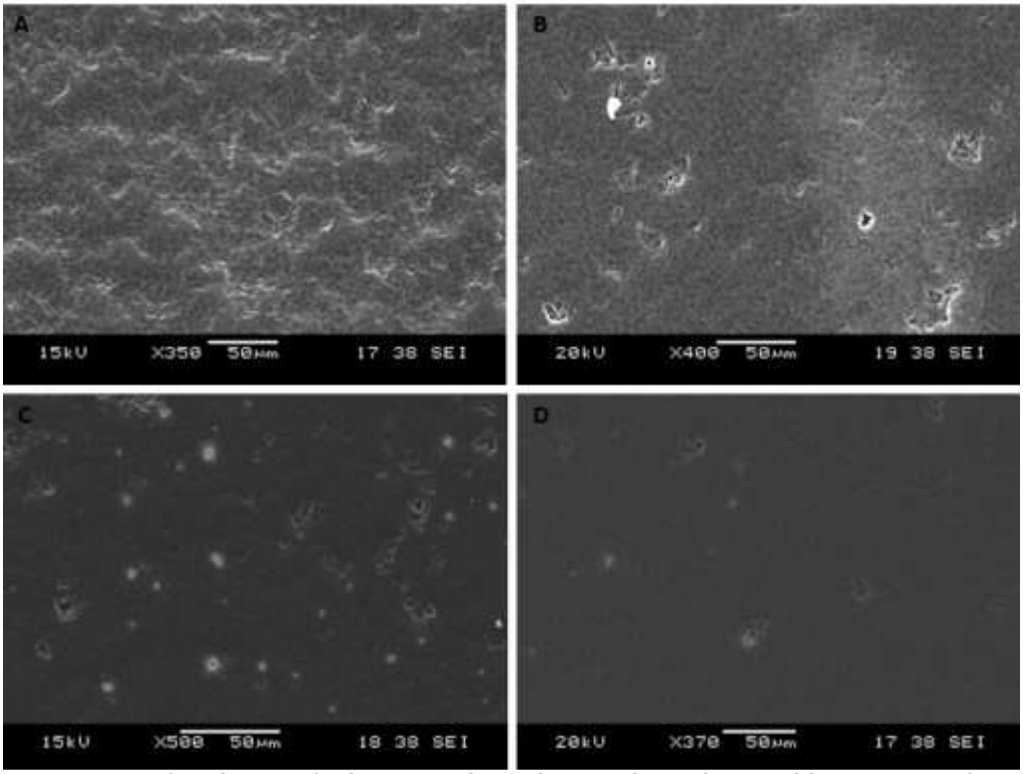

Figure 35- Top surface image of: A) untreated membrane, B) Membrane with a top coat of 50% PEGDA, C) Membrane with a top coat of PEG3000/PEGDA, D) Membrane with a top coat of PEG35000/PEGDA

In Figure 36 is presented the untreated and top coated membranes cross-section. From the images obtained, it can be distinguished the dense hydrogel layer formed on the top of the membrane. The thickness of the membranes coatings is between 2-5 µm. The membrane prepared with 3 coatings (Figure 36 C) does not show thicker coating comparing to the other pictures. Also it can be seen that the membrane prepared with the PEG with high molecular

weight (Figure 36 E) as a thicker and denser coating. Unfortunately, the low resolution of the SEM does not allowed to see a clearer picture of the hydrogel coating.

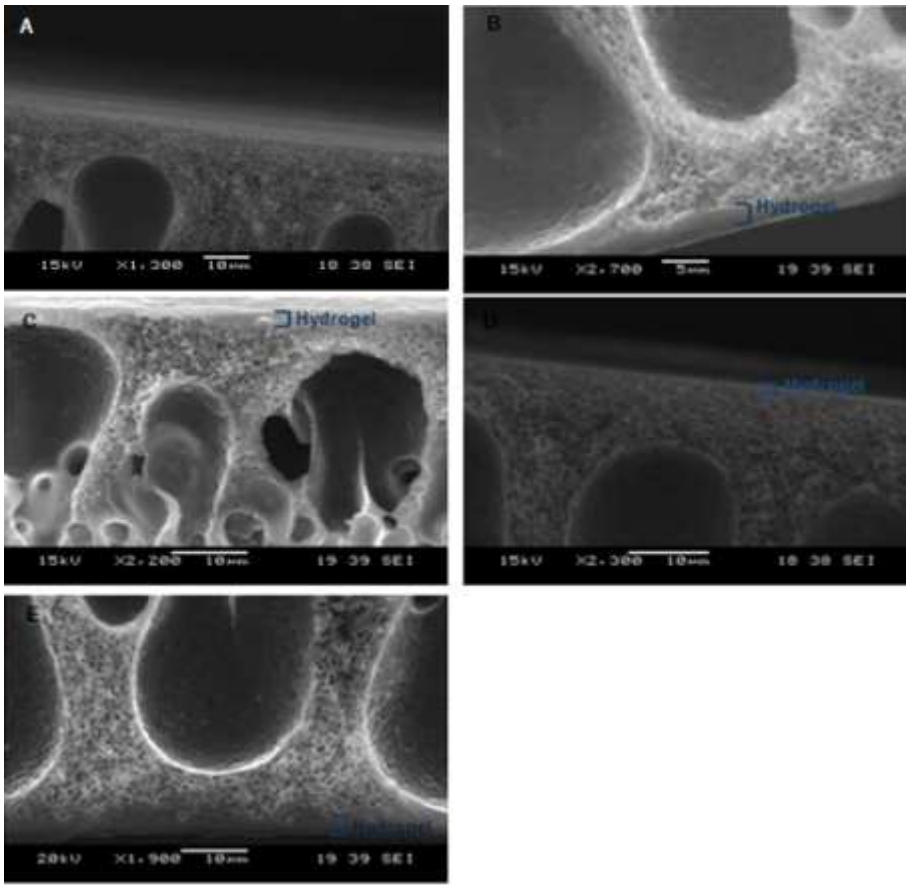

Figure 36 - Cross-section image of: A) untreated membrane, B) Membrane with a top coat of 50% PEGDA, C) Membrane with 3 top coatings of 50% PEGDA D) Membrane with a top coat of PEG3000/PEGDA, E) Membrane with a top coat of PEG35000/PEGDA

The SEM images of the bottom surface of the untreated and bottom coated membranes are presented in Figure 37. From the images obtained, it can be seen that there is no uniform coating formed, which means that the hydrogel sinks through the membrane support. Also it can be seen, that the support fibbers from the treated membranes (Figure 37 B and C) appear to a have a coating (brighter zone), which can be due to the presence of hydrogel.

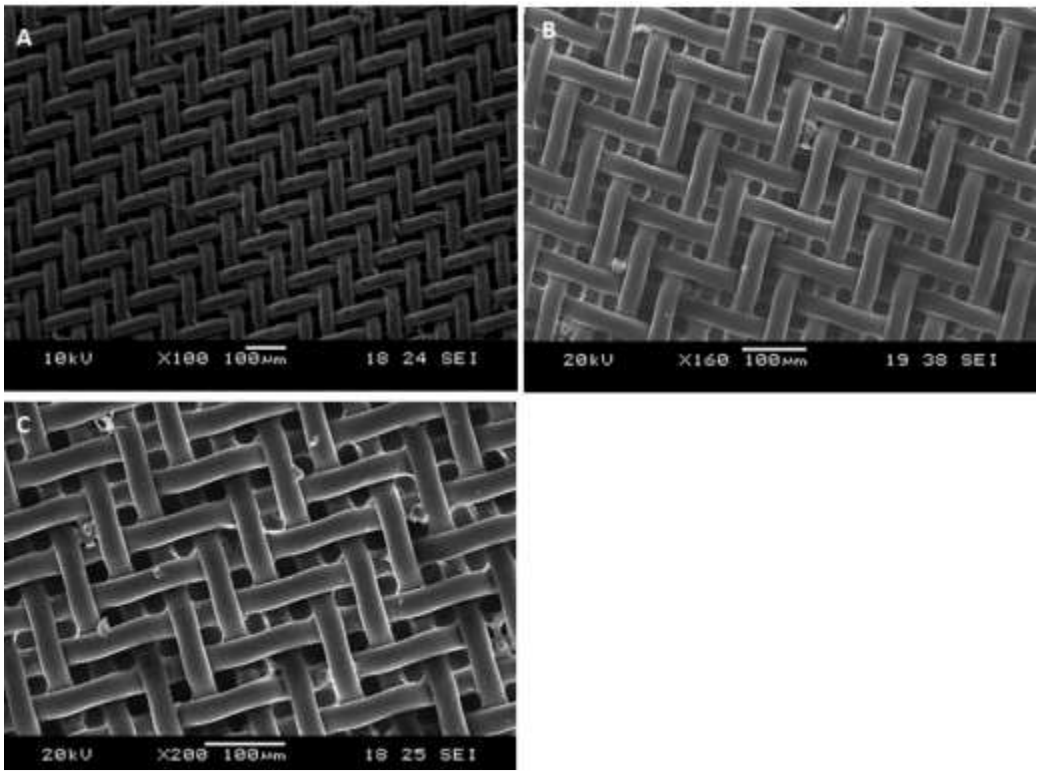

Figure 37 – Bottom surface image of: A) untreated membrane, B) Membrane with a bottom coat of 50% PEGDA, C) Membrane with a bottom coat of PEG35000/PEGDA

It should be notice that all SEM images were obtained in dry state; during FO the hydrogel of the modified membranes would be in a swollen state and its structure would significantly differ from the images in dry state. A possible solution to catch a more accurate image is by using an environmental scanning electron microscope (ESEM), which allows the option of collecting electron micrographs of materials wet and uncoated.

b. The influence of the hydrogel thickness in water flux

Figure 38 shows the influence of the hydrogel free-standing films thickness over the water flux, as expected the flux decreases with thickness. From the results obtained from SEM pictures (see Figure 36) is known that the membrane thickness is somewhere between 2-5 µm, so even if the difference in thickness is small the influence in water flux can be great.

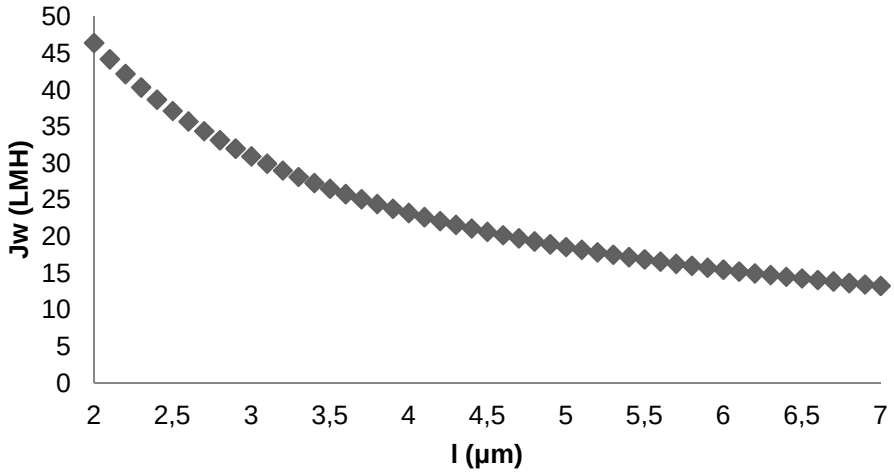

Figure 38 - The influence of hydrogel thickness in water flux

c. Thermogravimetric analisys

The weight loss of the individual compounds of the membranes and the membranes versus temperature were investigated by TGA, the results are shown in Figure 39 and 40 respectively.

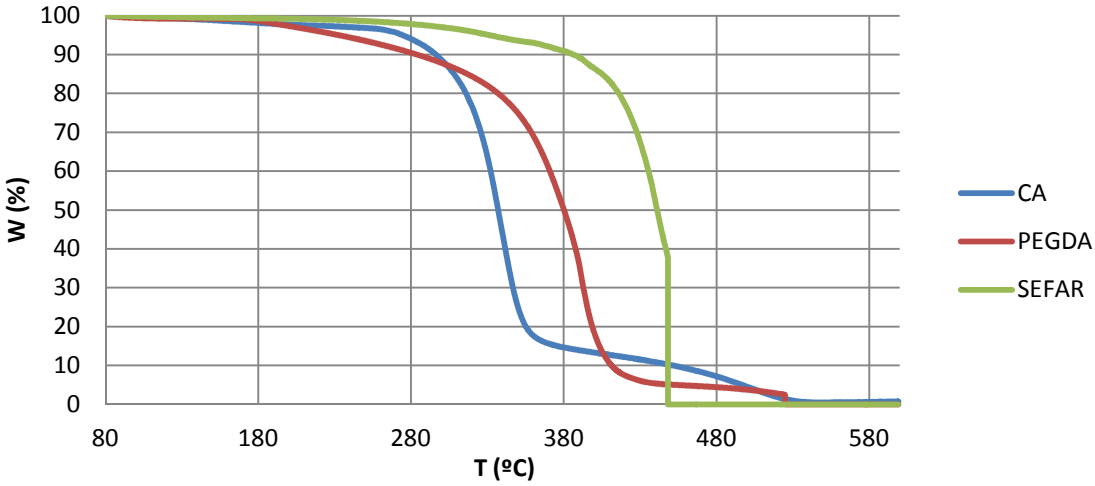

Figure 39- TGA curves of the individual membrane components

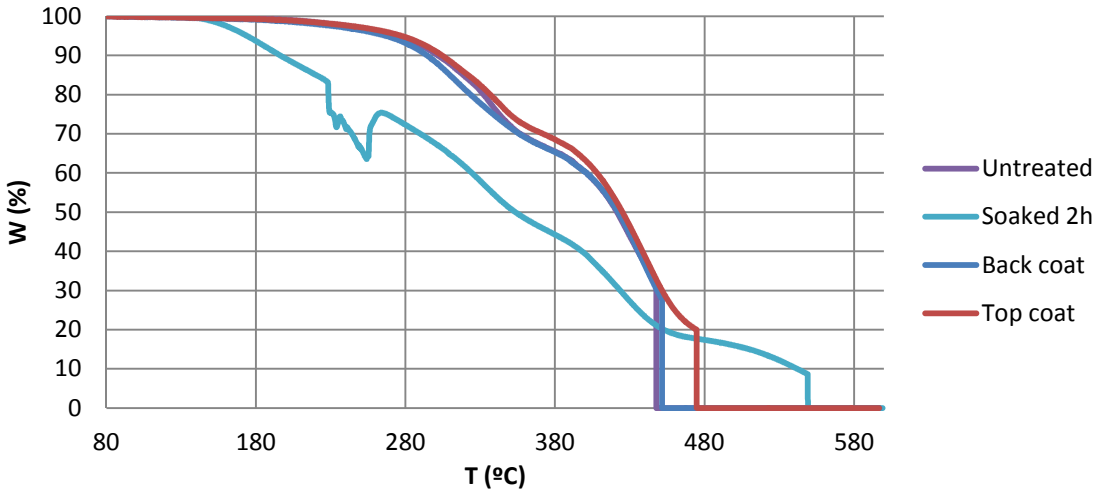

Figure 40 – TGA curves of the untreated membrane and the membranes prepared with different hydrogels impregnations techniques (coating and soaking)

Figure 39 shows the results of the individual components of the membrane, as it can be seen the decomposition temperature gap of the 3 components overlaps, between 280-400ºC, differing only in the rate of weight loss. Cellulose acetate loses more quickly than the other components, and the SEFAR support loses more slowly.

The membranes analysis results, in Figure 40, shows that the membranes with the hydrogel coatings have similar behavior as the untreated membrane meaning that the amount of hydrogel in the membrane is very small. In the case of the membrane soaked for two hours in a hydrogel solution show a bigger weight loss than the others, meaning that the amount of hydrogel impregnated in the membrane is superior, between 10-20% of the total mass of the membrane.

d. Coated membranes performance

The water flux and permeability were evaluated for the different hybrid CA membranes. Both sides of the membrane were tested in crossflow mode. The draw solution, for all experiments, was 47.6 $g.L^{-1}$ $MgCl_2$ and the feed was DIW or 35 $g.L^{-1}$ NaCl .The tests results are shown in Table 15 - 10. To minimize the errors due to the mass balance differences from the balances, the fluxes and permabilities showed correspond to the average flux between, the flux calculate from the weight change in the feed side and the draw side. Also, the first minutes of every

experience weren't considered because, in most cases, the first values didn't match with the behaviour of the other values.

The results of the membranes performance will be separated according to the type of treatment used, to be easier to understand

Membrane with a top coat

Table 15 present the performance results for the membranes prepared with one coating on the active layer.

Table 15- Performance of CA membrane, untreated and prepared with 1 coating on the top of the active layer.

Entry nº	Membrane	Feed solution	Draw solution	J_W (LMH)	A_W (LMH.bar^{-1})	R (%)
1	Untreated	DIW	0.5 M $MgCl_2$	4.91 ± 0.07	0.12 ± 0.002	-
2		0.6 M NaCl	0.5 M $MgCl_2$	0.95 ± 0.08	0.06 ± 0.005	92.1 ± 2.3
3	1 coating **top** 25%PEGDA(Mw=700)	DIW	0.5 M $MgCl_2$	3.91 ± 0.27	0.10 ± 0.008	-
4		0.6 M NaCl	0.5 M $MgCl_2$	0.80 ± 0.01	0.05 ± 0.001	99.2 ± 0.8
5	1 coating **top** 50%PEGDA(Mw=700)	DIW	0.5 M $MgCl_2$	5.73 ± 0.65	0.15 ± 0.020	-
6		0.6 M NaCl	0.5 M $MgCl_2$	1.90 ± 0.18	0.12 ± 0.016	99.8 ± 0.0
7	1 coating **top** 75%PEGDA(Mw=700)	DIW	0.5 M $MgCl_2$	4.56 ± 0.42	0.11 ± 0.011	-
8		0.6 M NaCl	0.5 M $MgCl_2$	1.39 ± 0.27	0.09 ± 0.018	99.7 ± 0.3
9	1 coating **top** PEG3000/PEGDA	DIW	0.5 M $MgCl_2$	5.14 ± 0.22	0.13 ± 0.006	-
10		0.6 M NaCl	0.5 M $MgCl_2$	1.14 ± 0.18	0.07 ± 0.012	98.4 ± 0.8
11	1 coating **top** PEG35000/PEGDA	DIW	0.5 M $MgCl_2$	3.77 ± 0.21	0.09 ± 0.005	-
12		0.6 M NaCl	0.5 M $MgCl_2$	0.98 ± 0.01	0.06 ± 0.001	98.1 ± 1.1

Entry nº	Membrane	Feed solution	Draw solution	J_W (LMH)	A_W (LMH.bar^{-1})	R (%)
1	Untreated	DIW	0.5 M $MgCl_2$	3.54 ± 0.41	0.09 ± 0.011	-
2		0.6 M NaCl	0.5 M $MgCl_2$	0.82 ± 0.08	0.05 ±0.005	93.9 ± 2.5
3	1 coating **top** 25%PEGDA(Mw=700)	DIW	0.5 M $MgCl_2$	3.17 ± 0.06	0.06 ± 0.013	-
4		0.6 M NaCl	0.5 M $MgCl_2$	0.71 ± 0.08	0.04 ± 0.004	100 ± 0.0
5	1 coating **top** 50%PEGDA(Mw=700)	DIW	0.5 M $MgCl_2$	4.67 ± 0.16	0.11 ± 0.002	-
6		0.6 M NaCl	0.5 M $MgCl_2$	2.15 ± 0.95	0.13 ± 0.061	99.6 ± 0.4
7	1 coating **top** 75%PEGDA(Mw=700)	DIW	0.5 M $MgCl_2$	3.90 ± 0.47	0.10 ± 0.012	-
8		0.6 M NaCl	0.5 M $MgCl_2$	1.10 ± 0.31	0.07 ± 0.021	100 ± 0.0
9	1 coating **top** PEG3000/PEGDA	DIW	0.5 M $MgCl_2$	4.09 ± 0.32	0.10 ± 0.010	-
10		0.6 M NaCl	0.5 M $MgCl_2$	1.30 ± 0.11	0.09 ± 0.020	97.3 ± 0.6
11	1 coating **top** PEG35000/PEGDA	DIW	0.5 M $MgCl_2$	3.72 ± 0.09	0.09 ± 0.002	-
12		0.6 M NaCl	0.5 M $MgCl_2$	0.71 ± 0.18	0.04 ± 0.011	98.3 ± 1.2

The FO experimental results demonstrate that coating hydrogel on the active layer of CA membrane affects the membrane rejection positively. Most of the results show a rejection of 100% and some show an improvement of salt rejection. In some membranes the rejection

results have significant values of standard deviations, which is not good for desalination membrane. These results can be explained by the non-uniformity of the hydrogel coating layer (see section5.6 a), which may cause the variation of the rejection results. The membranes PEG3000/PEGDA and PEG35000/PEGDA show an improvement in the salt rejection (comparing to the untreated membrane), but also without a constant value. These results were not expected since the coating film appeared to be more uniform than the latter treatments (see section 5.6 a). However it was possible to verify that small air bubbles trapped in the prepolymerization solution cause some imperfections on the hydrogel layer which could affect the final rejection.

Figure 41 shows the effect of the hydrogel top coating on the membrane flux. In general, the water flux of the treated membranes is almost the same as the untreated membrane. However when the coating used is PEGDA 50% the water flux shows an improvement of 100% from the original water flux. The addition of the monomer PEG to this prepolymerization solution, decreases slightly the water flux, comparing to the results for the original solution, this can be explained by the increasing thickness of the coating.

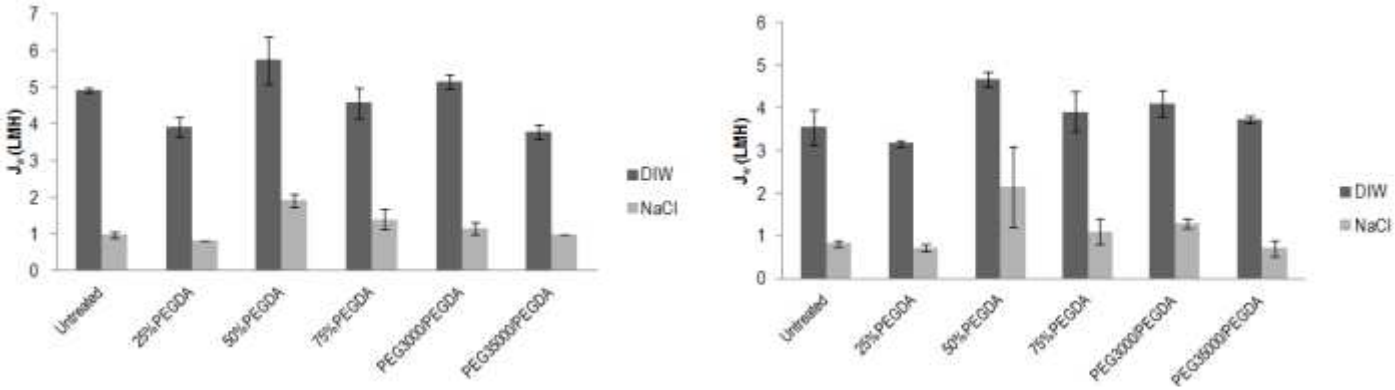

Figure 41- Effect of the hydrogel top coating on the membrane flux; left side PRO mode and right side FO mode

Membrane with a bottom coat

The FO performance results for the membranes with one coat on the bottom surface are presented in Table 16.

Table 16 - Performance of CA membrane, untreated and prepared with 1 coating on the top of the porous support layer.

Entry nº	Membrane	Feed solution	Draw solution	J_W (LMH)	A_W (LMH.bar^{-1})	R (%)
1	Untreated	DIW	0.5 M $MgCl_2$	4.91 ± 0.07	0.12 ± 0.002	-
2		0.6 M NaCl	0.5 M $MgCl_2$	0.95 ± 0.08	0.06 ± 0.005	92.1 ± 2.3
3	1 coating **bottom**	DIW	0.5 M $MgCl_2$	4.98 ± 0.12	0.13 ± 0.003	-
4	25%PEGDA(Mw=700)	0.6 M NaCl	0.5 M $MgCl_2$	1.31 ± 0.09	0.08 ± 0.005	97.9 ± 0.2
5	1 coating **bottom**	DIW	0.5 M $MgCl_2$	7.49 ± 0.20	0.19 ± 0.013	-
6	50%PEGDA(Mw=700)	0.6 M NaCl	0.5 M $MgCl_2$	2.13 ± 0.07	0.14 ±0.006	98.6 ± 0.2
7	1 coating **bottom**	DIW	0.5 M $MgCl_2$	3.99 ± 0.39	0.10 ± 0.010	-
8	75%PEGDA(Mw=700)	0.6 M NaCl	0.5 M $MgCl_2$	1.14 ± 0.31	0.07 ±0.020	99.4 ±0.6
9	1 coating **bottom**	DIW	0.5 M $MgCl_2$	4.87 ± 0.40	0.12 ± 0.011	-
10	PEG3000/PEGDA	0.6 M NaCl	0.5 M $MgCl_2$	1.23 ±0.03	0.08 ± 0.002	95.4 ± 4.2
11	1 coating **bottom**	DIW	0.5 M $MgCl_2$	3.87 ± 0.16	0.10 ± 0.004	-
12	PEG35000/PEGDA	0.6 M NaCl	0.5 M $MgCl_2$	1.08 ± 0.17	0.07 ± 0.011	98.7 ± 1.3

Entry nº	Membrane	Feed solution	Draw solution	J_W (LMH)	A_W (LMH.bar^{-1})	R (%)
1	Untreated	DIW	0.5 M $MgCl_2$	3.54 ± 0.41	0.09 ± 0.011	-
2		0.6 M NaCl	0.5 M $MgCl_2$	0.82 ± 0.08	0.05 ±0.005	93.9 ± 2.5
3	1 coating **bottom**	DIW	0.5 M $MgCl_2$	3.91 ± 0.19	0.08 ± 0.017	-
4	25%PEGDA(Mw=700)	0.6 M NaCl	0.5 M $MgCl_2$	1.07 ± 0.04	0.08 ± 0.016	99.2 ± 0.9
5	1 coating **bottom**	DIW	0.5 M $MgCl_2$	5.06 ± 0.09	0.13 ± 0.003	-
6	50%PEGDA(Mw=700)	0.6 M NaCl	0.5 M $MgCl_2$	1.63 ± 0.07	0.11 ± 0.006	99.6 ±0.4
7	1 coating **bottom**	DIW	0.5 M $MgCl_2$	3.24 ± 0.28	0.08 ± 0.008	-
8	75%PEGDA(Mw=700)	0.6 M NaCl	0.5 M $MgCl_2$	0.77 ± 0.06	0.05 ± 0.004	99.9 ± 0.1
9	1 coating **bottom**	DIW	0.5 M $MgCl_2$	3.73 ± 0.02	0.09 ±0.001	-
10	PEG3000/PEGDA	0.6 M NaCl	0.5 M $MgCl_2$	0.93 ± 0.07	0.06 ± 0.005	98.6 ± 0.8
11	1 coating **bottom**	DIW	0.5 M $MgCl_2$	3.72 ± 0.39	0.09 ± 0.010	-
12	PEG35000/PEGDA	0.6 M NaCl	0.5 M $MgCl_2$	0.69 ± 0.12	0.04 ± 0.001	99.5 ± 0.8

The results obtained show an improvement in the salt rejection, although without a constant value for each treatment. These results can be explained by the non-uniformity of the hydrogel coating layer (see section 5.6 a), which may cause the variation of the rejection results. The worst result was observed with the concentration of 25%PEGDA (PRO mode), which can be explained by the salt transport properties in the hydrogel, which as the highest values for this mixture (see section 5.5). For the membranes prepared with a mixture PEG/PEGDA, the results obtained show an improvement in the salt rejection, without a constant value for each treatment. These results can be explained by the images obtained from SEM (see section 5.6 a); the

uneven coating formed when the membrane is coated on the bottom (the hydrogel sinks through the porous support) and the small air bubbles trapped in the prepolymerization solution causing some imperfections on the hydrogel layer, which could affect the final rejection.

The water fluxes results for the membranes with one coat on the bottom are presented in Figure 42. In general, the water flux of the treated membranes does not change. However, the membrane coated with the prepolymerization mixture of 50%PEGDA, show an improvement of 120% from the original flux value. This improvement can be explained by the good results obtained by this hydrogel (see section 5.5). Again, the addition of PEG to the prepolymerization show a decrease in the water flux comparing to the original solution.

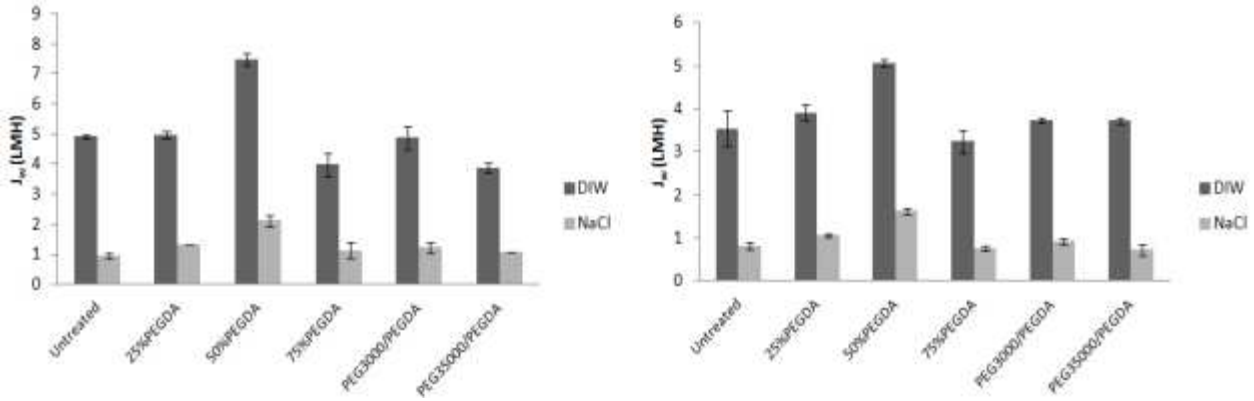

Figure 42 - Effect of the hydrogel bottom coating on the membrane flux; left side PRO mode and right side FO mode

Membrane prepared with 3 coatings

The results obtained for the membranes prepared with 3 coatings are show in Table 17.

Table 17- Performance of CA membrane, untreated and prepared with 3 coating on the top/bottom

PRO mode

Entry nº	Membrane	Feed solution	Draw solution	J_W (LMH)	A_W (LMH.bar^{-1})	R (%)
1	Untreated	DIW	0.5 M $MgCl_2$	4.91 ± 0.07	0.12 ± 0.002	-
2		0.6 M NaCl	0.5 M $MgCl_2$	0.95 ± 0.08	0.06 ± 0.005	92.1 ± 2.3
3	3 coatings **top** 25%PEGDA(Mw=700)	DIW	0.5 M $MgCl_2$	3.77 ± 0.39	0.09 ± 0.010	-
4		0.6 M NaCl	0.5 M $MgCl_2$	0.80 ± 0.10	0.05 ± 0.006	99.4 ± 0.6
5	3 coatings **bottom** 25%PEGDA(Mw=700)	DIW	0.5 M $MgCl_2$	4.31 ± 0.14	0.10 ± 0.01	-
6		0.6 M NaCl	0.5 M $MgCl_2$	1.12 ± 0.12	0.07 ± 0.013	98.9 ± 0.9
7	3 coatings **top** 50%PEGDA(Mw=700)	Damaged by the hydrogel -				
8	3 coatings **bottom** 50%PEGDA(Mw=700)	DIW	0.5 M $MgCl_2$	4.41 ± 0.22	0.10 ± 0.013	-
9		0.6 M NaCl	0.5 M $MgCl_2$	1.12 ± 0.11	0.07 ± 0.013	98.9 ± 0.1
10	3 coatings **top/bottom** 75%PEGDA(Mw=700)	Damaged by the hydrogel				

FO mode

Entry nº	Membrane	Feed solution	Draw solution	J_W (LMH)	A_W (LMH.bar^{-1})	R (%)
1	Untreated	DIW	0.5 M $MgCl_2$	3.54 ± 0.41	0.09 ± 0.011	-
2		0.6 M NaCl	0.5 M $MgCl_2$	0.82 ± 0.08	0.05 ±0.005	93.9 ± 2.5
3	3 coatings **top** 25%PEGDA(Mw=700)	DIW	0.5 M $MgCl_2$	3.25 ± 0.54	0.08 ± 0.014	-
4		0.6 M NaCl	0.5 M $MgCl_2$	0.60 ± 0.17	0.04 ± 0.01	99.8 ± 0.2
5	3 coatings **bottom** 25%PEGDA(Mw=700)	DIW	0.5 M $MgCl_2$	3.78 ± 0.14	0.09 ± 0.003	-
6		0.6 M NaCl	0.5 M $MgCl_2$	0.82 ± 0.04	0.05 ± 0.003	99.9 ± 0.1
7	3 coatings **top** 50%PEGDA(Mw=700)	Damaged by the hydrogel				
8	3 coatings **bottom** 50%PEGDA(Mw=700)	DIW	0.5 M $MgCl_2$	3.54 ± 0.58	0.08 ± 0.013	-
9		0.6 M NaCl	0.5 M $MgCl_2$	0.76 ± 0.13	0.04 ± 0.012	98.8 ± 1.2
10	3 coatings **top/bottom** 75%PEGDA(Mw=700)	Damaged by the hydrogel				

The membranes treated show an improvement in salt rejection (comparing to the untreated membrane), although without a constant value for each treatment. These results shows that, increasing the number of coatings of hydrogel do not make the hydrogel layer more uniform.

Figure 43 show the influence of the 3 coatings treatment on the membrane performance. The water flux is almost the same for all the membranes, which means that increasing the number of coatings does not provoke changes in the membranes performance.

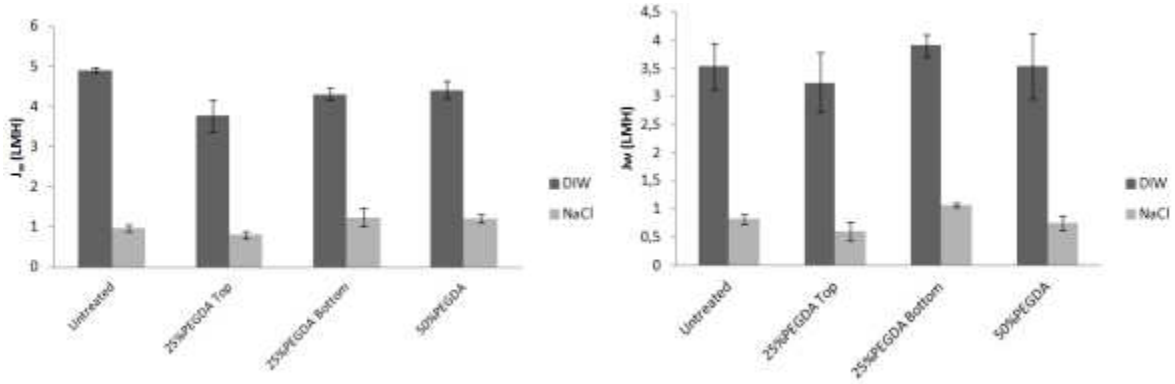

Figure 43- Effect of the 3 coatings of hydrogel on the membrane flux; left side PRO mode and right side FO mode

Membranes prepared by soaking

Table 18 show the results obtained for the membranes treated by soaking in the FO system.

Table 18- Performance of CA membrane, untreated and prepared by soaking

Entry nº	**Membrane Orientation**	**Membrane**	**Feed solution**	**Draw solution**	**J_W (LMH)**	**A_W (LMH.bar^{-1})**	**R (%)**
1	PRO	Untreated	DIW	0.5 M $MgCl_2$	4.91	0.12	-
2			0.6 M NaCl	0.5 M $MgCl_2$	0.95	0.06	92.1 ± 2.3
3	PRO	25%PEGDA (Mw=700)	DIW	0.5 M $MgCl_2$	No Flux		
4			DIW	1.5 M $MgCl_2$	0.37	0.002	N/A
6	-	50%PEGDA (Mw=700)	Damaged by the hydrogel				
7	-	75%PEGDA (Mw=700)	Damaged by the hydrogel				

The results obtained show a significantly decrease in the water fluxes reaching almost zero. Also, most of the membranes prepared cannot stand the amount of hydrogel impregnated, becoming damaged. These results show that soaking is not a good technique treatment.

Water flux vs osmotic pressure

Since the 50%PEGDA coated membranes show the best performance (the greatest water flux and a constant value for rejection), they were chosen to test the influence of increasing driving force in membrane performance. Figure 44 shows the results obtained for these experiments.

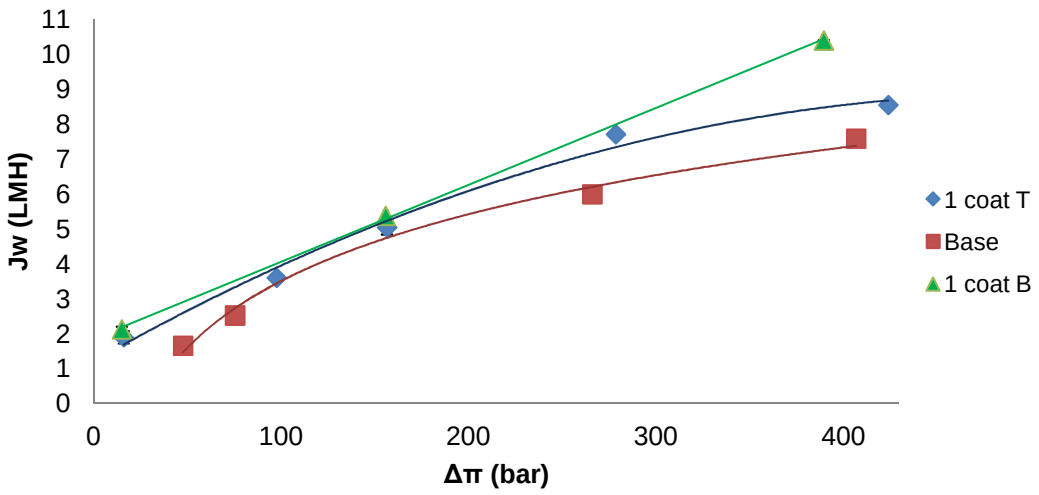

Figure 44 – 50% Coated and base membrane performance over a range of osmotic pressure differences; PRO mode

From the results obtained it can be seen that the treatment which is not affected by the increasing osmotic diving force (less influenced by the internal CP effects) is the membrane bottom coated, because part of the pores are covered/filled with hydrogel, reducing the concentrative internal CP effect.

The membrane top coated shows a slightly improvement in water flux (comparing to the base membrane), however with the increasing driving force the flux tends to decline, due to the internal CP effects in the membrane porous support (concentrative internal CP).

For an efficient FO desalination process, it is also imperative that salt rejection be high. Rejection data for the latter experiments is presented in Table 19.

Table 19- Water flux and NaCl rejection results for the FO runs carried out under settled feed solution concentration and increasing draw solution concentration (PRO mode)

1 coating **Top** 50%PEGDA (Mw=700)					
C_F (M)	**C_D (M)**	**$\Delta\pi$ (bar)**	**J_w (LMH)**	**A_w (LMH.bar^{-1})**	**R (%)**
0.6	0.5	16.1	1.90	0.12	99.8
0.6	1.0	97.7	3.60	0.03	99.4
0.6	1.5	156.6	5.05	0.03	99.6
0.6	2.6	278.6	7.71	0.03	N/A
0.6	3.7	423.9	8.55	0.02	N/A

1 coating **Bottom** 50%PEGDA (Mw=700)					
C_F (M)	**C_D (M)**	**$\Delta\pi$ (bar)**	**J_w (LMH)**	**A_w (LMH.bar^{-1})**	**R (%)**
0.6	0.5	15.1 ± 0.1	2.13 ± 0.07	0.14	98.6
0.6	1.5	155.9	5.38	0.03	99.2
0.6	3.7	389.5	10.40	0.03	99.3

The results indicate that NaCl rejection increases with increasing water flux. However, for the top coated membrane the rejection value is almost constant. The increasing rejection is due to the “dilution effect” (McCutvheon, et al., 2006), which occurs when water flux is increased without a subsequent increase in salt flux. Increasing the osmotic pressure driving force only affects water flux and not the salt flux, and rejection is thereby improved (McCutvheon, et al., 2006).

Salt concentration in the permeate as a function of time

The membrane with more constant value of rejection, 50 % top coated, was chosen to test the evolution of salt concentration in draw solution with time; the results are presented in Figure 45.

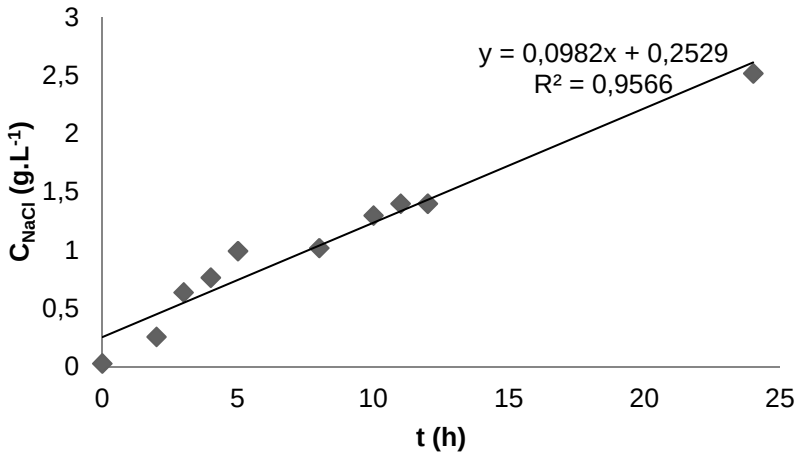

Figure 45 – Draw solution salt concentration over time; performance of 50% coated membrane

The results obtained show that the evolution of salt concentration in the draw solution through time is constant, i. e., the amount of salt passing with the permeate water in the first hour is the same as after twenty four hours of operation. This means that the hydrogel coating does not loose properties during the FO experiments.

e. Coated membranes water transport properties

In Table 20 are presented the membrane contact angle results. The contact angle characterizes the membrane relative surface hydrophilicity (Ju, et al., 2009).

Table 20 – Membrane contact angle measurements

Membrane	Contact angle (°)
Untreated	57.0 ± 1.7
25%PEGDA	45.8 ± 3.5
50%PEGDA	33.6 ± 2.1
75%PEGDA	37.2 ± 1.6
PEG3000/PEGDA	31.6 ± 5.8
PEG35000/PEGDA	39.3 ± 3.1

The results obtained show that treating the membrane with hydrogel improves the membrane affinity to water, i.e. hydrophilicity. For the films prepared, the contact angle decreases as prepolymerization water content decreases. The addition of the monomer PEG to the prepolymerization mixture, maintaining the same prepolymerization water content, does not affect significantly the coating surface hydrophilicity.

The membrane with high hydrophilic properties is 50%PEGDA. This high affinity to water can explain the water flux results obtained, which show an increase for both top and bottom.

The membranes water uptake values are present in Table 21.

Table 21 – Membrane water uptakes.

Membrane	ω (wt%)
Untreated	94.9 ± 14.2
25%PEGDA **Top**	108.1 ± 2.3
25%PEGDA **Bottom**	94.9 ± 2.3
25% PEGDA **3 coat Top**	108.1 ± 10.5
25% PEGDA **3 coat Bottom**	97.0 ± 0.7
50%PEGDA **Top**	132.5 ± 0.5
50%PEGDA **Bottom**	130.4 ± 39.5
50%PEGDA **3 coat Bottom**	120.4 ± 4.0
75%PEGDA **Top**	120.1 ± 24.1
75%PEGDA **Bottom**	130.9 ± 11.5
PEG3000/PEGDA **Top**	104.2 ± 4.2
PEG3000/PEGDA **Bottom**	98.1 ± 9.0
PEG35000/PEGDA **Top**	104.0 ± 2.3
PEG35000/PEGDA **Bottom**	107.3 ± 3.7

The results obtained show that the hydrogel films change their properties when used as coatings, i.e. the linearity between the water content in the prepolymertization mixture and the water uptake of the coating is not manifested.

The membranes with higher water uptake (50% PEGDA top and bottom) also have the highest value of water flux, which can be also a possible explanation for these results.

The 25% PEGDA treatments show that increasing the number of coatings doesn't change the water uptake of the membranes, and also the water flux. In the case of 50%PEGDA, the water uptake decreases slightly with the number of coatings and also the water flux, this situation can be explained by the fact that the 3 coatings have more tight structure than just one coating.

An important thing to notice is the standard deviation values of the water uptake, which are very high, showing that the coating preparation is difficult to replicate.

Comparing the results from Table 20 and 21, it can be seen that the membranes with higher water uptake also have the smallest values for contact angle, which is due to the presence of more water in the coating structure (Ju, et al., 2009).

f. Coated membranes parameters

The membranes parameters are present in Table 22.

Table 22 - Membrane parameters.

Membrane	k_m (10^{-6}m.s^{-1})	S (mm)	τ
Untreated	4.94	0.28	1.56
25%PEGDA **Top**	3.74	0.40	1.98
25%PEGDA **Bottom**	4.45	0.34	1.67
25% PEGDA **3 coat Top**	3.74	0.40	1.98
25% PEGDA **3 coat Bottom**	4.39	0.34	1.69
50%PEGDA **Top**	7.61	0,20	1.00
50%PEGDA **Bottom**	6.26	0.24	1.18
50%PEGDA **3 coat Bottom**	6.16	0.24	1.20
75%PEGDA **Top**	4.79	0.31	1.55
75%PEGDA **Bottom**	6.55	0.23	1.13
PEG3000/PEGDA **Top**	6.55	0.23	1.13
PEG3000/PEGDA **Bottom**	4.11	0.37	1.80
PEG35000/PEGDA **Top**	4.58	0.33	1.62
PEG35000/PEGDA **Bottom**	6.37	0.24	1.16

The results obtained show that coating the membranes with hydrogel, in some cases, decreases the S value, i.e. the propensity for the occurrence of internal CP, which can explain the better results obtained for membrane performance (comparing to the untreated membrane).

6. CONCLUSIONS

In this work the forward osmosis membrane limitations (salt rejection and ICP effects) were improved by surface modification of a cellulose acetate forward osmosis membrane, via coating. Primarily a base membrane was selected, in order to achieve a membrane with a small structural parameter. Therefore, different CA membranes were tested, by varying the dope solutions composition (pure dioxane; 1:3 acetone:dioxane; 1:1 acetone:dioxane; 3:1 acetone:dioxane) and the porous supports (PET and nylon). The best result was achieved by the membrane prepared with the dope solution of cellulose acetate and pure dioxane, using nylon as the porous support. The base membrane presents a NaCl rejection between 89-96% and is limited by internal concentration polarization effects.

PEG-based hydrogels were synthesized and applied as coatings to cellulose acetate forward osmosis membranes. The hydrogels have high water uptake and low salt permeability, making them interesting candidates as forward osmosis coating materials. The water flux of coated membranes, in most, cases decreases slightly when compared to the uncoated membranes, except for the prepolymerization mixture of 50%PEGDA, which in all treatments have a slightly improve in water flux in the PRO orientation (100 and 120%, coating on the active layer and on the porous support, respectively). All the coated membranes show a higher NaCl rejection (≈ 100%), which proves that the application of hydrogel coatings benefits the performance of the cellulose acetate membranes. However, this improvement is not constant in value, i.e., the salt rejection varies from membrane to membrane, even when the prepolymerization mixture viscosity is increased. The internal CP effect was proved to be decreasing; the 50%PEGDA coated membrane showed a linear behaviour with the increasing osmotic driving force.

7. FUTURE WORK

In this work, was proved that PEG-based hydrogel coatings upgrade the cellulose acetate forward osmosis membranes. However, some developments are still needed, as the

improvement of the coating thickness and its uniformity (ensure a gap-free structure), and also guaranty that the entire membrane surface is covered with the coating.

In future work, some experimental procedures could be improved: and (i) in order to control the membrane thickness and the covered area, a drawdown coating machine could be used; thus by controlling the type of rod and the coating speed different coatings could be obtained; (ii) also, another impregnation technique could be employed, utilizing vacuum to impregnate hydrogel into the membrane pores, which could be a more efficient way to fill the membrane porous without comprimising the membrane integrity. For the improvement of the coating uniformity other monomers could be tested, such as PEG with different molecular weights, poly(ethylene glycol) acrylate, 2-hydroxyethyl acrylate, and acrylic acid; that were already tested to coat RO membranes (La, et al., 2011; Sagle, et al., 2009). Finally test the treated membranes for long term operation and in actual seawater, in order to obtain the coating/membrane stability during a real life situation.

8. BIBLIOGRAPHY

Achilli, A., Cath, T. and Childress, A. 2009. Journal of Membrane Science. *Power generation with pressure retarded osmosis: An experimental and theoretical investigation.* 2009, Vol. 343, pp. 42-52.

Achilli, A., Cath, T. Y. and Childress, A. E. 2010. Journal of Membrane Science. *Selection of inorganic-based draw solutions for forward osmosis applications.* 2010, Vol. 364, pp. 233-241.

Achilli, A., et al. 2009. Desalination. *The forward osmosis membrane bioreactor: A low fouling alternative to MBR processes.* 2009, Vol. 239, pp. 10-21.

Adham, S., et al. 2007. *Dewatering reverse osmosis concentrare from water reuse using forward osmosis.* s.l. : WateReuse Foundation, 2007.

Anderson, D. K. 1977. *Concentraton of dilute wastes by direct osmosis.* University of Rhode Island, Providence : s.n., 1977.

Applin, K. R. and Lasaga, A. C. 1984. Geochmica et Cosmochimica Acta. *The determination of SO42-, NaSO4-, and MgSO40 tracer diffusion coefficients and their application to diagenetic flux calculations.* 1984, Vol. 48, pp. 2151-2162.

Aslow, F. 1998. Oregon State University. *Analysis of Dual Stage Sanitary Land fill Leachate Treatment of Heavy and Toxic Metal.* [Online] 1998. http://www.chemistry.oregonstate.edu/courses/ch361-464/ch461/461specproj.htm.

Avlontis, S. A., Kouroumbas, K. and Vlachakis, N. 2003. Desalination. *Energy consumption and membrane replacement cost for seawater RO desalination plants.* 2003, Vol. 157, pp. 151-158.

Babu, B. R., Rastogi, N. K. and Raghavarao, K. S. M. S. 2006. Journal of Membrane Science. *Mass transfer in osmotic membrane distillation of phycocyanin colorant and sweet-lime juice.* 2006, Vol. 272, pp. 58-69.

Babu, B. R., Rastogi, N. K. and Raghavarao, K.S.M.S. 2006. Journal of Membrane Science. *Effect of process parameters on transmembrane flux during direct osmosis.* 2006, Vol. 280, pp. 185-194.

Baker, R. W. 2000. *Membrane Technology and Applications.* s.l. : WILEY, 2000.

Bamaga, O. A., et al. 2011. Desalination. *Hybrid FO/RO desalination system: preliminary assessment of osmotic energy recovery and designs of new FO membrane module configurations.* 2011, Vol. 268, pp. 163-169.

Batchelder, G. w. 1965. *Process for the desmineralization of water. US Patent 3,171,799* 1965.

Belfer, S., et al. 2001. Desalination. *Effect of surface modification in preventing fouling of commercial SWRO membranes at the Eilat seawater desalination pilot plant.* 2001, Vol. 139, pp. 169-176.

Belfer, S., et al. 2004. Journal of Membrane Science. *Modification of NF membrane properties by in situ redox initiated graft polymerization with hydrophilic monomers.* 2004, Vol. 239, pp. 55-64.

Belfer, S., Purinson, Y. and Kedem, O. 1998. Acta Polymerica. *Surface modificationof commercial polyamide reverse osmosis membranes by radical graftin: an ATR-FT-IR study.* 1998, Vol. 49, pp. 574-582.

Bolto, B., et al. 2009. Progress in Polymer Science. *Crosslinked poly(vinyl alcohol) membranes.* 2009, Vol. 34, pp. 969-981.

Cartinella, J. L., et al. 2006. Environmental Science & Technology. *Removal of natural steroid hormones from wastewater using membrane contactor processes.* 2006, Vol. 40, pp. 7381–7386.

Cath, T. Y, et al. 2005. Journal of Membrane Science. *Membrane contactor processes for wastewater reclamation in space Part I. Direct osmotic concentration as pretreatment for reverse osmosis.* 2005, Vol. 257, pp. 85-98.

Cath, T. Y., Adams, D. and Childress, A. E. 2005. Journal of Membrane Science. *Membrane contactor processes for waste water reclamation in space: II. Combined direct osmosis, osmotic destillation, and membrane distillation for treatment of metabolic wastewater.* 2005, Vol. 257, pp. 111-119.

Cath, T. Y., Childress, A. E. and Elimelech, M. 2006. Journal of Membrane Science. *Forward osmosis: Principles, applications, and recent developments.* 2006, Vol. 281, pp. 70-80.

Cath, T. Y., et al. 2012. Desalination. *Standard Methodology for evaluating membrane performance in osmotically driven membrane processes.* Manuscript, 2012.

Cath, T. Y., et al. 2010. Journal of Membrane Science. *A multi-barrier osmotic dilution process for simultaneous desalination and purification of impaired water.* 2010, Vol. 362, pp. 417–426.

Changrue, V., et al. 2008. Journal of Food Engineering. *Effect of osmotic dehydration on the dielectric properties of carrots and strawberries.* 2008, Vol. 88, pp. 280-286.

Chay, S. L. Nanyang Technological University. *Low Cost Seawater Desalination – Forward Osmosis Membrane Desalination .* [Online] http://www.ntu.edu.sg/HOME/MSCLOW/FO%20White%20Paper.pdf.

Choi, H., et al. 2012. Desalination. *Surface modification of seawater reverse osmosis (SWRO) membrane using methyl methacrylate-hydroxy poly(oxyethylene) methacrylate (MMA-HPOEM) comb-polymer and its performance.* 2012, Vol. 291, pp. 1-7.

Chou, S. at all. 2010. Desalination. *Characteristic and potential applications of a novel forward osmosis hollow fiber membrane.* 2010, Vol. 26, pp. 365-372.

Chung, T., et al. 2012. Desalination. *Forward osmosis processes: Yesterday, today and tomorrow.* 2012, Vol. 287, pp. 78-81.

Cornelissen, E. R., et al. 2008. Journal of Membrane Science. *Membrane fouling and process performance of forward osmosis membranes on activated sludge.* 2008, Vol. 319, pp. 158-168.

Crespo, J. G. and Afonso, C. A. M. 2005. *Green Separation Processes.* s.l. : WILEY-VCH, 2005.

El-Aouar, Â. A., et al. 2006. Journal of Food Engineering. *Influence of the osmotic agent on the osmotic dehydration of papaya (Carica papaya L.).* 2006, Vol. 75, pp. 267-274.

Elimelech, M. and Phillip, W. A. 2011. Science. *The Future of Seawater Desalination: Energy, Technology, and the Environment.* 2011, Vol. 333, pp. 712-717.

Elimelech, M. 2006. Journal of Water Supply: Research and Technology. *The global challenge for adequate and safe water.* 2006, Vol. 55.1, pp. 3-10.

Eren, I. and Kaymak-Ertekin, F. 2007. Journal of Food Engineering. *Optimization of osmotic dehydration of potato using response surface methodology.* 2007, Vol. 79, pp. 344-352.

Frank, B. S. 1972. *Desalination of seawater. US Patent 3,670, 897* 1972.

Full Scale Experience of Direct Osmosis Concentration Applied to Leachate Management. **York, R. J., Thiel, R. S. and Beaudry, E. G. 1999.** Sardinia : Proceedings for Sardinia '99 Seventh International Landfill Symposium, 1999.

Ganji, F., Vasheghani-Farahani, S. and Vasheghani-Farahani, E. 2010. Iranian Polymer Journal. *Theoretical Description of Hydrogel Swelling: A Review.* 2010, Vol. 19 (5).

García, M., et al. 2010. Food Research International. *Effects of chitosan coating on mass transfer during osmotic dehydration of papaya.* 2010, Vol. 43, pp. 1656-1660.

Garcia-Castello, E. M. and McCutcheon, J. R. 2011. Journal of Membrane Science. *Dewatering press liquor derived from orange production by forward osmosis.* 2011, Vol. 372, pp. 97-101.

Garcia-Castello, E. M., McCutcheon, J. R. and Elimelech, M. 2009. Journal of Membrane Science. *Performance evaluation of sucrose concentration using forward osmosis.* 2009, Vol. 338, pp. 61-66.

Ge, Q., et al. 2011. Water Research. *Exploration of polyelectrolytes as draw solutes in forward osmosis processes.* 2011, Vol. 46, pp. 1318-1326.

Gekas, V. and Hallström, B. 1987. Journal of Membrane Science. *Mass transfer in the membrane concentration polarization layer under turbulent cross flow: I. Critical literature review and adaptation of existing sherwood correlations to membrane operations.* 1987, Vol. 30, pp. 153-170.

Gerstandt, K., et al. 2008. Desalination. *Membrane processes in energy supply for an osmotic power plant.* 2008, Vol. 224, pp. 64-70.

Glew, D. N. 1965. *Process for liquid recovery and solution concentration. US Patent 3,216, 930* 1965.

Goosens, I. and Van-Haute, A. 1978. Desalination. *The use of Direct Osmosis tests as complementary experiments to determine the water and salt permeabilities of cellulose acetate membranes.* 1978, Vol. 26, pp. 299–308.

Gostoli, C. 1999. Journal of Membrane Science. *Thermal effects in osmotic distillation.* 1999, Vol. 163, pp. 75-91.

Gray, G. T., McCutcheon, J. R. and Elimelech, M. 2006. Desalination. *Internal concentration polarization in forward osmosis: role of membrane orientation.* 2006, Vol. 197, pp. 1-8.

Gray, G., McCutcheon, J. and Elimelech, M. 2006. Desalination. *Internal concentration polarization in forward osmosis: role of membrane orientation.* 2006, Vol. 197, pp. 1-8.

Hancock, N. T. and Cath, T. Y. 2009. Environ. Sci. Technol. *Solute Coupled diffusion in osmotically driven membrane processes.* 2009, Vol. 43, pp. 6769-6775.

Hatakeyama, E. S., et al. 2009. Journal of Membrane Science. *New protein-resistant coatings for water filtration membranes based on quaternary ammonium and phosphonium polymers.* 2009, Vol. 330, pp. 104-116.

Herbig, S. M., et al. 1995. Journal of Controlled Release. *Asymmetric-membrane tablet coatings for osmotic drug delivery.* 1995, Vol. 35, pp. 127-136.

Holloway, R. W., et al. 2007. Water research. *Forward Osmosis for concentration of anaerobic digester centrate.* 2007, Vol. 41, pp. 4005-4014.

Hoover, L. A., et al. 2011. Environmental Science & Technology. *Forward with Osmosis: Emerging Applications for Greater Sustainability.* 2011, Vol. 45, pp. 9824-9830.

Hough, W. T. 1970. *Process for extracting solvent from a solution. 3,702,820* US, 1970.

Irandoust, S. and Andersson, B. 1986. The Canadian Journal of Chemical Engineering. *Concentration-dependent diffusivity of benzoic acid in water and its influence on the liquid-solid mass transfer.* 1986, Vol. 64, pp. 954-959.

Jiao, B., Cassano, A. and Drioli, E. 2004. Journal of Food Engineering. *Recent advances on membrane processes for the concentration of fruit juices: a review.* 2004, Vol. 63, pp. 303-324.

Ju, H., et al. 2008. Journal of Membrane Science. *Crosslinked poly(ethylene oxide) fouling resistant coating materials for oil/water separation.* 2008, Vol. 307, pp. 260-267.

Ju, H., et al. 2009. Journal of Membrane Science. *Preparation and characterization of crosslinked poly(ethylene glycol) diacrylate hydrogels as fouling-resistant membrane coating materials.* 2009, Vol. 330, pp. 180-188.

Ju, H., et al. 2010. Journal of Membrane Science. *Characterization of sodium chloride and water transport in crosslinked poly(ehylene oxide) hydrogels.* 2010, Vol. 358, pp. 131-141.

Kang, G. and Cao, Y. 2012. Water Research. *Development of antifouling reverse osmosis membranes for water treatment: A review.* 2012, Vol. 46, pp. 584-600.

Karagiannis, I. C. and Soldatos, P. G. 2008. Desalination. *Water desalination cost literature: review and assessment.* 2008, Vol. 223, pp. 448-456.

Khaydarov, R. A. and Khaydarov, R. R. 2007. Desalination. *Solar power direct osmosis desalination.* 2007, Vol. 217, pp. 225-232.

Khayet, M. and Matsuura, T. 2011. *Membrane Destillation: Principles and Applications.* s.l. : Elsevier, 2011.

Khoyi, M. R. and Hesari, J. 2007. Journal of Food Engineering. *Osmotic dehydration kinetics of apricot using sucrose solution.* 2007, Vol. 78, pp. 1355-1360.

Kim, T., et al. 2011. Desalination. *Systematic approach for draw solute selection and optimal system design for forward osmosis desalination.* 2011, Vol. 284, pp. 253-260.

Kim, Y. and Lee, S. 2008. Water Quality Products. *Forward Osmosis & Water treatment.* 2008, Vol. 109, pp. 14-15.

Kock, K. and Strathmann, H. 1977. Desalination. *The formation mechanism of phase inversion membranes.* 1977, Vol. 21, pp. 241-255.

Kravath, R. E. and Davis, J. A. 1975. Desalination. *Desalination of Sea Water by Direct Osmosis.* 1975, Vol. 16, pp. 151–155.

Kulkarni, A., Mukherjee, D. and Gill, W. N. 1996. Journal of Membrane Science. *Flux enhancement by hydrophilization of thin film composite reverse osmosis membranes.* 1996, Vol. 114, pp. 39-50.

La, Y. H., et al. 2011. Journal of Membrane Science. *Bifunctional hydrogel coatings for water purification membranes: improved fouling resistance and antimicrobial activity.* 2011, Vol. 372, pp. 285-291.

La, Y., et al. 2012. Journal of Membrane Science. *Enhancing water permeability of fouling-resistant POSS-PEGM hydrogels using 'addition-extraction' of sacrificial additives.* 2012, Vols. 401-402.

Lampi, K., Beaudry, E. G. and Herron, J. 2005. *Forward osmosis pressurized device and process for generating potable water. 6,849,184* US, 2005.

Lee, K. L., Baker, R. W. and Lonsdale, H. K. 1981. Journal of Membrane Science. *Membranes for power generation by pressure-retarded osmosis.* 1981, Vol. 8, pp. 141-171.

Lee, S., et al. 2010. Journal of Membrane Science. *Comparision of fouling behavior in forward osmosis (FO) and reverse osmosis (RO).* 2010, Vol. 365, pp. 34-39.

Li, Q. and Xu, Z. Pinnau. 2007. Journal of Membrane Science. *Fouling of reverse osmosis membranes by biopolymers in wastewater secondary effluent: Role of membrane surface properties and initial permeate flux.* 2007, Vol. 290, pp. 173-181.

Lin, Y. and Ho, H. 2003. Journal of Controlled Release. *Investigations on the drug releasing mechanism from an asymmetric membrane-coated capsule with an in situ formed delivery orifice.* 2003, Vol. 89, pp. 57-69.

Ling, M. M. and Chung, T. S. 2011. Desalination. *Desalination process using super hydrophilic nanoparticles via forward osmosis integrated with ultrafiltration regeneration.* 2011, Vol. 278, pp. 194-202.

Liu, L., et al. 2009. Recent Patens in Chemical Engineering. *Current Patens of Forward Osmosis Membrane Processes.* 2009, Vol. 2, pp. 76-82.

Lobo, V. M. M. 1993. Pure & Appl. Chem. *Mutual diffusion coefficients in aqueous electrolyte solutions.* 1993, Vol. 65, pp. 2613-2640.

Loeb, S. 2002. Desalination. *Large-scale power production by pressure-retarded osmosis, using river water and sea water passing through a spiral modules.* 2002, Vol. 143, pp. 115-122.

Loeb, S. and Bloch, M. R. 1973. Desalination. *Countercurrent flow osmotic processes for the productions of solutions having a high osmotic pressure.* 1973, Vol. 13, pp. 207–215.

Loeb, S. and Mehta, G. D. 1978. Journal of Membrane Science. *Internal polarization in the porous substructure of a semipermeable membrane under pressure-retarded osmosis.* 1978, Vol. 4, pp. 261-265.

Loeb, S. and Sourirajan, S. 1962. Advances in Chemistry Series. *Sea Water Demineralization by Means of an Osmotic Membrane.* 1962, Vol. 38, pp. 117-132.

Loeb, S., et al. 1997. Journal of Membrane Science. *Effect of porous support fabric on osmosis through a Loeb-Sourirajan type asymmetric membrane.* 1997, Vol. 129, pp. 243-249.

Loeb, S., Hessen, F. V. and Shahaf, D. 1976. Journal of Membrane Science. *Production of energy from concentrated brines by pressure-retarded osmosis: II. Experimental results and projected energy costs.* 1976, Vol. 1, pp. 249-269.

Lombard, G. E., et al. 2008. Journal of Food Engineering. *Osmotic dehydration of pineaple as a pre-treatment for further drying.* 2008, Vol. 85, pp. 277-284.

Louie, J. S., et al. 2006. Journal of Membrane Science. *Effects of polyether-polyamide block copolymer coating on performance and fouling of reverse osmosis membranes.* 2006, Vol. 280, pp. 762-770.

Mallevialle, J., Odendaal, P. E. and Wiesner, M. R. 1996. *Water Treatment Membrane Processes.* USA : McGraw-Hill, 1996.

McCutcheon, J. R. and Elimelech, M. 2006. Journal of Membrane Science. *Influence of concentrative and dilutive internal concentration polarization on flux behaviour in forward osmosis.* 2006, Vol. 284, pp. 237-247.

McCutcheon, J. R., McGinnis, R. L. and Elimelech, M. 2005. Desalination. *A novel ammonia-carbon dioxide forward (direct) osmosis desalination process.* 2005, Vol. 174, pp. 1-11.

McCutvheon, J. R., McGinnis, R. L. and Elimalech, M. 2006. Journal of Membrane Science. *Desalination by ammonia-carbon dioxide forward osmosis; Influence of draw and feed solution concentrations on process performance.* 2006, Vol. 278, pp. 114-123.

McGinnis, R. and Elimelech, M. 2006. Desalination. *Energy requirements of ammonia-carbon dioxide forward osmosis desalination.* 2006, Vol. 207, pp. 370-382.

McGinnis, R. L. and Elimelech, M. 2010. Desalination. *Energy requirements of ammonia-carbon dioxide forward osmosis desalination.* 2010, Vol. 207, pp. 370-382.

McGinnis, R. L. 2002. *Osmotic desalination process. US Patent 6, 391, 205* 2002.

McPherson, T., et al. 1998. Langmuir. *Prevention of protein adsortion by tethered poly(ethylene oxide) layers: experiments and single-chain mean-field analysis.* 1998, Vol. 14, pp. 176-186.

Mehta, G. D. and Loeb, S. 1979. Journal of Membrane Science. *Performance of Permasep B-9 and B-10 membranes in various osmotic regions and at high osmotic pressures.* 1979, Vol. 4, pp. 335–349.

Mehta, G. D. 1982. Journal of Membrane Science. *Further results on the performance of present-day osmotic membranes in various osmotic regions.* 1982, Vol. 10, pp. 3-19.

Mi, B. and Elimelech, M. 2010. Journal of Membrane Science. *Organic fouling of forward osmosis mebranes: fouling reversibility and cleaning without chemical reagents.* 2010, Vol. 348, pp. 337-345.

Mulder, M. 1996. *Basic Principles of Membrane Technology.* London : Kluwer Academic Publishers, 1996.

Nagai, K., et al. 2001. Polymer. *Solubility and diffusivity of sodium chloride in phase-separated block copolymers of poly(2-dimethylaminoethyl methacrylate, poly(1,1'-dihydroperfluorooctyl methacrylate) and poly(1,1,2,2-tetrahydroperfluorooctyl acrylate).* 2001, Vol. 42, pp. 9941-9948.

Nayak, C. A. and Rastogi, N. K. 2010. Separation and Purification Technology. *Forward osmosis for the concentration of anthocyanin from Garcinia indica Choisy.* 2010, Vol. 71, pp. 144-151.

Nayak, C. A., Valluri, S. S. and Rastogi, N. K. 2011. Journal of Food engineering. *Effect of high or low molecular weight of components of feed on transmembrane flux during forward osmosis.* 2011, Vol. 106, pp. 48-52.

Nollet, J. A., Guérin, H. L. and Delatour, L. 1748. *Lecons de physique experimentale.* Paris : s.n., 1748.

Oriard, T. M. and Haggerty, P. D. 2007. *Forward osmosis utilizing a controllable osmotic agent. US Patent 0278153* 2007.

Ozdemir, M., et al. 2008. LWT-Food Science and Technology. *Optimization of osmotic dehydration of diced green peppers by response surface methodology.* 2008, Vol. 41, pp. 2044-2050.

Park, K. J., et al. 2002. Journal of Food Engineering. *Osmotic dehydration kinetics of pear D'anjou (Pyrus communis L.).* 2002, Vol. 52, pp. 293-298.

Park, M., et al. 2011. Journal of Membrane Science. *Determination of a constant membrane structure parameter in forward osmosis processes.* 2011, Vol. 375, pp. 241-248.

Pattle, R. E. 1954. Nature. *Production of Electric Power by mixing Fresh and Salt Water in the Hydroelectric Pile.* 1954, Vol. 174, pp. 660-660.

Peeva, L. G., et al. 2004. Journal of Membrane Science. *Effect of concentration polarization and osmotic pressure on flux in organic solvent nanofiltration.* 2004, Vol. 236, pp. 121-136.

Peeva, P. D., Million, N. and Ulbbritch, M. 2012. Journal of Membrane Science. *Factors affecting the behaviour of anti-fouling thin-layer cross-linked hydrogel polyethersulfone composite ultrafiltration membranes.* 2012, Vols. 390-391.

Peeva, P. D., Pieper, T. and Ulbricht, M. 2010. Journal of Membrane Science. *Tuning the ultrafiltration properties of antifouling thin-layer hydrogel polyethersulfone composite membranes by suited crosslinker monomers and photo-grafting conditions.* 2010, Vol. 362, pp. 560-568.

Peñate, B. and Rodríguez, L. G. 2012. Desalination. *Current trends and future prospects in the design of seawater reverse osmosis desalination technology.* 2012, Vol. 284, pp. 1-8.

Petersen, R. J. 1993. Journal of Membrane Science. *Composite reverse osmosis and nanofiltration membranes.* 1993, Vol. 83, pp. 81-150.

Petrotos, K. B. and Lazarides, H. N. 2001. Journal of Food Engineering. *Osmotic concentration of liquid foods.* 2001, Vol. 49, pp. 201-206.

Petrotos, K. B., Quantick, P. C. and Petropakis, H. 1999. Journal of Membrane Science. *Direct osmotic concentration of tomato juice in tubular membrane - module configuration. II. The effect of using clarified tomato juice on the process performance.* 1999, Vol. 160, pp. 171-177.

Petrotos, K. B., Quantick, P. and Petropakis, H. 1998. Journal of Membrane Science. *A study of the direct osmotic concentration of tomato juice in tubular membrane - module configuration. I. The effect of certain basic process parameters on the process performance.* 1998, Vol. 150, pp. 99-100.

Philip, W. A., Yong, J. S. and Elimelech, M. 2010. Environmental Science & Technology. *Reverse draw solute permeation in forward osmosis: modeling and experiments.* 2010, Vol. 44, pp. 5170-5176.

Phuntsho, S., et al. 2011. Journal of Membrane Science. *A novel low energy fertilizer driven forward osmosis desalination for direct fertigation: Evaluating the performance of fertilizer draw solutions.* 2011, Vol. 375, pp. 172-181.

Post, J. W., Hamelers, H. V. M. and Buisman, C. J. N. 2008. Environmental Science & Technology. *Energy recovery from controlled mixing salt and fresh water a reverse electrodialysis system.* 2008, Vol. 42, pp. 5785-5790.

Qin, J., Lay, W. and Kekre, K. 2012. Desalination and Water Treatment. *Recent developments and future challenges of forward osmosis for desalination: a review.* 2012, Vol. 39, pp. 123-136.

Qin, J.-J., et al. 2010. Journal of Membrane Science. *Development of novel backwash cleaning technique for reverse osmosis in reclamation of secondary effluent.* 2010, Vol. 346, pp. 8-14.

Ramon, G., Agnon, Y. and Dosoretz, C. 2010. Journal of Membrane Science. *Dynamics of an osmotic backwash cycle.* 2010, Vol. 364, pp. 157-166.

Ritger, P. L. and Peppas, N. A. 1987. Journal of Controlled Release. *A simple equatiton for description of solute release I. Fickian and non-Fickian release from non-swellable devices in the form of slabs, spheres, cylinders or discs.* 1987, Vol. 5, pp. 23-36.

Rogers, E., et al. 2000. Fundamentals of Chemistry. *Physical Properties of Solutions.* [Online] Copyright, 2000. http://www.chem.wisc.edu/deptfiles/genchem/sstutorial/Text11/Tx117/tx117.html.

Sagle, A. C., et al. 2009. Journal of Membrane Science. *PEG-coated reverse osmosis membranes: Desalination properties and fouling resistante.* 2009, Vol. 340, pp. 92-108.

Sagle, A. C., et al. 2009. Polymer. *PEG-based hydrogel membrane coatings.* 2009, Vol. 50, pp. 756-766.

Sairam, M., et al. 2011. Desalination. *Method for the preparation of cellulose acetate flat sheet composite membranes for forward osmosis-Desalination using MgSO4 draw solution.* 2011, Vol. 273, pp. 299-307.

Salter, R. J. 2005. Water Conditioning & Purification. *Forwar Osmosis.* 2005, Vol. 48, pp. 36–38.

Santus, G. and Baker, R. W. 1995. Journal of Controlled Release. *Osmotic drug delivery: a review of the patent literature.* 1995, Vol. 35, pp. 1-21.

Saren, Q., Qiu, C. Q. and Tang, C. Y. 2011. Environmental Science & Technology. *Synthesis and Characterization of Novel Forward Osmosis Membranes based on Layer-by-Layer Assembly.* 2011, Vol. 45, pp. 5201-5208.

Setiawan, L., et al. 2011. Journal of Membrane Science. *Fabrication of novel pol(amide-imide) forward osmosis hollow fiber membranes with a positively charged nanofiltration-like selective layer.* 2011, Vol. 369, pp. 196-205.

Shokri, J., et al. 2008. European Journal of Pharmaceutics and Biopharmaceutis. *Swellable elementary osmotic pump (SEOP): an effective device for delivery of poorly water soluble drugs.* 2008, Vol. 68, pp. 289-297.

Stache, K. 1989. *Apparatus for transforming sea water, brackish water, polluted water or the like into nutritious drink by means of osmosis. 4,879,030* US, 1989.

Strathmann, H. 1981. Journal of membrane science. *Membrane separation processes.* 1981, Vol. 9, pp. 121-189.

Su, J., et al. 2010. Journal of Membrane Science. *Cellulose acetate nanofiltration hollow fiber membranes for forward osmosis processes.* 2010, Vol. 355, pp. 36-44.

Talaat, K. M. 2009. Artificial Organs. *Forward osmosis process for dialysis fluid regeneration.* 2009, Vol. 33, pp. 1133-1135.

—. 2010. Saudi Journal of Kidney Diseases and Transplatation. *Dialysis fluid generation by forward osmosis: a feasible option dialysis systems.* 2010, Vol. 21, pp. 748-749.

Tan, C. H. and Ng, H. Y. 2010. Desalination and water treatment. *A novel hybrid forward osmosis - nanofiltration (FO-NF) process for seawater desalination: Draw solution selection and system configuration.* 2010, Vol. 13, pp. 356-361.

Tang, C. Y., et al. 2010. Journal of Membrane Science. *Coupled effects of internal concentration polarization and fouling on flux behavior of forward osmosis membranes during humic acid filtration.* 2010, Vol. 354, pp. 123-133.

Tang, C. Y., Kwon, Y. N. and Leckie, J. O. 2009. Desalination. *Effect of membrane chemistry and coating layer on physiochemical properties of thin film composite polyamide RO and NF membranes I. FTIR and XPS characterization of polyamide and coating layer chemistry.* 2009, Vol. 242, pp. 149-167.

—. 2007. Journal of Membrane Science. *Probing the nano- and micro- scales of reverse osmosis membranes- a comprehensive characterization of physiochemical properties of uncoated abd coated membranes by XPS, TEM, ATR-FTIR, and streaming potential measurements.* 2007, Vol. 287, pp. 146-156.

Thombre, A. G., et al. 1999. Journal of Controlled Release. *Asymmetric membrane capsules for osmotic drug delivery I. Development of a manufacturing process.* 1999, Vol. 57, pp. 55-64.

Torringa, E., et al. 2001. Journal of Food Engineering. *Osmotic dehydration as a pre-treatment before combined microwave-hot-air drying of mushrooms.* 2001, Vol. 49, pp. 185-191.

Trent, J. D., et al. 2010. *Algae bioreactor using submerged enclousures with semi-permeable membranes. US Patent 0216203* 2010.

Triwahyudi, W. 2007. Scribd. *Forward osmosis: " a sustainable desalination technology".* [Online] 2007. http://pt.scribd.com/doc/62171924/Forward-Osmosis-Desalination.

Uddin, M. B., Ainsworth, P. and Ibanoglu, S. 2004. Journal of Food Engineering. *Evaluation of mass exchange during osmotic dehydration of carrots using response surface methodology.* 2004, Vol. 65, pp. 473-477.

Van Wagner, E. M., et al. 2010. Journal of Membrane Science. *Surface modification of commercial polyamide desalination membranes using poly(ehtylene glycol) diglycidyl ether to enhance membrane fouling.* 2010, Vol. 367, pp. 273-287.

Veerman, J., et al. 2009. Journal of Membrane Science. *Reverse electrodialysis: Performance of a stack with 50 cells on the mixing of sea and river water.* 2009, Vol. 327, pp. 136-144.

Votta, F., Barnett, S. M. and Anderson, D. K. 1974. *Concentration of industrial waste by direct osmosis: completion report.* University of Rhode Island, Providence,RI : s.n., 1974.

Wang, K. Y., Chung, T. and Amy, G. 2012. AIChE Journal. *Developing thin-film-composite forward osmosis membranes on the PES/SPSf substrate through interfacial polymerization.* 2012, Vol. 58, pp. 770-781.

Wang, K. Y., et al. 2011. Chemical Engineering Science. *Integrated forward osmosis-membrane distillation (FO-MD) hybrid system for the concentration of protein solutions.* 2011, Vol. 66, pp. 2421-2430.

Wang, K. Y., Ong, R. C. and Chung, T. 2010. Ind. Eng. Chem. *Double-Skinned Forward Osmosis Membranes for Reducing Internal Concentration Polarization within the Porous Sublayer.* 2010, Vol. 49, pp. 4824-4831.

Wang, R., et al. 2010. Journal of Membrane Science 355. *Characterization of novel forward osmosis hollow fiber membranes.* 2010, Vol. 355, pp. 158-167.

Wang, X., et al. 2006. Journal of Membrane Science. *High performance ultrafiltration composite membranes based on poly(vinyl alcohol) hydrogel coating on crosslinked nanofibrous poly(vinyl alcohol) scaffold.* 2006, Vol. 278, pp. 261-268.

Wieland, P. O. 1994. NASA. *Design for human presence in space: an introduction to environmental control and life support systems.* [Online] 1994. http://flightprojects.msfc.nasa.gov/book/rp1324.pdf.

Wijmans, J. G. and Baker, R. W. 1995. Journal of membrane Science. *The solution-diffusion model: a review.* 1995, Vol. 107, pp. 1-21.

Wilbert, M. C., Pellegrino, J. and Zydney, A. 1998. Desalination. *Bench-scale testing of surfactant-modified reverse osmosis/nanofiltration membranes.* 1998, Vol. 115, pp. 15-32.

Wu, S. Y., et al. 1997. Journal of Applied Polymer Science. *Plasma modification of aromatic polyamide reverse osmosis composite membrane surface.* 1997, Vol. 64, pp. 1923-1926.

Wu, Y., et al. 2010. Journal of Membrane Science. *Water uptake, transport and structure characterization in poly(ehylene glycol) diacrylate hydrogels.* 2010, Vol. 347, pp. 197-208.

Xiao, D., et al. 2011. Journal of Membrane Science. *Modeling salt accumulation in osmotic membrane bioreactors: Implication for FO membrane selection and system operation.* 2011, Vol. 366, pp. 314–324.

Xie, Y. J., et al. 2007. Journal of Environmental Sciences. *Improvement of antifouling characteristics in a bioreactor of polypropylene microporous membrane by the adsorption of Tween 20.* 2007, Vol. 19, pp. 1461-1465.

Xu, J. B., et al. 2005. Journal of Membrane Science. *Alginic acid-silica hydrogel coatings for the protection of osmotic distillation membranes against wet-out by surface-active agents.* 2005, Vol. 260, pp. 19-25.

Yaeli, J. 1992. *Method and apparathus for processing liquid solutions of suspensions particularly useful in the desalination of saline water. US Patent 5,098,575* 1992.

Yang, Q., Wang, K. Y. and Chung, T.-S. 2009. Separation and Purification Technology. *A novel dual-layer forward osmosis membrane for protein enrichment and concentration.* 2009, Vol. 69, pp. 269-274.

Yang, R., et al. 2011. Chemistry of Materials. *Surface-tethered zwitterionic ultrathin antifouling coatings on reverse osmosis membranes by initiated chemical vapor deposition.* 2011, Vol. 23, pp. 1263-1272.

Yangali-Quintanilla, V., Li, Z. and Valladares, R. 2011. Desalination. *Indirect desalination of Red Sea water with forward osmosis and low pressure reverse osmosis for water reuse.* 2011, Vol. 280, pp. 160-166.

Yanq, Q., Wang, K. Y. and Chung, T. S. 2009. Environ. Sci. Technol. *Dual-layer hollow fibers with enhanced flux as novel forward osmosis membranes for water production.* 2009, Vol. 43, pp. 2800–2805.

Yasuda, H., Lamaze, C. E. and Ikenberry, L. D. 1968. Die Makromolekulare Chemie. *Permeability of solutes though hydrated polymer membranes. Part I. Diffusion of sodium chloride.* 1968, Vol. 118, pp. 19-35.

Yip, N. Y., et al. 2011. Environmental Science & Technology. *Thin-film composite pressure retarded osmosis membranes for sustainable power generation from salinity gradients.* 2011, Vol. 45, pp. 4360-4369.

Young, J., Phillip, W. A. and Elimelech, M. 2011. Journal of membrane science. *Coupled reverse draw solute permeation and water flux in forward osmosis with neutral draw solutes.* 2011, Vols. 392-393, pp. 9-17.

Yu, H. Y., et al. 2007. Water Research. *Surface modification of polypropylene microporous membrane to improve its antfouling characteristics in an SMBR: N2 plasma treatment.* 2007, Vol. 41, pp. 4703-4709.

Zhang, F., Brastad, K. S. and He, Z. 2011. Environmental Science & Tecnology. *Integrating Forward Osmosis into Microbial Fuel Cells for Wastewater Treatment, Water Extraction and Bioelectricity Generation.* 2011, Vol. 45, pp. 6690-6696.

Zhao, S., et al. 2012. Journal of Membrane Science. *Recent developments in forward osmosis: Opportunities and challenges.* 2012, Vol. 396, pp. 1-21.

Zhap, S. and Zou, L. 2011. Journal of Membrane Science. *Relating solution physicochemical properties to internal concentration polarization in forward osmosis membranes during humic acid filtration.* 2011, Vol. 379, pp. 459-467.

Zhou, Y., et al. 2009. Separation and Purification Technology. *Surface modification of thin film composite polyamide membranes by electrostatic self deposition of polycations for improved fouling resistance.* 2009, Vol. 66, pp. 287-294.

Zhu, H., et al. 2011. Bioresource Technology. *Feasibility of applying forward osmosisto the simultaneous thickening, digestion, and direct dewatering of waste activated sludge.* 2011, Vol. 30, pp. 207-213.

Zou, L., et al. 2011. Journal of Membrane Science. *Surface hydrophilic modification of RO membranes by plasma polymerization for low organic fouling.* 2011, Vol. 369, pp. 420-428.

Zou, S., et al. 2011. Journal of Membrane Science. *The role of physical and chemical parameters on forward osmosis membrane fouling during algae separation.* 2011, Vol. 366, pp. 356-362.

Appendixes

Appendix 1 - Techniques for membrane preparation

Synthetic membranes can be prepared by different techniques; the main techniques are resumed in Table 23.

Table 23- Main techniques for the preparation synthetic membranes

Technique	Type of membrane	Description
Sintering	Porous (0.1-10 μm)	A powder of known size particles is compressed and sintered at elevated temperatures. During the sintering the interfaces between the contacting particles disappears.
Stretching	Porous (0.1-3 μm)	A extruded film, of a partially crystalline polymeric material, is stretched perpendicular to the direction of the extrusion
Track-etching	Porous (0.02-10 μm)	A film is subjected to high energy particle radiation, and then is immersed in acid or alkaline bath.
Template leaching	Porous (≈5 μm)	A melted mixture of three components is cooled down, creating two phases (insoluble and soluble). The soluble phase is then leached out by an acid or base.
Phase inversion	Nonporous	Involves the precipitation of casting solution by immersion in a nonsolvent (e.g. water) bath. This method as a variety of techniques such as precipitation by solvent evaporation, precipitation from the vapor phase, precipitation by controlled evaporation, thermal precipitation and immersion precipitation.
Interfacial polymerization	Nonporous	Used to prepare thin film composite membranes (TFC). The method consists in polymerizing an extremely thin layer of polymer at the surface of a microporous support layer.
Coating	Nonporous	Used to produce composite membranes, which consist of a thick, porous, non-selective supporting layer covered with an ultra-thin barrier. To prepare these membranes, one or more thin, dense polymer layers are solution coated onto the surface of a microporous support. The coating procedures can be: dip coating, plasma polymerization, interfacial polymerization and in-situ polymerization.

The phase inversion process is the most common and reproducible process of membrane preparation, which will be emphasized in this review, more specifically by the immersion precipitation method.

a. Phase inversion method

The phase inversion method is used to prepare asymmetric skin type membranes, in which a homogeneous polymer solution is transformed into a two phase system, i.e., a solid polymer-rich phase which forms the membrane structure and a liquid polymer-poor phase which forms the membrane pores (Strathmann, 1981). The process of solidification is very often initiated by the transition from one liquid state into two liquids (liquid-liquid demixing). At a certain stage during demixing, one of the liquid phases (the polymer-rich phase) will solidify so that a solid matrix is formed (Baker, 2000).

This “phase separation” of the cast polymer solution into a polymer-rich and a polymer-lean phase can be induced by immersion in a non-solvent bath (“immersion precipitation”), by evaporating the volatile solvent from a polymer that was dissolved in a solvent/non-solvent mixture (“controlled evaporation”), by lowering the temperature (“thermal precipitation”) or by placing the cast film in a vapor phase that consists of a non-solvent saturated with a solvent (“precipitation from vapor phase”) (Crespo, et al., 2005). By controlling the initial stage of phase transition the membrane morphology can be controlled, i. e., porous as well as nonporous membranes can be prepared (Mulder, 1996). Figure 46 shows several typical membranes structures.

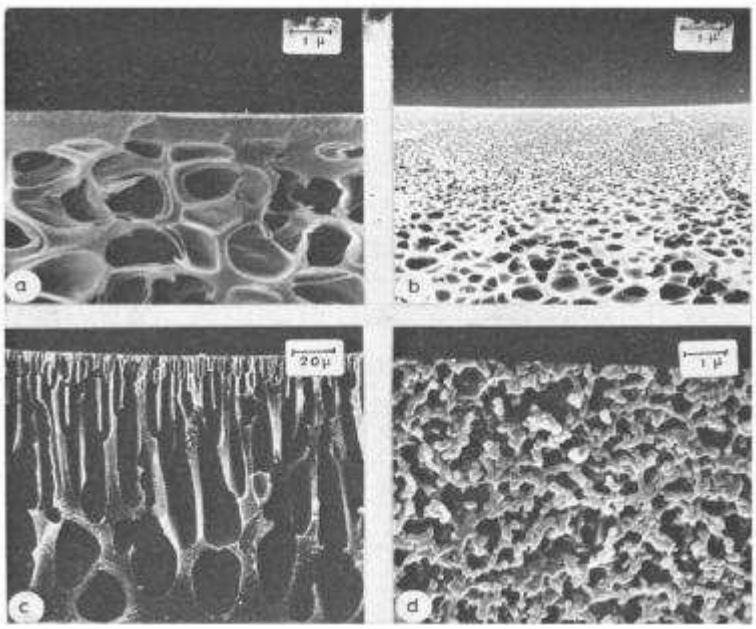

Figure 46- Scanning electron micrographs of membrane cross sections with typical structures: a) Asymmetric membrane with uniform-pore substructure; b) Asymmetric

membrane with a graded-pore substructure; c) Asymmetric membrane with a finger-pore substructure; d) Symmetric microporous membrane without a skin (Kock, et al., 1977)**.**

The photograph Figure 46 a) shows a microporous membrane with a “sponge” type structure and a dense homogeneous skin on the top side and a relative uniform pore distribution over the entire cross-section. In Figure 46 b) shows, also, a “sponge” type structure with a dense skin at the top surface and a graded pore structure underneath, with increasing pore size from the top to the bottom side. Figure 46 c) shows a microporous membrane with a “finger” type structure, with a dense top skin on the top side and large pores penetrating the entire membrane cross-section. The pores, generally, increase in diameter from the top to the bottom side. Finally, Figure 46 d) presents a microporous membrane with a “sponge-like” structure, rather uniform over the entire membrane cross-section, and no skin on top or bottom surface. This membrane was prepared by introducing the precipitant from the vapor phase, while a)-c) membranes where prepared by immersing the polymer solution into a precipitation fluid.

The phase inversion process consists, at the least, in a three component system, a polymer, a solvent and a non-solvent for the polymer. In some cases, is added to the polymer solution/non-solvent bath, a co-solvent (often more-volatile solvents), small amounts of non-solvent, and additives (of organic, inorganic or polymeric nature). After the membrane casting, solvent evaporation can take place over a certain time period at a given temperature. The composition and temperature of the coagulation medium are the subsequent parameters, while a final post-treatment of the membranes has often proven extremely important for the final membrane performance. Such post-treatment can consist of exposing the membranes to solvents or acids, annealing, for instance in water, cross-linking, drying by exchanges in a series of solvents or treating with conditioning agents like lube oil. This method can induce the formation of a structure with macrovoids (Crespo, et al., 2005).

Immersion Precipitation

This membrane preparation procedure, developed by Loeb and Sourirajan (Loeb, et al., 1962), produce skin-type membranes, which exists in two typical subclasses, “sponge” and “finger” structure (see Figure 46 a)-c)). In immersion precipitation process, the phase separation

of the cast polymer solution is made by immersion the solution in a nonsolvent bath. This stage is very important because defines whether the top layer will be more open (porous) or very dense (nonporous).

In immersion precipitation, a polymer solution consisting of a polymer and a solvent is cast as a thin film upon a support (e.g. non-woven support, glass plate) and then immersed in a nonsolvent bath. The solvent diffuses into the coagulation bath whereas the nonsolvent will diffuse into the cast film. After a given period of time the exchange of solvent and nonsolvent has proceeded so far that the solution becomes thermodynamically unstable and demixing takes place (liquid-liquid demixing). Finally a solid is obtained with an asymmetric structure (Mulder, 1996). The liquid-liquid demixing process is often illustrated by a ternary phase diagram, see Figure 47. This diagram is a description of an equilibrium state. It reflects the conditions under which a multicomponent mixture is either stable as a homogeneous phase, or decays into two separate phases.

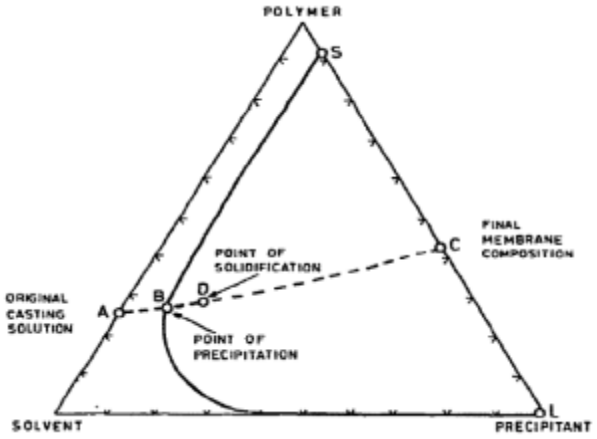

Figure 47-Schematic phase diagram of the system polymer-solvent-precipitant showing the precipitation pathway of the casting solution during membrane formation (Kock, et al., 1977)**.**

The corners of the ternary phase diagram represent the pure components, polymer, solvent and nonsolvent. A point located on one of the sides of the triangle represents a mixture consisting of the two corner components. Any point within the triangle represents a mixture of the three components. This system consists of two regions: a one phase region where all components are miscible and a two-phase region where the system separates into a polymer-rich phase (generally solid) and a polymer-poor phase (generally liquid).

During membrane formation the system changes from a composition A, which represents the initial casting solution to a composition C, which represents the final membrane. At composition C, two phases are in equilibrium, a solid (polymer-rich) phase which forms the membrane structure, represented by point S, and a liquid (polymer-poor) phase which constitutes the membrane pores filled with precipitant, represent by point L. The position C on the line S-L determines the overall membrane porosity. The entire precipitation process is thus represented by the path A to C, during which the solvent is exchanged by the precipitant. The point B along the path is the concentration at which the first polymer precipitates. At some point, the viscosity is high enough for the precipitated polymer to be regarded as a solid and further bulk movement of the polymer is hindered (composition D).

The membrane formation can occur instantaneously or slowly, which at the end will affect the membrane structure and performance. Different factors have a major effect upon the membrane structure. These are: choice of polymer, choice of solvent and nonsolvent, composition of casting solution, composition of casting solution, composition of coagulation bath, gelation and crystallisation behaviour of the polymer, location of the liquid-liquid demixing gap, temperature of the casting solution and the coagulation bath and evaporation time. By varying one or more of these parameters, which are not independent of each other the membrane structure can be changed.

b. Factors affecting membrane structure

The mechanism of membrane formation is influenced by different factors: polymer-solvent-precipitant selection, the concentration of polymer in the casting solution and the addition of non-solvent to the casting solution or precipitant.

Selection of the polymer-solvent precipitant system

The precipitant and the solvent used in membrane preparation determine both the activity coefficient of the polymer in the solvent-precipitant mixture and the concentration of polymer at the point of precipitation and solidification. Unfortunately, the activity coefficient values for the

polymer, the solvent, or the precipitant, and the dependence of these coefficients on the composition, are not available and are experimentally difficult to obtain. So the polymer-solvent interaction can be approximately expressed in terms of the disparity of the solubility parameter of polymer and solvent. The smaller the solubility parameter disparity of solvent and polymer the better is their compatibility, the more time it takes to remove the solvent from the polymer structure, and slower is the precipitation of the polymer. Therefore, when all other parameters are kept constant, the tendency for a change from a sponge to a finger structure increases with decreasing compatibility of solvent and polymer. The compatibility of polymer and precipitant can also be expressed in terms of the solubility parameter disparity. The higher this disparity, the less compatible are polymer and precipitant, the higher will be the activity coefficient of the polymer in the solvent-precipitant mixture, and the faster will be the precipitation. The tendency to change from a sponge to a finger structure will increase with decreasing compatibility of polymer and precipitant (Kock, et al., 1977).

Concentration of polymer

The polymer concentration in the casting solution has a significant effect on membrane structure. A low polymer concentration in the casting solution tends to precipitate in a finger-structure, while high polymer concentrations tend to form sponge-structure membranes. High concentration of the polymer in the casting solution result in a more concentrated interface casting solution/non-solvent during phase inversion, which slows down the solvent/non-solvent exchange leading to delayed demixing, tending to form a sponge-structured membranes. The increasing viscosity of the casting solution has the same effect (Mulder, 1996; Kock, et al., 1977).

Addition of non-solvent to the casting solution or precipitant

The effect of additives to the casting solution or precipitant on membrane structure can be explained by changes of the activity coefficient of the polymer, the solvent, or the precipitant. These activities are again directly related to the rate of precipitation. Certain additives to the precipitant such salts, sugars, glycerine, etc., reduce the rate of precipitation and clearly favour

a more dense sponge structure. The same additives in the casting solution generally increase the rate of precipitation and therefore favour a finger structure, while other additives in the casting solution (e.g. benzene) reduce the rate of precipitation and therefore favour a sponge structure.

Appendix 2 - Membrane surface modification

The physicochemical properties of membrane surface, such as hydrophilicity, roughness and electrostatic charge, are major factors influencing membrane performance (e.g. fouling mitigating).

The increase of membrane hydrophilicity offers better fouling resistance, because many foulants are hydrophobic in nature. A pure water layer is easily formed on highly hydrophilic surface, which can prevent the adsorption and deposition of hydrophobic foulants onto membrane surface (thus reducing fouling), and increase water permeability (Figure 48 a) (Kang, et al., 2012; Peeva, et al., 2010).

A smoother membrane surface is commonly expected to experience less particle interaction, presumably because foulant particles are more likely to be entrained by rougher topologies than by smoother surfaces. Therefore, increasing membrane rejection.

The membrane surface charge is also an important factor influencing membrane fouling, if the forces between the membrane surface and foulant are repulsive (Figure 48 b). So, the antifouling membranes should be developed according to the electrostatic character of foulants in practical situation.

Finally, some previous research results showed that the surface-bound long chain hydrophilic molecules (e.g. polyethylene glycol, PEG) were very effective in preventing adsorption of macromolecules such as protein onto membrane surface due to the steric repulsion mechanism (McPherson, et al., 1998). When hydrophilic polymer chains are grafted or created on membrane surface, this diffused hydrophilic layer will exert steric repulsion to hydrophobic proteins that reach surface (Figure 48 c) (Kang, et al., 2012).

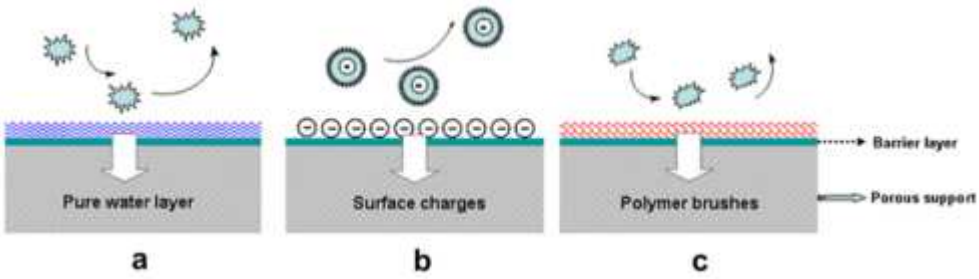

Figure 48 – Schematic diagrams of antifouling mechanisms: (a) pure water layer; (b) electrostatic repulsion; (c) steric repulsion (Kang, et al., 2012)**.**

Surface modification of existing membranes is also considered as a potential and effective route to enhance membrane performance. So far, there are many articles related to the surface modification of conventional RO membranes to improve the surface morphology and properties, thus enhancing the antifouling ability. The surface modification method ranges from physical to chemical treatments (Peeva, et al., 2010; Kang, et al., 2012).

a. Physical method

Surface adsorption

Physical adsorption is a simple tool for modification and structuring of polymer surfaces. Some researchers adopted this method to modify the surface properties of water filtration membranes (Xie, et al., 2007; Zhou, et al., 2009). For example, Wilbert et al. (Wilbert, et al., 1998) used a homologous series of polyethylene-oxide surfactants to modify the surface of commercial cellulose acetate blend and polyamide RO membranes. The tests showed that the roughness of polyamide RO membrane after treatment was reduced, and it exhibited improved antifouling property in a vegetable broth solution compared to the unmodified membrane. However, the results of cellulose acetate RO membrane were inconclusive.

Surface coating

Surface coating is a convenient and efficient technique for membrane surface modification, and it has been widely adopted to tailor the surface properties of conventional RO membranes.

Here, the coating acts as a protective layer to reduce or eliminate the adsorption and deposition of foulants onto membrane surface. This technique is a simple way and easily operated, so it has been paid much attention by many researchers and membrane manufacters so far (Kang, et al., 2012).

Louie et al. (Louie, et al., 2006) performed a physical coating study of commercial polyamide RO membranes PEBAX® 1657 (high hydrophilic block copolymer of nylon-6 and poly(ethylene glycol). The coating greatly reduced surface roughness without significant change in the contact angle, also, slow down the flux decline for long-term fouling test with an oil/surfactant/water emulsion. However, the coating resulted in large water flux reduction for high-flux RO membranes (ESPA1 and ESPA3).

The researchers from Freeman group developed a series of fouling resistant coating materials by lightly cross-linking, which were used for the surface modification of water filtration membranes including commercial RO membrane (Ju, et al., 2008; Hatakeyama, et al., 2009; La, et al., 2011; Sagle, et al., 2009). The results obtained were very promising. In this method, the liquid prepolymer mixture (monomer, crosslinker and photoinitiator) was firstly coated on surface of RO membrane and then photopolymerized to form a water-insoluble coating. For example, Sagle et al. (Sagle, et al., 2009) modified commercial RO membranes with crosslinked PEG-based hydrogels using poly(ethylene glycol) diacrylate (PEGDA) as the crosslinker and poly(ethylene glycol) acrylate (PEGA), 2-hydroxyethyl acrylate (HEA), or acrylic acid (AA) as comonomers. The results obtained indicated that the surface-coated membranes exhibited improved fouling resistance and an improved ability to be cleaned after fouling.

So far, the materials used for surface coating to improve membrane antifouling property are hydrophilic polymers containing hydroxyl, carboxyl or ethylene oxide groups (Kang, et al., 2012). This is consistent to the results obtained by Tang group (Tang, et al., 2007; Tang, et al., 2009), which fully characterized several widely used commercial RO and NF polyamide membranes by AFM, transmission electron microscopy (TEM), contact angle measurement and streaming potential analysis, and found that some commercial RO membranes were coated with aliphatic polymeric alcohol (PVA). The presence of the coating layer could significantly enhance hydrophilicity and reduce surface charge and roughness of membrane, rendering a better antifouling property.

Note that, the coated materials may increase the membrane permeation resistance, resulting in the decline of water flux. Therefore, for practical purposes, the coating layer should have an inherently high water permeability and be made sufficiently thin to maintain the water flux as possible. On the other hand, the modifiers in physical modification are only connected with membrane surface by van der Waals attractions, hydrogen bonding or electrostatic interaction, so the antifouling property of modified RO membranes may be gradually deteriorated due to the loss or leaching of coating layer during long-term operation (Kang, et al., 2012).

b. Chemical method

Hydrophilization treatment

As already mentioned, membrane surface hydrophilization is advantageous to enhance fouling resistance. This treatment can be made by using hydrophilizing agents (e.g. hydrofluoric, hydrochloric, sulphuric, phosphoric and nitric acids) to modify membrane surface (Kulkarni, et al., 1996).

Radical grafting

In the radical grafting process, the free radicals are produced from the initiators and transferred to the polymer to react with monomer, realizing the modification of membrane material (Kang, et al., 2012).

Belfer group (Belfer, et al., 2004; Belfer, et al., 2001; Belfer, et al., 1998) developed a successful system, which is based on a redox-initiated radical grafting of vinyl monomers onto polyamide RO or NF membranes surface. A redox system, composed of potassium persulfate and potassium metabisulfite, was used to generate radicals. They attacked the polymer backbone, initiating the grafting of monomers to the membrane surface. Polymerization then occurred via propagation. The hydrophilic monomers used were acrylic acid (AA), methacrylic acid (MA), poly(ethylene glycol) methacrylate (PEGMA), 3-sulfopropylmethacrylate (SPM), vinylsulfonic acid (VSA) and 2-acrylamido-2-methylpropane-sulfonic acid (AMPS). In general,

the tests results showed that the modified membranes presented less adsorption of foulants and were more easily cleaned than the unmodified membranes.

Chemical coupling

Membranes with surface containing free reactive groups (e.g. polyamide membranes (Petersen, 1993)) can modify their surface via chemical reaction or coupling.

Van Wagner et al. (Van Wagner, et al., 2010) modified commercial polyamide RO membranes based on the reaction of primary amine groups with the epoxy end groups of poly(ethylene glycol) diglycidyl ether (PEGDE). Although modified membranes experienced minimal changes in surface properties (e.g. surface charge, hydrophilicity and roughness), they generally presented improved fouling resistance.

Plasma polymerization or plasma-induced polymerization

Plasma treatment is a technique for the surface modification of polymer materials to improve the surface properties. This method includes plasma polymerization and plasma-induced polymerization. Plasma polymerization is a one-step process, as the plasma is used to deposit the polymer onto membrane surfaces. Plasma-induced polymerization utilizes plasma to activate the surface to generate oxide or hydroxide groups, which can then be used in conventional polymerization methods (two-step method) (Zou, et al., 2011). So far plasma treatment has been utilized on a variety of materials including the surface modification of TFC RO membranes (Yu, et al., 2007; Wu, et al., 1997).

Initiated chemical vapor deposition

Initiated chemical vapor deposition (iCVD) is an all-dry free-radical polymerization technique performed at low temperatures and low operating pressures. In this method, the modifiers are covalently bond with membrane surface, belonging to permanent modification. Therefore, this technique is better for long-term operation.

Yang et al. (Yang, et al., 2011) synthesized a copolymer containing poly-(sulfobetaine) zwitterionic groups, which was covalently grafted on to RO membrane for surface modification. The modified membrane exhibited superior antifouling performance compared to the bare RO membrane.